

ปฏิริยาไฮโดรจีนชั้นในวฏภาคของเหลวบนตัวเร่งปฏิริยาแพลเลเดียมบนตัวรองรับซึ่งอะลูมินาที่เตรียมโดย
วิธีโซลโวลเทอรัล



นาย วีรชัย สิริขจร

สถาบันวิทยบริการ

จุฬาลงกรณ์มหาวิทยาลัย

วิทยานิพนธ์นี้เป็นส่วนหนึ่งของการศึกษาตามหลักสูตรปริญญาวิศวกรรมศาสตรมหาบัณฑิต

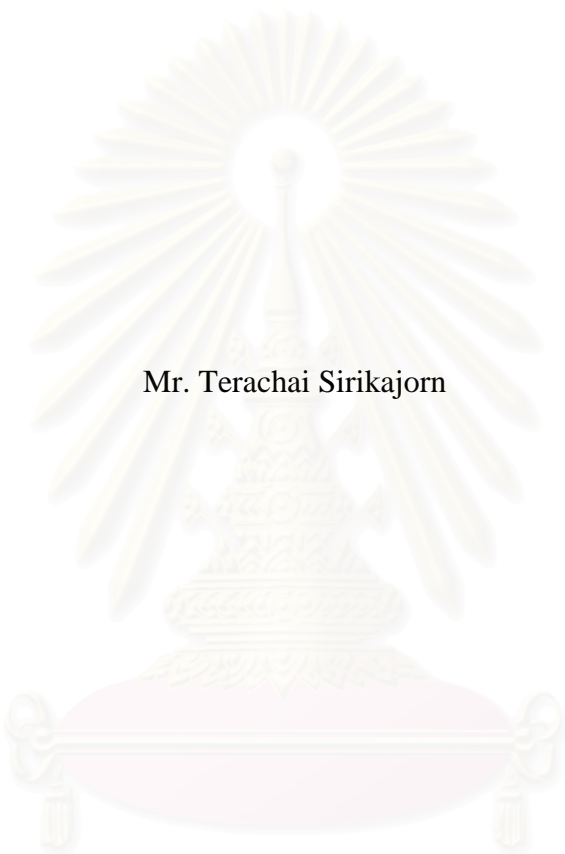
สาขาวิชาวิศวกรรมเคมี ภาควิชาวิศวกรรมเคมี

คณะวิศวกรรมศาสตร์ จุฬาลงกรณ์มหาวิทยาลัย

ปีการศึกษา 2549

ลิขสิทธิ์ของจุฬาลงกรณ์มหาวิทยาลัย

LIQUID-PHASE HYDROGENATION ON Pd CATALYST SUPPORTED ON
SOLVOTHERMAL-DERIVED ZnAl_2O_4



Mr. Terachai Sirikajorn

สถาบันวิทยบริการ
จุฬาลงกรณ์มหาวิทยาลัย

A Thesis Submitted in Partial Fulfillment of the Requirements
for the Degree of Master of Engineering Program in Chemical Engineering

Department of Chemical Engineering

Faculty of Engineering

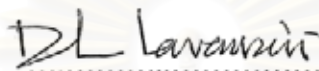
Chulalongkorn University

Academic Year 2006


Copyright of Chulalongkorn University

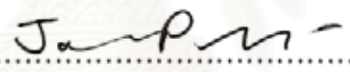
Thesis Title LIQUID-PHASE HYDROGENATION ON Pd CATALYST
SUPPORTED ON SOLVOTHERMAL-DERIVED ZnAl₂O₄
By Mr. Terachai Sirikajorn
Field of Study Chemical Engineering
Thesis Advisor Assistant Professor Joongjai Panpranot, Ph.D.


Accepted by the Faculty of Engineering, Chulalongkorn University in Partial
Fulfillment of the Requirements for the Master's Degree

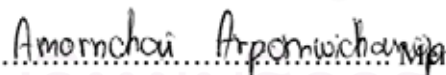

..... Dean of the Faculty of Engineering
(Professor Direk Lavansiri, Ph.D.)

THESIS COMMITTEE


..... Chairman
(Associate Professor ML. Supakanok Thongyai, Ph.D.)


..... Thesis Advisor
(Assistant Professor Joongjai Panpranot, Ph.D.)


..... Member
(Akawat Sirisuk, Ph.D.)


..... Member
(Amornchai Arpornwichanop, D.Eng.)


..... Member
(Assistant Professor Okorn Mekasuwandumrong, D.Eng.)

ธีรชัย สิริขจร: ปฏิริยาไฮโดรจิเนชันในวัฏภาคของเหลวบนตัวเร่งปฏิริยาแพลเลเดียมบนตัวรองรับซิงค์อะลูมิเนตที่เตรียมโดยวิธีโซลโวเทอร์มอล (LIQUID-PHASE HYDROGENATION ON Pd CATALYST SUPPORTED ON SOLVOTHERMAL-DERIVED $ZnAl_2O_4$) อ. ที่ปรึกษา: ผ.ศ. ดร. จุใจ ปั้นประณต, 108 หน้า.

วิทยานิพนธ์นี้ศึกษาเปรียบเทียบลักษณะเฉพาะและคุณสมบัติการเร่งปฏิริยาของตัวเร่งปฏิริยาแพลเลเดียมบนตัวรองรับซิงค์อะลูมิเนต อะลูมินา และ ซิงค์ออกไซด์ ในเทอมของความว่องไวของการเกิดปฏิริยาไฮโดรจิเนชันในวัฏภาคของเหลวของเฮปไทน์ การเลือกเกิดของเฮปทีนและการเสื่อมสภาพของตัวเร่งปฏิริยา พบตัวรองรับทั้งสามชนิดที่เตรียมขึ้นมีโครงสร้างผลึกเป็นแบบผลึกเดี่ยวในช่วงอุณหภูมิที่ใช้ในการเผา (500-1150°C) จากการศึกษาคุณสมบัติการเร่งปฏิริยาและการเลือกเกิดของตัวเร่งปฏิริยาพบว่า ตัวเร่งปฏิริยาแพลเลเดียมที่อยู่บนตัวรองรับซิงค์อะลูมิเนตและอะลูมินาที่เตรียมด้วยวิธีโซลโวเทอร์มอลซึ่งเผาที่อุณหภูมิสูงจะให้ประสิทธิภาพดีกว่าตัวเร่งปฏิริยาที่อยู่บนตัวรองรับซิงค์อะลูมิเนตและอะลูมินาที่เผาที่อุณหภูมิต่ำ นอกจากนี้ยังพบว่าตัวเร่งปฏิริยาแพลเลเดียมบนตัวรองรับอัลฟาอะลูมินาที่เตรียมโดยวิธีโซลโวเทอร์มอลมีความว่องไวในการเกิดปฏิริยามากกว่าตัวเร่งปฏิริยาแพลเลเดียมบนตัวรองรับอัลฟาอะลูมินาเกรดทางการค้า สำหรับการเสื่อมสภาพของตัวเร่งปฏิริยา พบว่า ตัวเร่งปฏิริยาแพลเลเดียมที่อยู่บนตัวรองรับที่เผาที่อุณหภูมิสูงกว่าจะมีปริมาณการถูกชะล้างของแพลเลเดียมน้อยกว่า

สถาบันวิทยบริการ
จุฬาลงกรณ์มหาวิทยาลัย

ภาควิชา.....วิศวกรรมเคมี..... ลายมือชื่อนิสิต..... ธีรชัย สิริขจร
สาขาวิชา.....วิศวกรรมเคมี..... ลายมือชื่ออาจารย์ที่ปรึกษา..... ผ.ศ. ดร. จุใจ ปั้นประณต
ปีการศึกษา.....2549.....

4870326021: MAJOR CHEMICAL ENGINEERING

KEYWORDS: LIQUID-PHASE HYDROGENATION/ ZnAl_2O_4 SUPPORTED
PALLADIUM CATALYSTS

TERACHAI SIRIKAJORN: LIQUID-PHASE HYDROGENATION ON Pd
CATALYST SUPPORTED ON SOLVOTHERMAL-DERIVED ZnAl_2O_4

THESIS ADVISOR: ASST. PROF. JOONGJAI PANPRANOT Ph.D., 108 pp.

The characteristics and catalytic properties of solvothermal derived ZnAl_2O_4 supported palladium catalysts were investigated and compared in terms of catalytic activities for liquid-phase hydrogenation of 1-hetyne, 1-heptene selectivities and catalyst deactivation to those of solvothermal derived Al_2O_3 and ZnO supported Pd catalysts. It was found that the solvothermal derived ZnAl_2O_4 , Al_2O_3 , and ZnO formed single crystallite. The palladium catalysts supported on solvothermal derived ZnAl_2O_4 and Al_2O_3 calcined at higher temperature exhibited better performances than those supported on the supports calcined at lower temperatures. Moreover, it was found that Pd catalyst support on solvothermal-derived alpha alumina exhibited the higher activity than those supported on commercial one. For catalyst deactivation, Pd catalysts on the supports calcined at high temperature showed lower amount of Pd leaching.

สถาบันวิทยบริการ
จุฬาลงกรณ์มหาวิทยาลัย

Department Chemical Engineering.....

Field of Study..... Chemical Engineering.....

Academic year2006.....

Student's signature

Advisor's signature

Terachai Sirikajorn

Joongjai Panpranot

ACKNOWLEDGEMENTS

The author would like to express his sincere gratitude and appreciation to his advisor, Assistant Professor Joongjai Panpranot, for his invaluable suggestions, encouragement during his study, and useful discussion throughout this research. Without the continuous guidance and comments from Professor Piyasan Praserttham, this work would never have been achieved. In addition, the author would also be grateful to Associate Professor ML. Supakanok Thongyai, as the chairman, and Dr. Akawat Sirisuk, Dr. Amornchai Arpornwichanop, and Assistant Professor Okorn Mekasuwandumrong as the members of the thesis committee. The financial supports of the Thailand Research Fund (TRF), TJTTP-JBIC and Graduate School of Chulalongkorn University are gratefully acknowledged.

Most of all, the author would like to express his highest gratitude to his parents who always pay attention to his all the times for their suggestions and have provided support and encouragements. The most success of graduation is devoted to his parents.

Finally, the author wishes to thank the members of the Center of Excellence on Catalysis and Catalytic Reaction Engineering, Department of Chemical Engineering, Faculty of Engineering, Chulalongkorn University for their friendship and assistance.

สถาบันวิทยบริการ
จุฬาลงกรณ์มหาวิทยาลัย

CONTENTS

	Page
ABSTRACT (IN THAI)	iv
ABSTRACT (IN ENGLISH)	v
ACKNOWLEDGMENTS	vi
CONTENTS	vii
LIST OF TABLES	xi
LIST OF FIGURES	xii
CHAPTER	
I INTRODUCTION	1
1.1 Rationale.....	1
1.2 Objective.....	3
1.3 Research Scopes.....	3
II THEORY	4
2.1 Aluminium Oxides or Alumina (Al_2O_3)	4
2.2 Aluminate.....	4
2.3 Zinc Oxides (ZnO)	5
2.4 Aluminate (ZnAl_2O_4)	5
2.5 Hydrothermal Synthesis.....	6
2.5.1 Synthesis of New Phases.....	6
2.5.2 Growth of Single Crystals.....	7
2.6 Solvothermal Synthesis.....	8
2.7 Hydrogenation Reaction.....	8
2.8 Hydrogenation of Alkenes and Alkynes.....	9
2.8.1 Hydrogenation of Alkenes.....	9
2.8.2 Hydrogenation of Alkynes.....	10
2.9 Hydrogenation Catalyst.....	10
2.10 Catalyst Deactivation (Satterfield, 1980)	11
2.10.1 Poison.....	11
2.10.2 Fouling.....	11
2.10.3 Reduction of Active Area by Sintering or Migration.....	13

CHAPTER

2.10.4 Loss of Active Species (Leaching)	13
2.11 Sintering.....	14
III LITERATURE REVIEWS.....	16
3.1 Synthesis of Zinc Aluminate.....	16
3.2 Supported Pd Catalysts in Liquid Phase Hydrogenation...	18
3.3 Supported Noble Metal Catalysts in 1-Heptyne Selective Hydrogenation.....	21
3.4 Deactivation of Supported Pd Catalysts in Liquid-Phase Reaction.....	23
IV EXPERIMENTS.....	24
4.1 Catalyst Preparation.....	24
4.1.1 Materials	
4.1.2 Equipment	
4.1.3 Synthesis of Zinc Aluminate	
4.1.4 Synthesis of Alumina	
4.1.5 Synthesis of Zinc Oxide	
4.1.6 Palladium Loading	
4.2 The Reaction Study in Liquid-Phase Hydrogenation.....	28
4.2.1 Instruments and Apparatus.....	28
4.2.2 Liquid-Phase Hydrogenation Procedure.....	28
4.3 Catalyst Characterization.....	30
4.3.1 N ₂ Physisorption.....	30
4.3.2 X-Ray Diffraction (XRD)	30
4.3.3 Transmission Electron Microscopy (TEM)	30
4.3.4 CO-Pulse Chemisorption.....	30
4.3.5 X-Ray Photoelectron Spectroscopy (XPS).....	31
4.3.6 Atomic Absorption Spectroscopy (AAS).....	31
V RESULTS AND DISCUSSIONS.....	32
5.1 Pd Catalysts Supported on the Solvothermal-derived ZnAl ₂ O ₄ , Al ₂ O ₃ , and ZnO in 1-Heptyne Hydrogenation.....	32
5.1.1 Characterization of the Catalysts.....	32

CHAPTER

5.1.1.1 Transmission Electron Microscopy (TEM)	32
5.1.1.1.1 TEM Results of ZnAl ₂ O ₄	33
5.1.1.1.2 TEM Results of Al ₂ O ₃	39
5.1.1.1.3 TEM Results of ZnO.....	43
5.1.1.2 N ₂ Physisorption.....	44
5.1.1.2.1 Surface Area and Pore Measurement of ZnAl ₂ O ₄ Supports and Pd/ZnAl ₂ O ₄ Catalysts.....	44
5.1.1.2.2 Surface Area and Pore Measurement of Al ₂ O ₃ Supports and Pd/Al ₂ O ₃ Catalysts.....	46
5.1.1.2.3 Surface Area and Pore Measurement of ZnO Supports and Pd/ZnO Catalysts.....	48
5.1.1.3 X-Ray Diffraction (XRD).....	50
5.1.1.3.1 X-Ray Diffraction (XRD) Patterns of ZnAl ₂ O ₄ , Al ₂ O ₃ , and ZnO Supports.....	50
5.1.1.3.2 X-Ray Diffraction (XRD) Patterns of Supported Pd Catalysts.....	50
5.1.1.4 X-Ray Photoelectron Spectroscopy (XPS) ...	58
5.1.1.5 CO-Pulse Chemisorption.....	61
5.1.2 Reaction Study in 1-Heptyne Hydrogenation.....	63
5.1.3 Catalyst Deactivation.....	68
5.2 Comparison of Pd Catalysts on the Solvothermal-derived Supports and the Commercial Ones in 1-Heptyne Hydrogenation	70
5.2.1 Characterization of the Commercial Catalysts.....	70
5.2.1.1 Transmission Electron Microscopy (TEM)...	70
5.2.1.2 N ₂ Physisorption.....	73

CHAPTER	page
5.2.1.3 X-Ray Diffraction (XRD).....	78
5.2.1.4 CO-Pulse Chemisorption.....	82
5.2.2 Reaction Study in 1-Heptyne Hydrogenation and Catalyst Deactivation.....	83
VI CONCLUSIONS AND RECOMMENDATIONS.....	86
6.1 Conclusions.....	86
6.2 Recommendations.....	87
REFERENCES.....	88
APPENDICES	
APPENDIX A. CALCULATION FOR CATALYST PREPARATION.....	93
APPENDIX B. CALCULATION OF THE CRYSTALLITE SIZE.....	94
APPENDIX C. CALCULATION FOR METAL ACTIVE SITES AND DISPERSION.....	98
APPENDIX D. CALIBRATION CURVES.....	99
APPENDIX E. CALCULATION OF PHENYLACETYLENE CONVERSION AND SELECTIVITY.....	102
APPENDIX F. CALCULATION OF TURNOVER OF FREQUENCY.....	104
APPENDIX G. LIST OF PUBLICATIONS.....	105
VITAE.....	108

LIST OF TABLES

TABLE	Page
5.1	N ₂ physisorption properties of zinc aluminate supports and Pd catalysts..... 45
5.2	N ₂ physisorption properties of alumina supports and Pd catalysts..... 47
5.3	N ₂ physisorption properties of alumina supports and Pd catalysts..... 49
5.4	Crystallite sizes of supports and catalysts..... 51
5.5	Atomic concentrations of catalysts from XPS..... 59
5.6	Binding energy position (eV) of catalysts from XPS..... 59
5.7	FWHM (eV) of catalysts from XPS..... 60
5.8	CO- pulse chemisorption results..... 62
5.9	Results of 1-heptyne hydrogenation..... 65
5.10	TOFs of various Pd catalysts..... 66
5.11	The actual amounts of palladium loading and the percentage of Pd leaching..... 69
5.12	N ₂ physisorption properties of various supports and Pd catalysts..... 74
5.13	Crystallite sizes of supports and catalysts..... 79
5.14	CO- pulse chemisorption results..... 82
5.15	Results of 1-heptyne hydrogenation..... 84
5.16	The actual amounts of palladium loading and the percentage of Pd leaching..... 84
D.1	Conditions uses in Shimadzu modal GC-14B..... 100

LIST OF FIGURES

FIGURE	Page
2.1 Structure of zinc aluminate.....	5
2.2 Formation of a neck during the sintering of two fine particles.....	14
4.1 Autoclave reactor and gas controlling system.....	25
4.2 A schematic diagram of the liquid-phase hydrogenation system.....	29
5.1 TEM micrographs and SAD patterns of ZnAl ₂ O ₄ (a), (b) ZnAl ₂ O ₄ -as syn (c), (d) ZnAl ₂ O ₄ -500 (e), (f) ZnAl ₂ O ₄ -700 (g), (h) ZnAl ₂ O ₄ -900 (i), (j) ZnAl ₂ O ₄ -1150.....	38
5.2 TEM micrographs and SAD patterns of Al ₂ O ₃ of (a), (b) Al ₂ O ₃ -as syn (c), (d) Al ₂ O ₃ -700 (e), (f) Al ₂ O ₃ -1150.....	42
5.3 TEM micrographs of ZnO-as syn.....	43
5.4 Pore size distributions of zinc aluminate calcined at various temperature.....	45
5.5 Pore size distributions of alumina calcined at various temperatures.....	47
5.6 Pore size distributions of zinc oxide calcined at various temperatures...	49
5.7 XRD patterns of ZnAl ₂ O ₄ calcined at various temperatures.....	52
5.8 XRD patterns of Al ₂ O ₃ calcined at various temperatures.....	53
5.9 XRD patterns of ZnO calcined at various temperatures.....	54
5.10 XRD patterns of Pd/ZnAl ₂ O ₄ calcined at various temperatures.....	55
5.11 XRD patterns of Pd/Al ₂ O ₃ calcined at various temperatures.....	56
5.12 XRD patterns of Pd/ZnO calcined at various temperatures.....	57
5.13 Performance curves of Pd/ZnAl ₂ O ₄ , Pd/Al ₂ O ₃ , Pd/ZnO catalysts in 1-heptyne hydrogenation.....	67

5.14	TEM micrographs and SAD patterns of commercial Al ₂ O ₃ of (a), (b) Al ₂ O ₃ -gamma com and (c), (d) Al ₂ O ₃ -alpha com.....	72
5.15	Pore size distributions of solvothermal gamma Al ₂ O ₃ and commercial gamma Al ₂ O ₃	75
5.16	Pore size distributions of solvothermal alpha Al ₂ O ₃ and commercial alpha Al ₂ O ₃	76
5.17	Pore size distributions of commercial SiO ₂ (15 nm)	77
5.18	XRD patterns of solvothermal-derived alumina and commercial gamma alumina.....	80
5.19	XRD patterns of Pd catalysts supported on solvothermal-derived alumina and commercial gamma alumina.....	80
5.20	XRD patterns of solvothermal-derived alumina-1150 and commercial alpha alumina.....	81
5.21	XRD patterns of Pd catalysts supported on solvothermal-derived alumina-1150 and commercial alpha alumina.....	81
5.22	Performance curves of various catalysts in 1-heptyne hydrogenation...	85
B.1	The diffraction peak of Pd/ZnAl ₂ O ₄ -900 for calculation of the crystallite size.....	96
B.2	The plot indicating the value of line broadening due to the equipment. (The data were obtained by using α-alumina as a standard).....	97
D.1	The calibration curve of 1-heptyne.....	101
D.2	The calibration curve of 1-heptene.....	101

CHAPTER I

INTRODUCTION

1.1 Rationale

Catalytic hydrogenation is one of the most useful, versatile, and environmentally acceptable reaction routes available for organic syntheses because the scope of the reaction type is very broad and many functional groups can be hydrogenated with high selectivity and high conversion. A large number of these reactions are carried out in liquid phase using batch type slurry processes.

Hydrogenation reactions are mostly catalyzed by noble metals or group VIII transition metals. The major advantages of noble metal catalysts are their relatively high activity, mild process conditions, easy separation, and better handling properties. Noble metals such as, Pt, Pd, Rh, and Ru are particularly effective in hydrogenation processes because they adsorb hydrogen with dissociation and the bonding is not too strong. The ability of the metal to dissociate the hydrogen molecules partly determines the activity of the catalyst. The hydrogenation activity generally decreases in the following sequence: Pd>Rh>Pt>Ru. Catalysis by noble metals is usually achieved via the high dispersion of low loading metals on an appropriate support. The supports are usually of relatively inexpensive oxide such as alumina, silica, and titania.

Several factors affecting the performance of noble metal catalysts in liquid phase hydrogenation have been extensively investigated. Typically, the factors can be classified into (i) the role of the liquid phase composition (substrate structure, solvent effect, etc.), (ii) the effect of catalysts (active sites composition and morphology, support effects, SMSI, modifiers, etc.), and (iii) the effect of reaction conditions (temperature, pressure, etc.) on reaction kinetics. A solvent in liquid-phase heterogeneous catalytic systems can have a significant effect on kinetic behavior. Mass transfer limitation is an obvious one, especially pore diffusion, but other

possibilities such as solvent properties and competitive adsorption of the solvent for sites may also occur.

The important problem in catalytic liquid phase hydrogenation is the activity and selectivity decay due to catalyst deactivation. The main causes of catalyst deactivation in liquid phase hydrogenation are

1. Sintering of metal particles and coalescence
2. Leaching of active phases and supports
3. Poisoning of strongly adsorbed molecules

Because the cost of these noble metal catalysts used in these reactions are very high, this problem must be concerned.

In order to improve the properties of catalytic materials, great interest has focused on the use of spinel-type structures. Among these materials, aluminates seem to be a good option because of their properties such as high thermal stability, high mechanical resistance, hydrophobicity, and low surface acidity. These properties make them interesting materials as catalysts and carriers for active metals to substitute the more traditional systems. Furthermore, it is known that some aluminate spinels, including zinc aluminate, tend to prevent sintering of noble metals due to a strong metal-support interaction. The sintering resistance and chemical stability of catalytically active phases are a very important problem for high-temperature processes.

Zinc aluminate catalysts or supports and ceramics are commonly prepared by high temperature calcination (above 1000 K) of mixed aluminium and zinc oxides, coprecipitated products or products of impregnating a porous alumina having a high surface area with a solution of zinc compound. A disadvantage of such materials for catalytic applications is the low surface area, usually about 20–50 m²/g, where conventional catalyst or supports are porous materials whose surface area require comprised between 100 and 300 m²/g. Better results may be obtained by sol-gel methods: ZnAl₂O₄ spinels prepared by controlled solvothermal method have surface areas in the range about 100 m²/g. Zinc aluminate spinel with single phase and

uniformly controlled particle size and morphology can be synthesized by solvothermal techniques. Presently, we report a solvothermal method for the preparation of nano-sized zinc aluminate spinel with a high surface area particularly useful for catalytic applications.

1.2 Objective

The objective of this research is to investigate the characteristics and catalytic properties of solvothermal-derived zinc aluminate spinel supported Pd catalysts in liquid-phase hydrogenation.

1.3 Research Scopes

1. Preparation of zinc aluminate, alumina and zinc oxide by solvothermal method with various particle sizes.
2. Preparation of zinc aluminate-supported palladium catalysts with 1% palladium loadings using incipient wetness impregnation method.
3. Preparation of zinc oxide (ZnO) and alumina (Al₂O₃)-supported palladium catalyst with 1% palladium loadings using incipient wetness impregnation method. Compare them with the zinc aluminate-supported palladium catalyst.
4. Characterization of various supported palladium catalysts using several techniques such as inductively coupled plasma (ICP), X-ray diffraction (XRD), scanning electron microscopy (SEM), transmission electron microscopy (TEM), N₂ physisorption, and pulse CO chemisorption
5. Reaction study of various supported palladium catalysts in liquid phase hydrogenation of an alkyne using stirring batch reactor (stainless steel autoclave 50 ml)
6. Study of catalyst deactivation after performing liquid-phase hydrogenation.

CHAPTER II

THEORY

2.1 Aluminium Oxides or Alumina (Al_2O_3)

Aluminum oxides, which are a term of alumina compounds, had transition phase and alpha phase alumina.

- Transition Alumina

The partial dehydration of aluminum hydroxides and oxyhydroxides leads to compounds with the crude formula $\text{Al}_2\text{O}_3 \cdot x \text{H}_2\text{O}$ with $0 < x < 1$, which generally are poorly crystallized. These compounds are used to apply as catalyst supports, Claus catalysts, and adsorbents. There are six principle phases designated by the Greek letters chi, kappa, eta, theta, delta, and gamma. The nature of the product obtained by calcination depends on the starting hydroxide (Gibbsite, boehmite and others) and on the calcination conditions. In effect, there exist several sequences during dehydration. In all cases, the ultimate product of dehydration is corundum (Al_2O_3). An excellent bibliographical review of transition alumina has been compiled by Leonard (1967). The situation can be reduced to a sample one on the basis of crystallographics, once one becomes aware that there are only two types of structures: spinel, for eta, gamma, delta, and theta and hexagonal, for chi and kappa.

2.2 Aluminate

A negative ion are usually given the formula AlO_2^- and derived from aluminum hydroxide. Solutions of aluminates are strongly basic.

2.3 Zinc Oxides (ZnO)

The crystal structure of zinc oxide is likely to stabilize defects, e.g., zinc excess or deficiency and inclusion of foreign ions, and therefore has useful semiconductor properties. Various doped oxides are used for photocopying, catalysts, and phosphors.

Zinc oxide, as an amphoteric material, reacts with acids to form zinc salts and with strong alkalies to form zincates. Zinc oxide reacts with carbon dioxide in moist air to form oxycarbonate. Acidic gases, i.e., hydrogen sulfide, sulfur dioxide, and chlorine, react with zinc oxide, and carbon monoxide or hydrogen reduce it to metal.

2.4 Zinc Aluminate (ZnAl₂O₄)

ZnAl₂O₄ is a binary oxide consisting of zinc oxides and aluminum oxides that crystallize in spinel structure. The unit cell of spinels is represented by formula of AB₂O₄. The Zn²⁺ ions occupy the tetrahedrally coordinated A site and Al³⁺ ions occupy the octahedrally coordinated B site. The structure of zinc aluminate is shown in Figure 2.1.

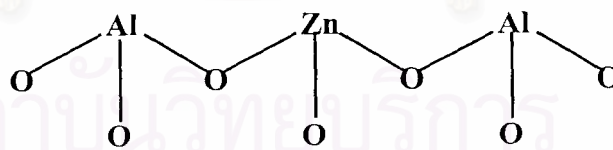


Figure 2.1 Structure of zinc aluminate

2.5 Hydrothermal Synthesis

Hydrothermal methods utilize water under pressure and at temperatures above its normal boiling point as means of speeding up the reactions between solids. The water performs two roles. The water-as liquid or vapour-serves as the pressure transmitting medium. In addition, some or all of the reactants to take place in, or with the aid of, liquid and/or vapour phases. Under these conditions, reactions may occur that, in the absence of water, would occur only at much higher temperatures. The method is therefore particularly suited for the synthesis of phases that are unstable at higher temperatures. It is also a useful technique for growth of single crystals; by arranging for a suitable temperature gradient to be present in the reaction vessel, dissolution of the starting material may occur at the hot end reprecipitation at the cooler end.

The design of hydrothermal equipment is basically a tube, usually of steel, closed at one end. The other end has a screw cap with a gasket of soft copper to provide a seal. Alternatively, the 'bomb' may be connected directly to an independent pressure source, such as hydraulic ram; this is known as the 'cold seal' method. The reaction mixture and an appropriate amount of water are placed inside the bomb, which is then sealed and placed inside an oven at the required temperature.

2.5.1 Synthesis of New Phases

Calcium silicate hydrates. Hydrothermal methods have been used successfully for the synthesis of many materials. A good example is the family of calcium silicate hydrates, many of which are important compounds of set cement and concrete. Typically, lime, CaO and quartz, SiO₂ are heated with water at temperature in the 150 to 500°C and pressure of 0.1 to 2.0 kbar. Each calcium silicate hydrate has, for its synthesis, optimum preferred conditions of composition of starting mix, temperature, pressure and time. For example, xonotlite, Ca₆Si₆O₁₇(OH)₂, may be preheated by heating equimolar mixtures of CaO and SiO₂ at saturated steam pressures in the range 150 to 350°C, by varying the experimental conditions, H.F.W. Taylor and others have been able to unravel the chemistry of this complex family of solids.

2.5.2 Growth of Single Crystals

For the growth of single crystals by hydrothermal methods it is often necessary to add a mineralizer. A mineralizer is any compound added to the aqueous solution that speeds up its crystallization. It usually operates by increasing the solubility of the solute through the formation of soluble species that would not usually be in the water. For instance, the solubility of quartz in water at 400°C and 2 kbar is too small to permit the recrystallization of quartz, in a temperature gradient, within a reasonable space of time. On addition of NaOH as a mineralizer, however, large quartz crystals may be readily grown. Using the following condition, crystals of kilogram size have been grown: quartz and 1.0 M NaOH solution are held at 400°C and 1.7 kbar; at this temperature some of the quartz dissolves. A temperature gradient is arranged to exist in the reaction vessel and at 360°C the solution is supersaturated with respect to quartz, which precipitates onto a seed crystal. In summary, therefore quartz dissolves in the hottest part of the reaction vessel, is transported throughout the vessel via convection currents and it precipitated in cooler parts of the vessel where its solubility in water is lower. Quartz single crystals are used in many devices in radar and sonar, as piezoelectric transducers, as monochromators in X-ray diffraction, etc. Annual world production of quartz single crystal, using hydrothermal and other methods, is currently is currently a staggering 600 tons!

Using similar methods, many substances have been prepared as high quality single crystals, e.g. corundum (Al_2O_3) and ruby (Al_2O_3 doped with Cr^{3+}).

สถาบันวิทยบริการ
จุฬาลงกรณ์มหาวิทยาลัย

2.6 Solvothermal Synthesis

Solvothermal synthesis is improved from the hydrothermal synthesis by using organic solvent as the reaction medium instead of water. This method is based on the decomposition of metal alkoxide at elevated temperature (200-300°C) under autogenous pressure. It is particularly suited for the synthesis of alumina in phase that is unstable at high temperature. It is also a useful technique for growing single crystals. In this method, parts or all of the reactants can dissolve in the organic solvent under high pressure. This feature enables the reaction to take place at lower temperature.

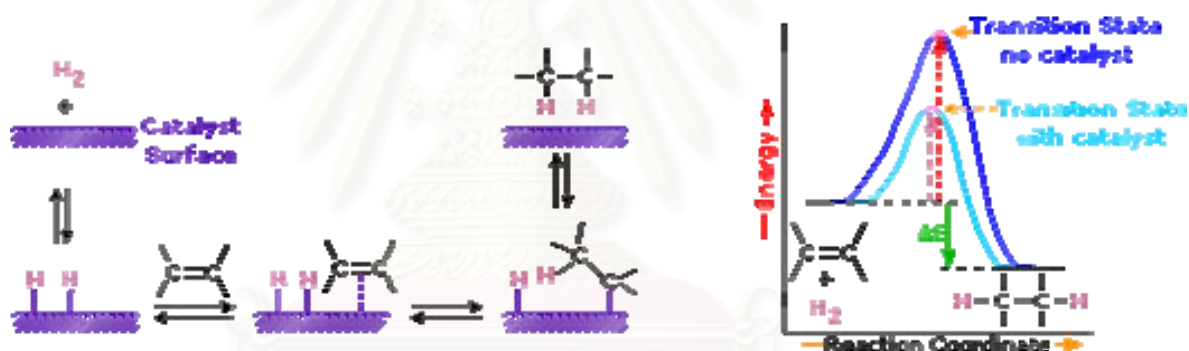
2.7 Hydrogenation Reaction

One of the oldest and most diverse catalytic processes is the selective hydrogenation of functional groups contained in organic molecules to produce (i) fine chemicals (ii) intermediates used in pharmaceutical industry (iii) monomers for production of various polymers and (iv) fats and oils for producing edible and nonedible products. Indeed there are more hydrogenation catalysts available commercially than any other type, and for good reason, because hydrogenation is one of the most useful, versatile and environmentally acceptable reaction routes for organic synthesis. Hydrogenation processes are often made on a small scale in batch reactor. Batch processes are usually most cost effective since the equipment need not to be dedicated to a single reaction. Generally, large stirred autoclave is capable of H₂ pressure up to 140 atm. Typically the catalyst is powdered and slurried with reactant; a solvent is usually present to influence product selectivity and to adsorb the reaction heat liberated by the reaction. Since most hydrogenations are highly exothermic, careful temperature control is required to achieve the desired selectivity and to prevent temperature runaway.

2.8 Hydrogenation of Alkenes and Alkynes

2.8.1 Hydrogenation of Alkenes

Addition of hydrogen to a carbon-carbon double bond is called hydrogenation. The overall effect of such an addition is the reductive removal of the double bond functional group. Regioselectivity is not an issue, since the same group (a hydrogen atom) is bonded to each of the double bond carbons. The simplest source of two hydrogen atoms is molecular hydrogen (H_2), but mixing alkenes with hydrogen does not result in any discernable reaction. Although the overall hydrogenation reaction is exothermic, the high activation energy prevents it from taking place under normal conditions. This restriction may be circumvented by the use of a catalyst, as shown in the following diagram.

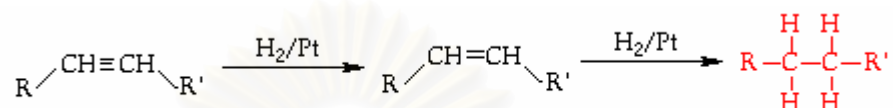


Catalysts are substances that change the rate (velocity) of a chemical reaction without being consumed or appearing as part of the product. Catalysts act by lowering the activation energy of reactions, but they do not change the relative potential energy of the reactants and products. Finely divided metals, such as platinum, palladium and nickel, are among the most widely used hydrogenation catalysts.

As shown in the energy diagram, the hydrogenation of alkenes is exothermic, and heat is released corresponding to the ΔE in the diagram. This heat of reaction can be used to evaluate the thermodynamic stability of alkenes having different numbers of alkyl substituents on the double bond.

2.8.2 Hydrogenation of Alkynes

This reaction is similar to hydrogenation of alkenes. In the hydrogenation of alkynes, alkyne is added by hydrogen to alkene, besides alkene may be overhydrogenated to alkane. However, overhydrogenation depends on the catalyst and reaction condition. The mechanism is shown as:



2.9 Hydrogenation Catalyst

The types of hydrogenation catalysts finding commercial applications include noble metals, group VIII transition metals, organometallic complexes and activated alloy catalysts that are either unsupported or supported. The major advantages of noble metal catalysts are their relatively high activity, mild process conditions, easy separation and better handling properties. The most commonly used noble metals are Pt, Pd, Rh and Ru. Generally Pd is the most active than Rh or Pt for many hydrogenation reactions on the same carbon carrier. In general, using of support allows the active component to have a larger surface area, which is particularly important in those cases where a high temperature is required to activate the active component. The supports may be as different as carbon, silica, alumina and polymer in order to obtain higher selectivity and activity. Supported catalyst may be prepared by a variety of methods, depending on the nature of active components as well as the characteristics of carriers such as decomposition, precipitation, coprecipitation, adsorption and ion-exchange etc.

2.10 Catalyst Deactivation (Satterfield, 1980)

A catalyst may lose its activity or its selectivity for a wide variety of reasons. The causes may be grouped loosely into

2.10.1 Poison

2.10.2 Fouling

2.10.3 Reduction of active area by sintering or migration

2.10.4 Loss of active species (leaching)

2.10.1 Poison

A catalyst poison is an impurity present in the feed stream that reduces catalyst activity. In a complex reaction it may affect one reaction step more than another; hence the selectivity towards a desired reaction may be improved by deliberately adding a poison. It adsorbs on active sites of the catalyst, and if not adsorbed too strongly, it is gradually desorbed when the poison is eliminated from the feed stream. The phenomenon is then temporary. If adsorption is strong, the effect is permanent. A desorption may be enhanced by reaction with the fluid. Thus in a hydrogenation reaction a metallic catalyst may be poisoned by adsorption of a sulfur compound, but desorption may be enhanced by its conversion to H₂ by reaction with H₂. If a reaction product is strongly adsorbed, the reaction may be termed self-poisoned or self-inhibited.

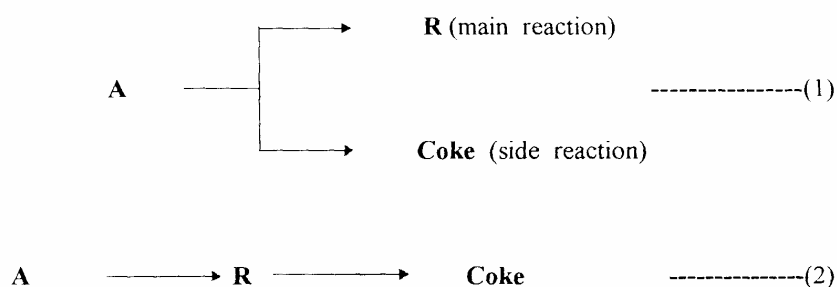
2.10.2 Fouling

The term fouling is generally used to describe a physical blockage such as the deposit of dust or fine powder or carbonaceous deposits (coke). In the latter case activity can usually be restored by removal of the coke by burning.

The fouling catalyst deactivation has been found by Butt (1972) and Levenspiel (1972) in Hughes (1984) and they have laid the foundations of a better understanding of fouling catalyst deactivation process. Fouling is a process of catalyst deactivation that may be either physical or chemical in nature. In general, much larger

amounts of material are responsible for deactivation in fouling processes than in poisoning. The most typical of fouling processes is that of the carbonaceous deposit or “coke” that forms on most catalysts used in the processing of petroleum fractions or other organic chemical feedstocks. Another class of fouling reactions is that of metal sulphide deposition arising from the organometallic constituents of petroleum which react with sulphur-containing molecules and deposit within the pores of the catalyst during hydrotreating operation (Newson, 1975). Liquid fuels derived from coals also give rise to similar deposits during hydrocracking of the resultant liquid (Davies, 1978). These last two examples may be termed impurity fouling, and as such they are not typical of the more general type of fouling associated with coke formation on the catalyst surface. The formation of carbonaceous or coke deposits (containing, in addition to carbon, significant amounts of hydrogen plus traces of oxygen, sulphur, and nitrogen) during the processing of organic based chemical feedstocks is the more usual example of fouling. It is important to recognize that the coke deposit in this case originates from the reactions occurring and is not an impurity. Because of this intrinsic association with the main chemical reactions, fouling by coke cannot be eliminated by purification of the feed or use of a guard catalyst; if reaction occurs, coke deposition must also necessarily occur according to the overall chemistry of the process. However, coke formation can be minimized by appropriate choice of reactor and operating conditions, and in some cases by modification of the catalyst.

In general, coke can originate from the reactant or product by reaction (1) or (2). Reaction (1) is called parallel fouling while (2) is called series fouling or consecutive fouling. Fouling may (and indeed often does for complex system) also occur by a combination of reactions (1) and (2). The extent of coke formation will depend on the orders of reaction with respect to the formation of the desired product R and the coke, and on the magnitudes of the temperature coefficients for each reaction.



2.10.3 Reduction of Active Area by Sintering or Migration

Sintering is an irreversible physical process leading to a reduction of effective catalytic area. It may consist of growth of metal crystallites on a support or of a decrease in area of a nonsupported catalyst.

2.10.4 Loss of Active Species (leaching)

The particular active species may also be converted to another form less active or selective, as is the case with certain complex metal oxides used in partial oxidation reactions. A complex metal oxide crystal may also decompose into other compounds, sometimes caused by loss of a particular element via volatilization of a compound. A somewhat amorphous catalyst may crystallize, or a compound active in one crystal habit may be converted into a less active crystalline form. A supported metal catalyst may be reduced in activity or selectivity by becoming alloyed with a metallic impurity or by reaction with the support; for example, a nickel/alumina catalyst may be converted to a nickel aluminate. However, the active species can be removed from support to bulk solution during the reaction.

2.11 Sintering

Sintering is the process by which small particles of material are bonded together by solid-state diffusion. In ceramic manufacturing, this thermal treatment results in the transformation of a porous compact into a dense, coherent product. In the sintering process, particles are coalesced by solid-state diffusion at very high temperatures yet lower than melting point of the compound being sintered. In sintering, atomic diffusion takes place between the contacting surfaces of the particles so that they become chemically bonded together, as shown in Figure 2.2. As the process proceeds, larger particles are formed at the expense of the smaller ones, while the porosity of the compacts decreases. Finally, at the end of the process, an “equilibrium grain size” is attained.

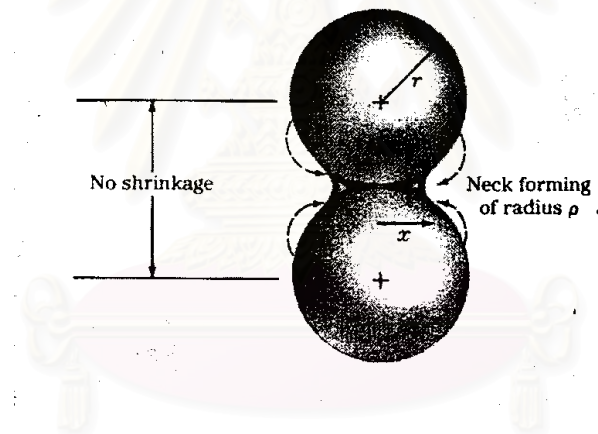


Figure 2.2 Formation of a neck during the sintering of two fine particles

Densification, recrystallization, and grain growth occur in the same temperature range. Therefore, strict control of the sintering process as well as small addition of grain growth inhibitor, e.g. MgO, to the alumina powders is essential to achieve a fully dense sintered body with fine-grained microstructure. In the course of sintering, the density increases with the logarithm of time, and the grain size increases with the one-third power of time.

The nature of the sintering atmosphere may influence the rate of sintering and the residual porosity. Many additives other than temporary binders have been used in sintering process for several purposes, such as crystal growth repression, crystal growth acceleration, acceleration of sintering or shrinkage rate, reduction in maturing temperature, porosity alteration, changes in physical or chemical properties, and removal of impurities. Many researchers have studied the effects of sintering additives on the sintering process in order to improve properties of material obtained.

The choice of sintering temperature, which is usually between 1600 and 1800°C, depends on surface energy, grain size distribution, and the additives of the alumina powder. The sintering time and particularly the heating rate should be adapted to the size and the wall thickness of the body to be sintered. Larger parts require a longer sintering time and a slower rate of heating-up. Smaller parts can be heated up more quickly, allowing a much shorter sintering time.



สถาบันวิทยบริการ
จุฬาลงกรณ์มหาวิทยาลัย

CHAPTER III

LITERATURE REVIEWS

3.1 Synthesis of Zinc Aluminate

M. Zawadzki *et al.* (2000) studied the hydrothermal synthesis of nanoporous zinc aluminate with high surface. Hydrothermal treatment at low temperatures is proposed for obtaining a nanocrystalline zinc aluminate spinel of interesting properties from catalytic point of view, including high specific surface area (up to 340 m²/g), nanoporosity, and narrow pore size distribution. The precursors for hydrothermal synthesis were basic aluminium nitrate having the empirical formula Al₂(OH)_{6-x}(NO₃)_x wherein x was equal or closed to 1, and hydrated zinc acetate. The proposed synthesis, in contrast to other methods, does not require a high temperature calcination to obtain the spinel phase. The properties of hydrothermally obtained zinc aluminate spinel make them an advanced material suitable for use in catalytic or high-tech ceramic applications.

J. Guo *et al.* (2004) studied the synthesis of high surface area MgAl₂O₄ spinel with a modified sol-gel route, by combining gelation and coprecipitation processes, was developed for the synthesis of high surface area MgAl₂O₄ precursors. The precursors were then calcined in flowing air at temperatures ranging from 500 to 900 °C. The result showed that the derived MgAl₂O₄ spinel is single-phase spinel powder with uniform pore size distribution was formed at temperatures as low as 600 °C. Thermal stability and degree of crystallinity of the as-synthesized spinels is higher than that reported by other preparation methods. The amount of PVA significantly affects the surface area of the samples. With increasing the molar ratio of M/PVA, the surface area of the resulting spinels increased accordingly. (M : metal ions and PVA : polyvinyl alcohol (PVA) monomer)

D. Chen *et al.* (2006) studied the synthesis and characterization of nanosized ZnAl₂O₄ spinel by sol-gel technique. Nanosized zinc aluminate spinel has been obtained by the thermal decomposition of Zn–Al gel prepared by sol-gel technique using oxalic acid as a chelating agent. Stirring an ethanol solution of zinc nitrate, aluminium nitrate and oxalic acid yields a gel precursor, followed by calcination of the resulting gel at different temperatures. Thermogravimetric analysis (TGA) and Differential scanning calorimetry (DSC) have been used to study the thermal behaviour of the precursor. Powder X-ray diffraction (XRD) show that the sample obtained by heating the precursor at 700 °C for 5 h is single-phase cubic material having the spinel-type structure, which can be confirmed by Infrared spectra (IR). The particle size of 15–20 nm has been measured by transmission electron microscopy (TEM). The specific surface area determined by BET surface area measurement was found to be 58 m² g⁻¹.

M. Zawadzki (2006) studied the synthesis of nanosized and microporous zinc aluminate spinel by microwave assisted hydrothermal method. The precursors for microwave-hydrothermal synthesis were aluminium hydroxy nitrate having the empirical formula Al₂(OH)_{6-x}(NO₃)_x, wherein x was equal or close to 1, and hydrated zinc acetate. The result showed that zinc aluminate powder is nano-size (mean particle size 2.4 nm with a narrow size distribution) and zinc aluminate has a spinel structure, high specific surface area (220 m²/g), microporosity and narrow pore size distribution. In contrast to other methods, is very rapid and does not require a high temperature heating to obtain the spinel phase. The potential application of such obtained ZnAl₂O₄ as convenient material for the preparation of thermal stable thin films coatings on different planar substrates is also reported.

3.2 Supported Pd Catalysts in Liquid-Phase Hydrogenation

S. David Jackson *et al.* (1999) studied the hydrogenation of cyclopentene, cyclohexene, cycloheptene and cis-cyclooctene over Pd/alumina, Pd/carbon, Pd/silica and Pd/zirconia catalysts. The hydrogenation reaction and the carbon deposition reaction both showed evidence for particle size sensitivity and the trend in activity with particle size was not the same for all the cycloalkenes, with cycloheptene hydrogenation increasing with particle size. This behavior can principally be related to the strength and mode of adsorption of the cycloalkene, although the adsorbed state of hydrogenation may also influence reactivity.

T. Nozoe *et al.* (2001) studied the non-solvent hydrogenation of solid alkynes and alkenes using supported palladium catalysts. Trans-stibene and carboxylic acid with α,β C=C bonds were employed as the alkene-type substrates for the non-solvent hydrogenation. Their hydrogenation proceeded over Pd/SiO₂ catalyst at room temperature. The hydrogenation rate of trans-stibene under the non-solvent condition was lower than the hydrogenation in tetrahydrofuran (THF).

Singh and Vannice (2001) studied liquid-phase citral hydrogenation over SiO₂-supported group VIII metals. The reaction was carried out in glass reactor at 300 K and atmospheric pressure. The initial TOF for citral hydrogenation exhibited the following trend: Pd > Pt > Ir > Os > Ru > Rh > Ni > Co >> Fe. With the exception of Ni/SiO₂, all catalysts exhibited substantial deactivation due to citral and/or unsaturated alcohol decomposition to yield adsorbed CO that poisoned active sites responsible for hydrogenation. In contrast, Ni/SiO₂ exhibited an initially low TOF that increased fourfold after 7 h of reactions after which time no deactivation was detected up to 84% conversion.

J. J. Ziolkowski *et al.* (2002) studied the rhodium complexes supported on zinc aluminate spinel as catalysts for hydroformylation and hydrogenation including the preparation and activity. The catalysts were prepared by the heterogenization of active homogeneous rhodium catalysts on zinc aluminate spinel. The ZnAl_2O_4 support was prepared by a hydrothermal process. The rhodium(I) complexes, $\text{Rh}(\text{acac})(\text{CO})_2$, $\text{Rh}(\text{acac})(\text{CO})(\text{PPh}_3)$, and $\text{RhCl}(\text{CO})(\text{PPh}_3)_2$, supported on the spinel, gave $\text{Rh}(\text{CO})^{2+}$, $\text{Rh}(\text{CO})(\text{PPh}_3)^+$, and $\text{Rh}(\text{CO})(\text{PPh}_3)^{2+}$ species, respectively, as confirmed by IR spectra. $\text{Rh}(\text{CO})^{2+}$ on the spinel with an excess of PPh_3 effectively catalysed the hydroformylation of 1-hexene under 1MPa of H_2/CO at 356 K. Aldehydes yield of 40–95% were obtained with an *n/iso* ratio of ca. 3. The coordination of 1-hexene to supported $\text{Rh}(\text{CO})^{2+}$ species was evidenced by the appearance of a $\nu(\text{CO})$ band at 2053 cm^{-1} . $\text{Rh}(\text{CO})^{2+}$ -supported on the spinel catalysed the hydrogenation of nitrobenzene and chloronitrobenzene at 1MPa of H_2 and 356K with a TON of 400–500 h^{-1} .

O. Dominguez-Quintero *et al.* (2003) investigated palladium nanoparticle in hydrogenation catalysis of different substrate (1-hexene, cyclohexene, benzene, 2-hexanone and benzonitrile). Palladium nanoparticles (1.9 nm) stabilized was obtained from the reduction of organometallic precursor (palladium(II)bis-dibenzylidene acetone) with hydrogen. The highest hydrogenation rate was found with 1-hexene with TOF of 38250 mole of product/mole of metal/h at 25°C and 30 psi pressure. They presented that the catalytic potential of the Pd/SiO₂ synthesized by organometallic route renders an extremely active nanomaterial which shows little aggregation after catalytic reaction even 145°C .

H. Yamada *et al.* (2003) studied the effect of solvents polarity on selective hydrogenation of unsaturated aldehyde in gas-liquid-solid three phase reactors. Pd/C, Pt/C and Co/Al₂O₃ were used as the catalysts. Experiments were carried out in a semi-batch stirred tank reactor. Hydrogen gas was introduced continuously in the reactor. The solvents were various normal alcohols and various aromatic compounds. They found that polar solvents activate a polar double bond C=O and non-polar solvents activate a non-polar double bond C=C.

J. Panpranot *et al.* (2004) studied the impact of the silica support structure on liquid phase hydrogenation on Pd catalysts. SiO₂ ($d_{\text{pore}} = 3$ nm), SiO₂ (large pore), MCM-41 ($d_{\text{pore}} = 3$ nm) and MCM-41 ($d_{\text{pore}} = 9$ nm), referred as S-3nm, S-large, M-3nm and M-9nm respectively, were used as supports. The catalysts were prepared by incipient wetness impregnation. The reaction was carried out at 25°C and 1 atm in a stainless steel Parr autoclave. The results showed that for the larger pore supports (S-large and M-9nm), Pd particles likely formed primarily in the pores, whereas use of smaller pore supports resulted in Pd particles primarily on the outside surface of the catalyst granules (S-3nm) or both inside and outside the support pores (M-3nm). All the catalysts exhibited similar TOFs for the liquid-phase hydrogenation of 1-hexene. The Pd particle size appeared to strongly determine this metal loss during reaction. However, it is also likely that the location on the silica support also played an important role.

J. Panpranot *et al.* (2004) studied the differences between Pd/SiO₂ and Pd/MCM-41 catalysts in liquid phase hydrogenation. SiO₂-small pore, SiO₂-large pore, MCM-41-small pore and MCM-41-large pore were used as supports. The catalysts were prepared by incipient wetness impregnation. The reaction was carried out at 25°C and 1 atm in a stainless steel Parr autoclave. The results showed that the characteristics and catalytic properties of the silica supported Pd catalysts in liquid-phase hydrogenation were affected by type of silica, pore size and pore structure. The catalyst activities were found to be merely dependent on the Pd dispersion, which as itself a function of the support pore structure. Among the four types of the supported Pd catalysts used in this study, Pd/MCM-41-large pore showed the highest Pd dispersion and the highest hydrogenation rate with the lowest amount of metal loss.

3.3 Supported Noble Metal Catalysts in 1-Heptyne Selective Hydrogenation

P. Argentiere *et al.* (2002) studied the supporting on γ -Al₂O₃ a palladium complex with chloride and tridecylamine as ligands. They found that it is possible to obtain an heterogeneous catalyst which is more active and selective for the 1-heptyne hydrogenation to 1-heptene than the classic Lindlar catalyst. At the same operational conditions, the supported palladium complex is also more active and selective than the same complex unsupported. The hydrogen pressure and the operational temperature showed to play an important role in the catalytic behavior of the catalysts under study. As determined by FTIR and X-ray photoelectron spectroscopy (XPS), the active species is the complex itself, which is stable under the reaction conditions. The obtained XPS results show that the palladium complex, supported or not, is tetra-coordinated, suggesting that its formula is [PdCl₂(NH₂(CH₂)₁₂CH₃)₂]. The highest activity and selectivity of the palladium supported complex can be attributed, at least partially, to electronic and geometrical effects.

Nijhuis *et al.* (2003) studied the silica-supported palladium catalysts for the selective liquid-phase hydrogenation of alkynes to alkenes. As a model reaction the hydrogenation of 3-methyl-1-pentyn-3-ol was chosen. The kinetics of this reaction was investigated. Different approaches were used to obtain an optimal catalyst system. The selectivity of the palladium catalysts was successfully improved by modifying the catalyst with copper and the effect of this modification on the reaction mechanism was studied. The addition of quinoline as a reaction modifier to the system was investigated as a manner to improve selectivity. Monolith supported catalysts were prepared to obtain a more convenient reactor configuration.

P. Argentiere *et al.* (2005) studied the catalytic behavior of Pd supported on γ -Al₂O₃ and on an activated pelletized carbon during the selective hydrogenation of 1-heptyne to 1-heptene under mild reaction conditions. They found that Pd/Al₂O₃ and Pd/C are good catalysts for this reaction, with the former showing better behavior. Under the same operating conditions, Pd/Al₂O₃ also presents a better performance than the classic Lindlar catalyst. The reduction and operating temperatures were found to play an important role in the catalytic behavior of the catalysts studied. The XPS results show that palladium in Pd/Al₂O₃ and Pd/C is electron-deficient. Within certain limits, the electron-deficient Pd species do not favor the further hydrogenation of 1-heptene to heptane, thus raising the selectivity to 1-heptene. The differences observed in the catalytic behavior of Pd/Al₂O₃ and Pd/C could be attributed, at least partially, to the differences in the support porosity.

E. Cagnola *et al.* (2006) studied the rhodium (I) complex containing chloro and hexylamine in the 1-heptyne semihydrogenation under mild conditions (303 K and 150 kPa) in homogeneous as well as heterogeneous systems using γ -alumina as support. Fourier transform infrared (FTIR) spectra indicate that the hexylamine molecule is one of the ligands present in the complex species. On the other hand, the analysis of the results of X-ray photoelectron spectroscopy (XPS) and elemental composition suggest that the complex is tetracoordinated with an empirical formula [RhCl(NH₂(CH₂)₅CH₃)₃], and that it attaches to the support and is not destroyed under reaction conditions. The absence of complex leaching from the supported catalyst was verified by XPS, atomic absorption analysis for Rh in solution, and catalyst reuse tests. When supported, the complex shows higher activity and selectivity than it does when it is unsupported, and also higher activity than the classic Lindlar catalyst used as a reference; this fact may be attributed, at least in part, to electronic and geometric effects.

3.4 Deactivation of Supported Pd Catalysts in Liquid-Phase Reaction

P. Albers *et al.* (2001) studied the major causes for deactivation such as particle growth, coke deposition and leaching. They found that the leaching of precious metal can be minimized by either improving the availability of hydrogen in the liquid reaction medium or by optimizing the catalyst side of the process. In term of modifying the catalyst site of the process two approaches are proposed (i) Using of smaller quantities of catalyst for reaction and/or (ii) decreasing the precious metal loading of catalyst. Unfavorable and undesired effect about sintering and agglomeration may be suppressed by means of adequate impregnation agents and procedures, temperature control and using suitable support materials.

R. G. Heidenreich *et al.* (2002) studied the parameter that influence the palladium leaching during and after Heck reactions of aryl bromides with olefins catalyzed by heterogeneous Pd on activated carbon systems. The results showed that the Pd concentration in solution correlated with the nature of the starting materials and products, the temperature, the solvent, the base and the atmosphere (argon and air). Lower temperature, higher concentration and stronger interaction of the bromoarenes with Pd⁰ clearly increase Pd leaching.

M. Besson and Pierre Gallezot (2003) reviewed the factors contributing to the deactivation of metal catalysts employed in liquid-phase reaction for the synthesis of fine or intermediate chemicals. The main causes of catalyst deactivation are particle sintering, metal and support leaching, deposition of inactive metal layers or polymeric species and poisoning by strongly adsorbed species. Leaching of metal atoms depends upon the reaction medium (pH, oxidation potential, chelating properties of molecules) and upon bulk and surface metal properties.

From literature reviews, Pd is the one of the most useful catalysts used in liquid-phase hydrogenation reaction. Furthermore types of solvent and support show the important roles in catalytic activity and catalyst deactivation. Catalyst deactivation such as leaching is the problem that usually occurs in these reactions.

CHAPTER IV

EXPERIMENTS

4.1 Catalyst Preparation

Catalyst supports used in this study are solvothermal-derived zinc aluminate, alumina, and zinc oxide calcined at various temperature are denoted as ZnAl₂O₄-as syn, ZnAl₂O₄-500, ZnAl₂O₄-700, ZnAl₂O₄-1150, Al₂O₃-as syn, Al₂O₃-700, Al₂O₃-1150, ZnO-as syn, ZnO-500, ZnO-700, and ZnO-1150, respectively.

4.1.1 Materials

The chemicals used in this study are specified as follows:

1. Aluminium Isopropoxide (AIP, [(CH₃)₂CHO]₃Al) available from Aldrich, 98%+
2. Zinc (II) acetylacetonate [CH₃COCH=C(O-)CH₃]₂Zn available from Merck, 95%+
3. Cobalt (II) acetylacetonate [CH₃COCH=C(O-)CH₃]₂Co available from Merck, 95%+
4. Copper (II) acetylacetonate [CH₃COCH=C(O-)CH₃]₂Zn available from Merck, 95%+
5. Toluene (C₆H₅CH₃) available from Carlo Erba Reagenti, 99.5%
6. Palladium (II) nitrate hydrate from Aldrich.
7. Heptyne (C₇H₁₂) available from Aldrich, 99.9%
8. Ethanol (C₂H₅OH) available from Aldrich, 99.9%
9. Zinc acetate (Zn(CH₃COO)₂H₂O) available from Aldrich, 98%+
10. Acetic acid (CH₃COOH) from Aldrich, 98%+
11. De-ionized water

4.1.2 Equipment

Zinc aluminate and alumina preparation by solvothermal method requires an autoclave reactor as shown in Figure 4.1 with the following specifications.

Autoclave reactor

- Made from stainless steel
- Volume of 200 cm³
- Maximum temperature of 350°C
- Pressure gauge in the range of 0-300 bar
- Relief valve used to prevent runaway reaction
- Test tube was used to contain the reagent and solvent
- A temperature program controller was connected to a thermocouple attached to the reagent in the autoclave.
- Electrical furnace (heater) supplied the required heat to the autoclave for the reaction.
- Nitrogen was set with a pressure regulator (0-150 bar) and needle valves are used to release gas from autoclave.

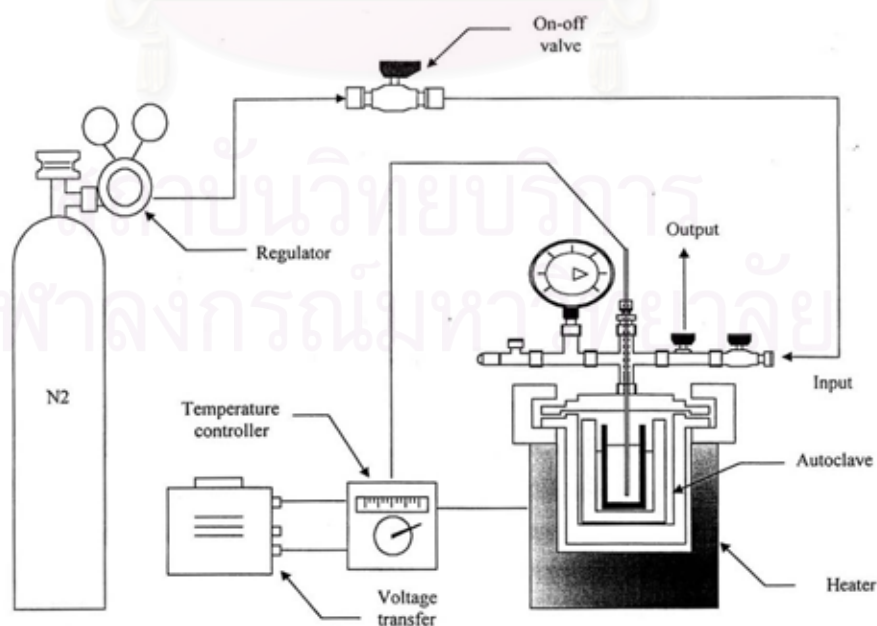


Figure 4.1 Autoclave reactor and gas controlling system

4.1.3 Synthesis of Zinc Aluminate

Zinc aluminate is used as catalyst support. In this experiment, Zinc aluminate is synthesized by solvothermal method. ZnAl_2O_4 was prepared by the mixture of aluminium isopropoxide, 15.0 g and appropriate amount of zinc (II) acetylacetonate (Zn/Al molar ratio = 0.5). The starting materials were suspended in 100 mL of toluene in a beaker, and then set up in 300 mL autoclave. In the gap between the beaker and autoclave wall, 40 mL of toluene was added. After the autoclave was completely purged with nitrogen, the suspension was heated to 300 °C at the rate of 2.5°C/min and held at that temperature for 2 h. However, the same synthesis method is performed at various holding temperatures. Autogenous pressure during the reaction gradually increased as temperature was raised. Then the autoclave was cooled to room temperature. Then the autoclave was cooled to room temperature. After the autoclave was cooled, the resulting products were washed repeatedly with methanol by centrifugation and dried in air. The calcination of the thus-obtained product carried out in a furnace. The product was heated at the rate of 10 °C/min to a desired temperature (400, 500, 700, 900, 1150 °C) and held at that temperature for 1 h.

4.1.4 Synthesis of Alumina

An appropriate amount of aluminum isopropoxide (AIP), approximately 25 g, was suspended in 100 mL of toluene in a beaker, and then set up in 300 mL autoclave. In the gap between the beaker and autoclave wall, 40 mL of toluene was added. After the autoclave was completely purged with nitrogen, the suspension was heated to 300 °C at the rate of 2.5°C/min. and held at that temperature for 2 h. However, the same synthesis method is performed at various holding temperatures. Autogenous pressure during the reaction gradually increased as temperature was raised. Then the autoclave was cooled to room temperature. Then the autoclave was cooled to room temperature. After the autoclave was cooled, the resulting products were washed repeatedly with methanol by centrifugation and dried in air. The calcination of the thus-obtained product carried out in a furnace. The product was heated at the rate of 10 °C/min to a desired temperature and held at that temperature for 1 h.

4.1.5 Synthesis of Zinc Oxide

Zinc oxide was prepared by solvothermal method as same as ZnAl_2O_4 and Al_2O_3 , but using only zinc (II) acetylacetonate as a reactant.

4.1.6 Palladium Loading

In this experiment, incipient wetness impregnation is the method used for loading palladium. $\text{Pd}(\text{NO}_3)_2$ was used as precursor.

The incipient wetness impregnation procedure is as following

1. The certain amount of palladium (1% loading) was introduced into the water which its volume equals to pore volume of catalyst.
2. Zinc aluminate support was impregnated with aqueous solution of palladium. The palladium solution was dropped slowly to the zinc aluminate support.
3. The catalyst was dried in room condition for 6 hr.
4. The catalyst was dried in the oven at 100°C overnight.
5. The catalyst was calcined in air at 400°C for 6 h.

4.2 The Reaction Study in Liquid-Phase Hydrogenation

The liquid-phase hydrogenation was used to study the characteristic and catalytic properties of these prepared catalysts. An alkyne such as heptyne was used as reactant. The organic solvent was used as reaction medium.

4.2.1 Instruments and Apparatus

The schematic diagram of liquid-phase hydrogenation is shown in Figure 4.2. The main instruments and apparatus are explained as follow:

The autoclave reactor:

The 50 ml stainless steel autoclave was used as reactor. Hot plate stirrer with magnetic bar was used to heat up the reactant and to ensure that the reactant and the catalyst were well mixed.

Gas chromatography:

A gas chromatography equipped with flame ionization detector (FID) with GS-alumina capillary column will be used to analyze the feed and product

4.2.2 Liquid-Phase Hydrogenation Procedure

The liquid-phase hydrogenation procedures consist of 2 steps.

1. Reduction step

Approximately 0.2 gram of supported Pd catalyst was placed in glass cell using Micromeritics ChemiSorb 2750 (pulse chemisorption system). Then the catalyst was reduced by the hydrogen gas at the volumetric flow rate of 50 ml/min at 150°C for 2 h.

2. Reactant preparation and hydrogenation step

2 ml of heptyne and 98 ml of toluene were mixed in the volumetric flask. Next 10 ml of the mixture was taken into the autoclave reactor. Afterward the reactor was filled with hydrogen. The liquid phase hydrogenation was carried out at 30 ° C for 10 minutes. After the reaction the vent valve was slowly opened to prevent the loss of product. Then the product mixture was analyzed by gas chromatography with flame ionization detector (FID) and the catalyst was characterized by several techniques.

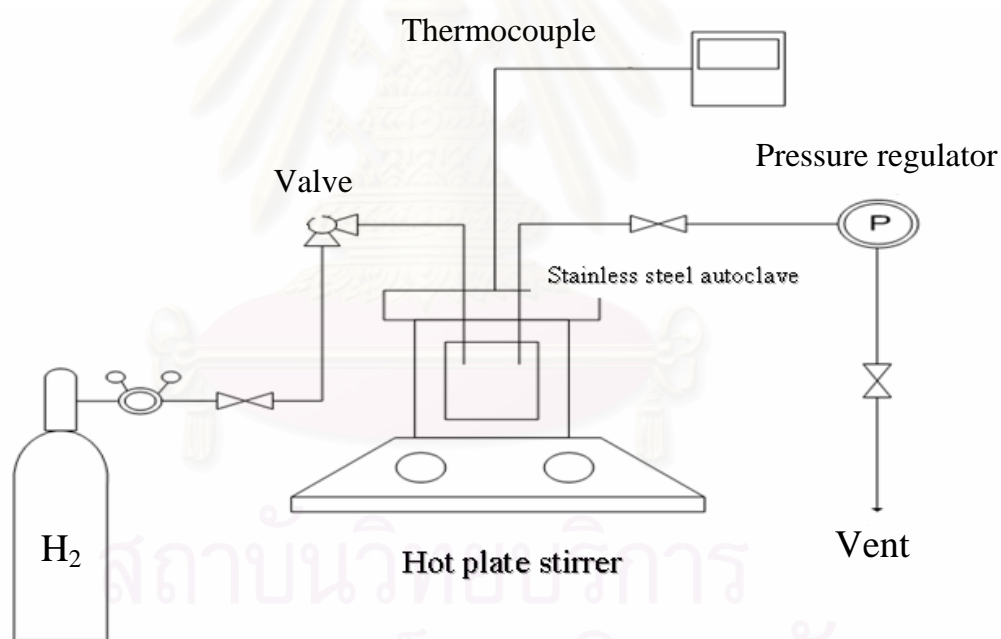


Figure 4.2 A schematic diagram of the liquid-phase hydrogenation system

4.3 Catalyst Characterization

The fresh and spent catalyst will be characterized by several techniques such as

4.3.1 N₂ Physisorption

The surface area of solid, pore volumes, average pore size diameters and pore size distribution were determined by physisorption of nitrogen (N₂) using Micromeritics ASAP 2020 (surface area and porosity analyzer)

4.3.2 X-Ray Diffraction (XRD)

The bulk crystal structure and chemical phase composition were determined by diffraction of an X-ray beam as a function of the angle of the incident beam. The XRD spectrum of the catalyst is measured by using a SIEMENS D5000 X-ray diffractometer and Cu K α radiation. The crystallite size was calculated from Scherrer's equation.

4.3.3 Transmission Electron Microscopy (TEM)

The morphology and crystallite size of the samples were observed by JEOL TEM-200cx Transmission Electron Microscope at the scientific and Technological Research Equipment Center, Chulalongkorn University (STREC).

4.3.4 CO-Pulse Chemisorption

The active sites and the relative percentage dispersions of palladium catalysts were determined by CO-pulse chemisorption technique using Micromeritics ChemiSorb 2750 (pulse chemisorption system).

4.3.5 X-Ray Photoelectron Spectroscopy (XPS)

The XPS spectra, the binding energy and the composition on the surface layer of the catalysts were determined by using a Kratos Amicus X-ray photoelectron spectroscopy. The analyses were carried out with these following conditions: Mg Ka X-ray source at current of 20 mA and 12 kV, 0.1 eV/step of resolution, and pass energy 75 eV and the operating pressure was approximately 1×10^{-6} Pa

4.3.6 Atomic Absorption Spectroscopy (AAS)

The bulk composition of palladium was determined using a Varian Spectra A800 atomic adsorption spectrometer at the Department of science service Ministry of science technology and environment.



สถาบันวิทยบริการ
จุฬาลงกรณ์มหาวิทยาลัย

CHAPTER V

RESULTS AND DISCUSSIONS

Supported noble metal catalysts are widely used in hydrogenation reactions. In this study the catalysts were prepared by impregnation method. The results and discussions in this chapter are divided into two parts. In the first part the characteristics and catalytic properties of catalysts prepared by impregnation method (Pd/ZnAl₂O₄, Pd/Al₂O₃, and Pd/ZnO) were investigated in selective 1-heptyne hydrogenation. The reaction was carried out at 30°C and pressure 1 bar. The catalysts were characterized by several techniques such as SEM, TEM, N₂ physisorption, XRD, XPS, and CO-pulse chemisorption. Furthermore, catalyst deactivations due to metal leaching were also investigated using AAS techniques. The second part describes the comparison of Pd catalysts on the solvothermal-derived supports and the commercial ones in 1-heptyne hydrogenation.

5.1 Pd Catalysts Supported on the Solvothermal-derived ZnAl₂O₄, Al₂O₃, and ZnO in 1-Heptyne Hydrogenation

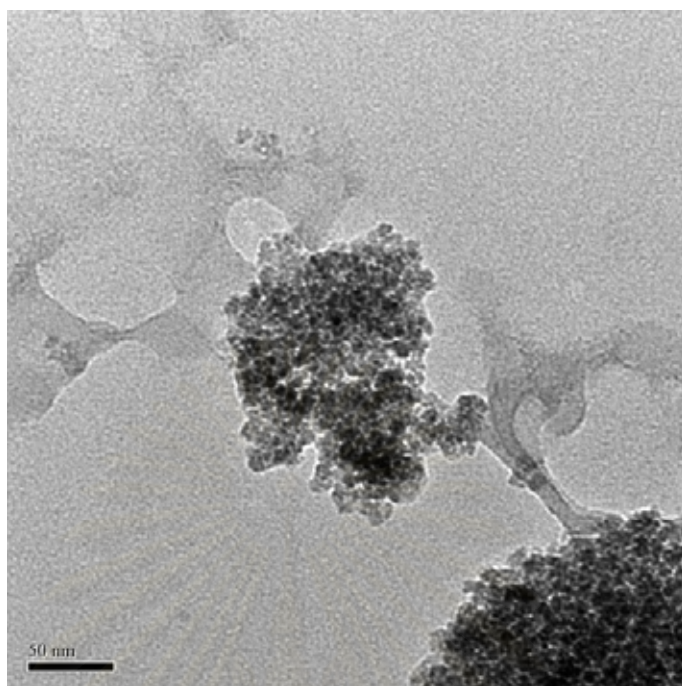
5.1.1 Characterization of the Catalysts

5.1.1.1 Transmission Electron Microscopy (TEM)

TEM micrographs were taken for zinc aluminate, alumina, and zinc oxide in order to physically measure the size of supports. TEM with diffraction modes were used to determine the crystallographic structure of the supports. The TEM micrographs results for zinc aluminate, alumina, and zinc oxide are shown in Figure 5.1, 5.2, and 5.3, respectively.

5.1.1.1.1 TEM Results of ZnAl₂O₄

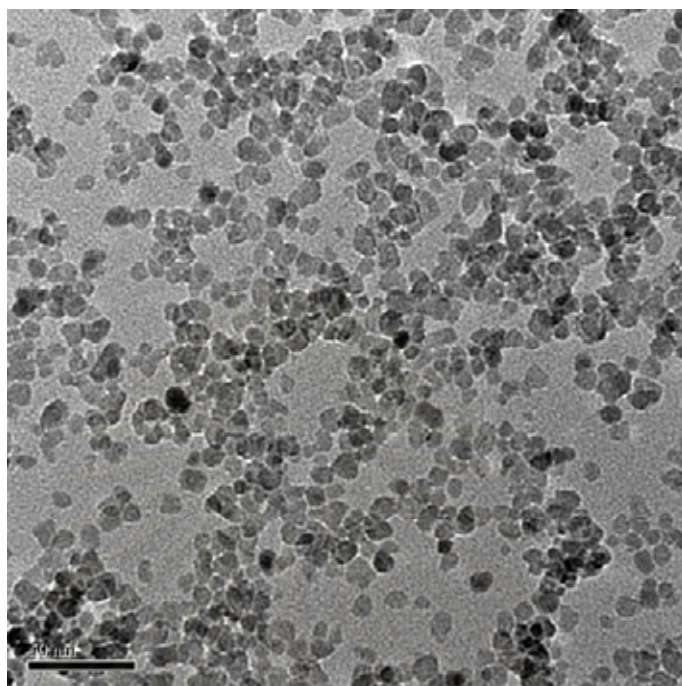
The morphology of solvothermally synthesized zinc aluminate as viewed by transmission electron microscope is shown in Fig. 5.1. It is revealed that the zinc aluminate-as syn is composed of many small particles with an average particle size of ca. 9 nm. It may be also noted from Fig. 1 that the corresponding selected area diffraction (SAD) patterns showing rings match d-spacings for the ZnAl₂O₄ confirm the structure of ZnAl₂O₄ (Ziolkowski *et al.*). After calcination with heat treatment, the particle sizes increased due to sintering of single particles. The particle size of zinc aluminate calcined at 500, 700, 900, 1150°C are 10, 16, 22, and 40 nm, respectively. The particle size is stable up to 500°C. These results confirmed the results of hydrothermal ZnAl₂O₄ preparation reported by Wrzyszc *et al.*. However, a solvothermal method usually produces single crystalline oxides, the large particles observed maybe the secondary particles formed by agglomeration of the primary nano-particles due to heat treatment during calcinations step. From the elemental diffraction results, they are revealed that ZnAl₂O₄-as syn and all ZnAl₂O₄ in calcined state are single crystalline.



(a)



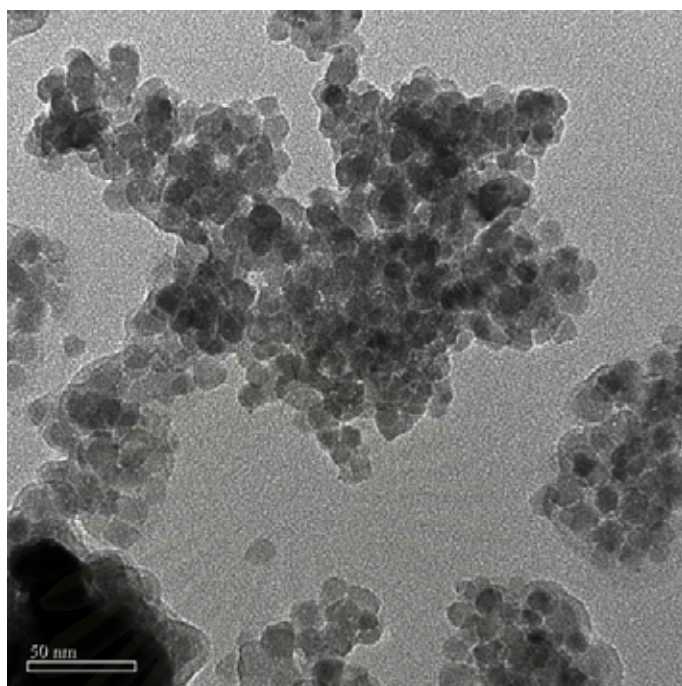
(b)



(c)



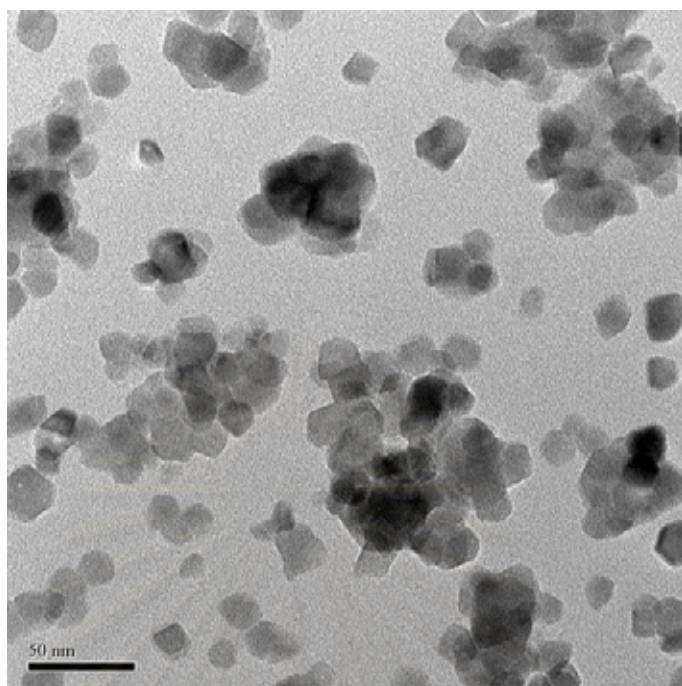
(d)



(e)



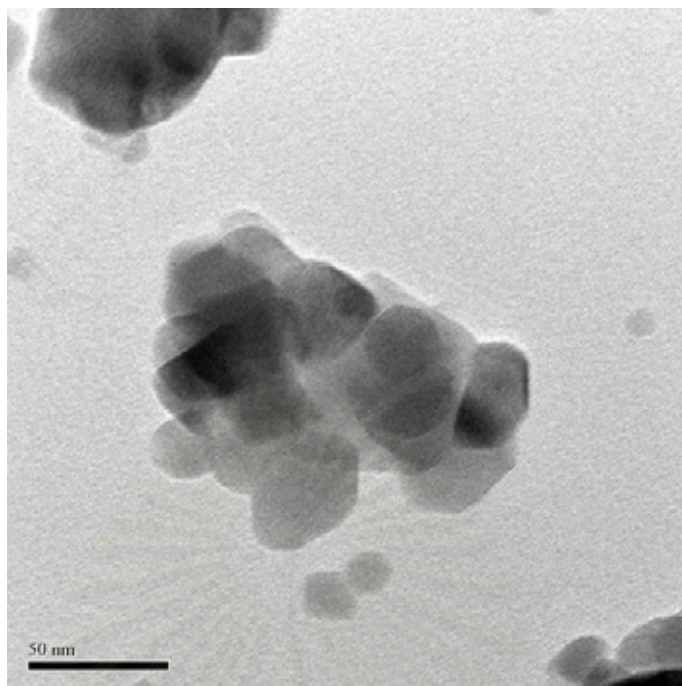
(f)



(g)



(h)



(i)



(j)

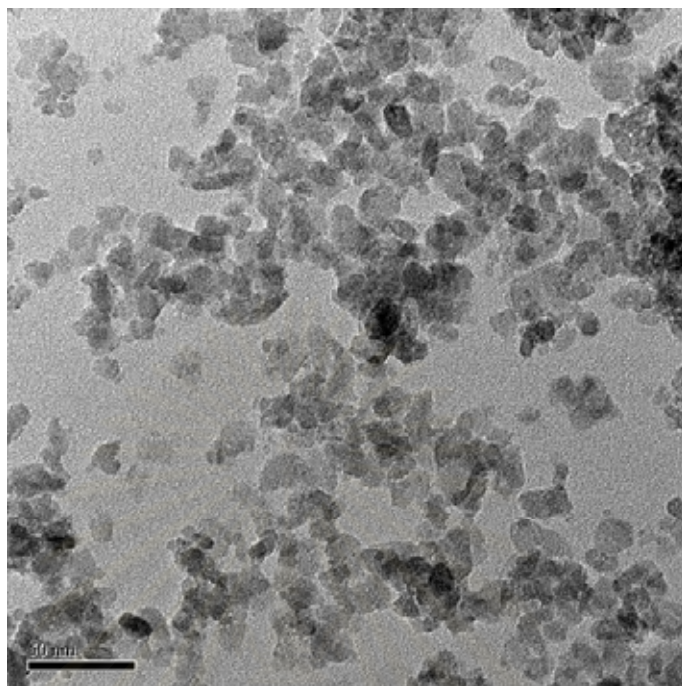
Figure 5.1 TEM micrographs and SAD patterns of ZnAl_2O_4 (a), (b) ZnAl_2O_4 -as syn, (c), (d) ZnAl_2O_4 -500, (e), (f) ZnAl_2O_4 -700, (g), (h) ZnAl_2O_4 -900, and (i), (j) ZnAl_2O_4 -1150

5.1.1.1.2 TEM Results of Al₂O₃

According to Figure 5.2, it is revealed that the alumina-as syn is composed of many small particles with an average particle size of ca. 10 nm. After calcination, the particle sizes increased due to sintering of single particles. The particle size of aluminate calcined at 700 and 1150°C are 20 and 80 nm, respectively. From the elemental diffraction results, it is revealed that the alumina-as syn, alumina-700, and alumina-1150 are single crystalline.



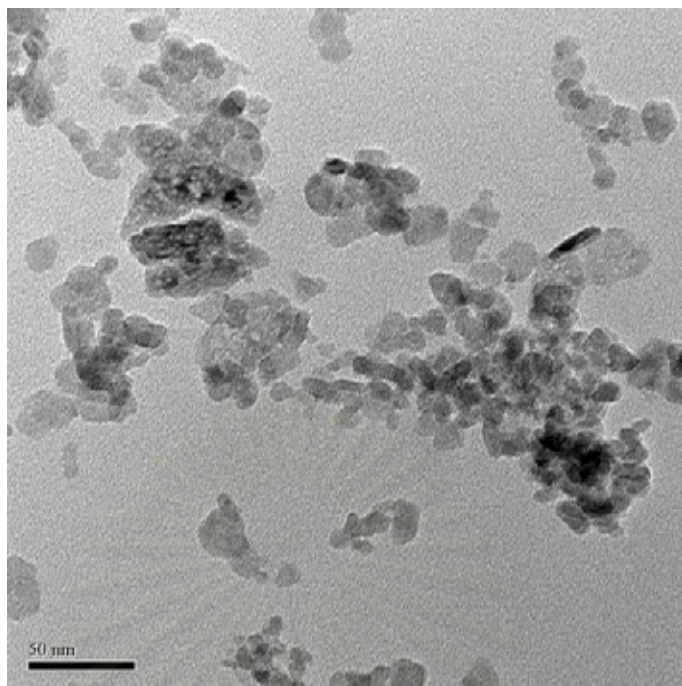
สถาบันวิทยบริการ
จุฬาลงกรณ์มหาวิทยาลัย



(a)



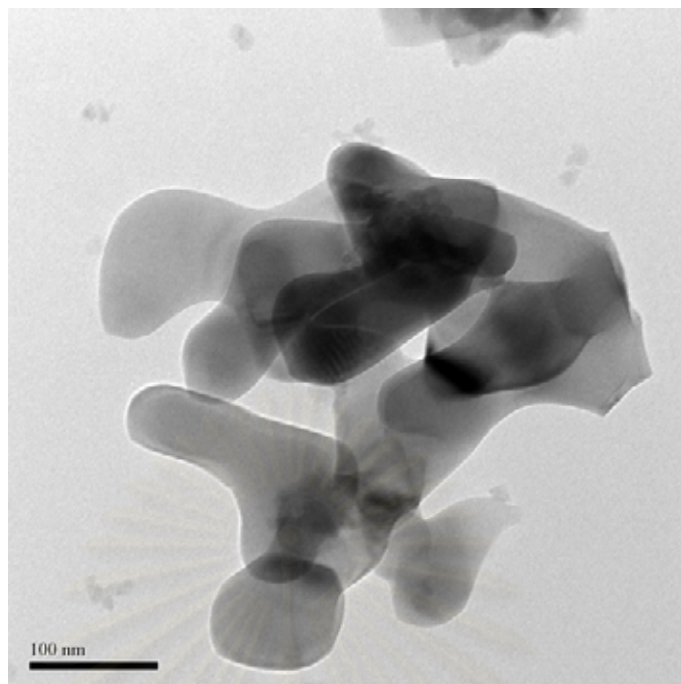
(b)



(c)



(d)



(e)



(f)

Figure 5.2 TEM micrographs and SAD patterns of Al₂O₃ of (a), (b) Al₂O₃-as syn, (c), (d) Al₂O₃-700, and (e), (f) Al₂O₃-1150

5.1.1.1.3 TEM Results of ZnO

According to Figure 5.3, it is revealed that the ZnO-as syn is quite large particles with an average particle size of ca. 120 nm.

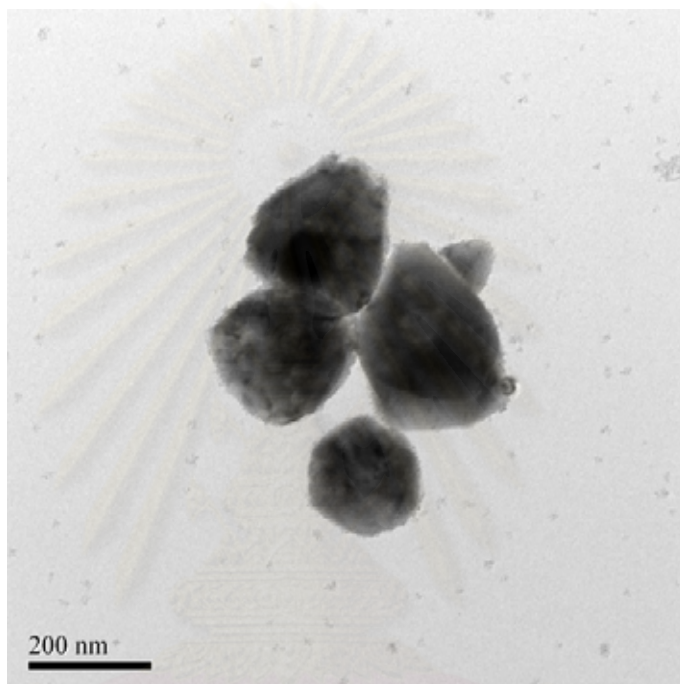


Figure 5.3 TEM micrographs of ZnO-as syn

สถาบันวิทยบริการ
จุฬาลงกรณ์มหาวิทยาลัย

5.1.1.2 N₂ Physisorption

BET surface areas, pore volumes, and pore diameters of zinc aluminate, zinc oxide, alumina, and supported Pd catalysts were determined by N₂ physisorption technique and are shown in Table 5.1, 5.2, and 5.3, respectively.

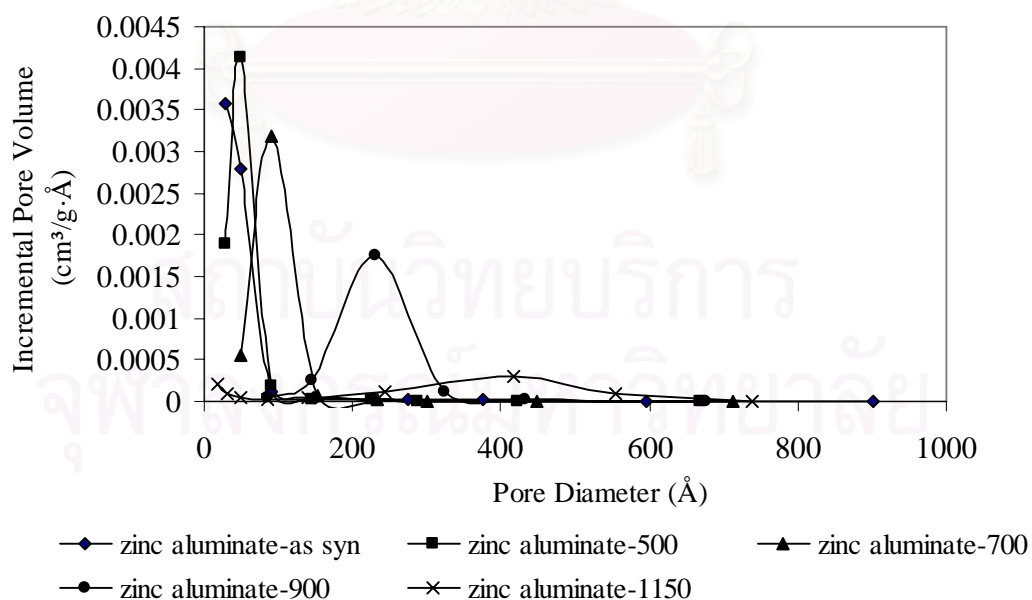
5.1.1.2.1 Surface Area and Pore Measurement of ZnAl₂O₄ Supports and Pd/ZnAl₂O₄ Catalysts

The pore size distributions of the zinc aluminate calcined at various temperatures are shown in Figure 5.4. It is indicated that the pores of as-syn and calcined zinc aluminate are meso-pores with average pore diameter around 2-50 nm. As shown in Table 5.1, BET surface areas of ZnAl₂O₄-as syn, ZnAl₂O₄-500, ZnAl₂O₄-700, ZnAl₂O₄-900, and ZnAl₂O₄-1150 were 130, 116, 63, 28, and 14 m²/g, and pore volumes were 0.17, 0.19, 0.20, 0.19, and 0.06 cm³/g, respectively. It is shown that BET surface areas of ZnAl₂O₄-as syn and ZnAl₂O₄-500 are slightly different whereas those of ZnAl₂O₄-700, ZnAl₂O₄-900, and ZnAl₂O₄-1150 dramatically decreased due to thermal sintering. It is suggested that the solvothermal derived zinc aluminate was stable up to 500° C. Moreover, it revealed that pore volumes of the zinc aluminate remained unchanged up to 900°C, but the pore sizes are increased in this temperature range. Such results suggest that the meso-pores of zinc aluminate are melted together during the heat treatment (Li *et al.*). When calcination temperature is above 900°C, the pore volume of zinc aluminate rapidly decreased, and the pore size distribution shifted toward larger size. All these changes in pore structure were attributed to the collapse of micro and meso pores caused by powder densification (Li *et al.*).

After Pd loading, BET surface areas of Pd/ZnAl₂O₄-as syn, Pd/ZnAl₂O₄-500, Pd/ZnAl₂O₄-700, Pd/ZnAl₂O₄-900, and Pd/ZnAl₂O₄-1150 were 106, 104, 66, 28, and 16 m²/g, and their pore volumes were 0.2, 0.21, 0.21, 0.18, 0.1 cm³/g, respectively. It can be seen that BET surface areas of the Pd catalysts slightly decreased; furthermore, there were no significant change in the average pore diameters and pore volume from their supports. Such results indicate that only a small amount of Pd was deposited in the pores of the zinc aluminate.

Table 5.1 N₂ physisorption properties of zinc aluminate supports and Pd catalysts

Samples	Surface Area (m ² /g)	N ₂ Physisorption	
		Pore Volume (cm ³ /g)	Avg. Pore Diameter(nm)
ZnAl ₂ O ₄ -as syn	130	0.18	4.2
ZnAl ₂ O ₄ -500	116	0.19	4.6
ZnAl ₂ O ₄ -700	63	0.2	8.5
ZnAl ₂ O ₄ -900	28	0.19	22.0
ZnAl ₂ O ₄ -1150	15	0.08	36.6
Pd/ZnAl ₂ O ₄ -as syn	106	0.2	4.6
Pd/ZnAl ₂ O ₄ -500	104	0.21	4.8
Pd/ZnAl ₂ O ₄ -700	66	0.21	8.9
Pd/ZnAl ₂ O ₄ -900	28	0.18	21.5
Pd/ZnAl ₂ O ₄ -1150	16	0.1	29.2

**Figure 5.4** Pore size distributions of zinc aluminate calcined at various temperatures

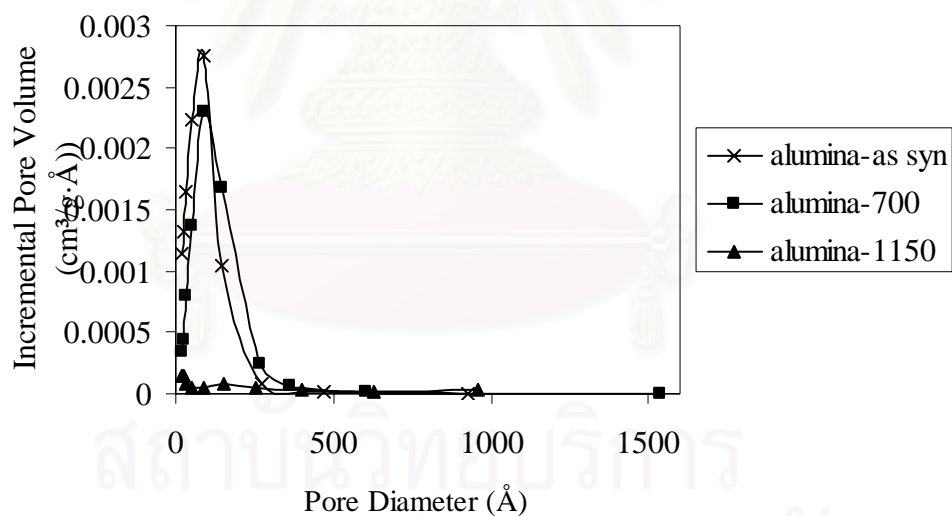
5.1.1.2.2 Surface Area and Pore Measurement of Al₂O₃ Supports and Pd/Al₂O₃ Catalysts

The pore size distributions of the alumina-as syn and those calcined at 700, 1150°C are shown in Figure 5.5. The BET surface areas, pore volumes, and pore diameters of the alumina are shown in Table 5.2. The BET surface areas of Al₂O₃-as syn, Al₂O₃-700, and Al₂O₃-1150 are 170, 133, and 11 m²/g, and pore volume are 0.39, 0.41, and 0.05 cm³/g, respectively. It is shown that the pore size distributions shifted toward larger size, and pore volume as well as BET surface areas diminished at higher calcinations temperature. Nevertheless, the BET surface areas and pore volumes of Al₂O₃-as syn and Al₂O₃-700 are slightly different whereas those of Al₂O₃-1150 dramatically decreased due to thermal sintering as well as pore collapse. Moreover, it is indicated that the pores of various alumina are meso-pores with average pore diameter around 5-20 nm. These results were similar to those of ZnAl₂O₄.

Moreover, it can be seen that BET surface area, pore volume, and average pore sizes of Pd catalysts prepared from Al₂O₃ supports slightly diminished in the same as those of the Pd/ZnAl₂O₄. The BET surface areas of Pd/Al₂O₃-as syn, Pd/Al₂O₃-700, and Pd/Al₂O₃-1150 are 152, 116, and 10 m²/g, and their pore volumes are 0.29, 0.33, and 0.05 cm³/g, respectively.

Table 5.2 N₂ physisorption properties of alumina supports and Pd catalysts

Samples	Surface Area (m ² /g)	N ₂ Physisorption	
		Pore Volume (cm ³ /g)	Avg. Pore Diameter(nm)
Al ₂ O ₃ -as syn	170	0.39	6.4
Al ₂ O ₃ -700	133	0.41	8.2
Al ₂ O ₃ -1150	11	0.05	14.5
Pd/Al ₂ O ₃ -as syn	152	0.29	5.2
Pd/Al ₂ O ₃ -700	116	0.33	6.6
Pd/Al ₂ O ₃ -1150	10	0.05	17.3

**Figure 5.5** Pore size distributions of alumina calcined at various temperatures

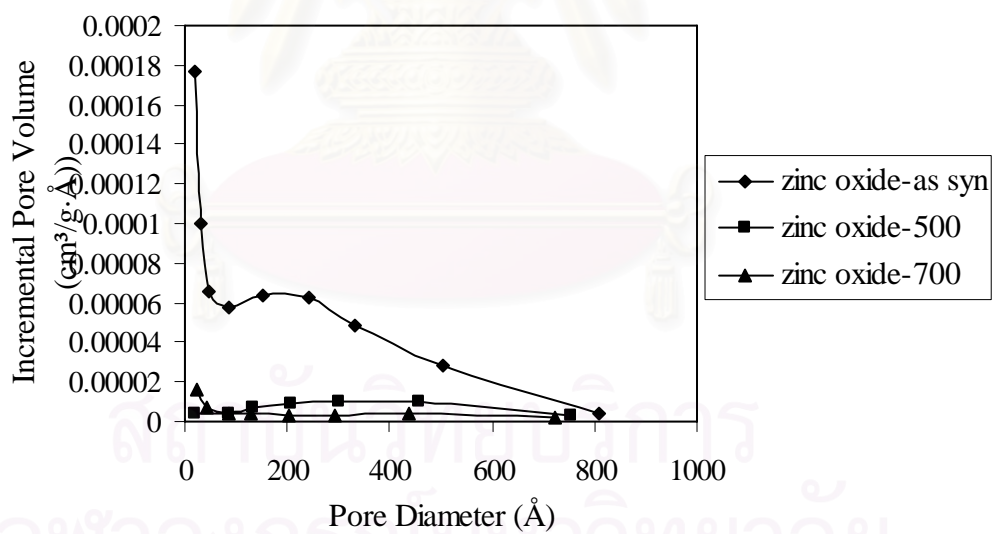
5.1.1.2.3 Surface Area and Pore Measurement of ZnO Supports and Pd/ZnO Catalysts

The pore size distributions of the zinc oxide calcined at various temperatures are shown in Figure 5.6. It is indicated that the pores of as-syn and calcined zinc oxide are meso-pores with average pore size around 10-30 nm. As shown in Table 5.3, the BET surface areas of ZnO-as syn, ZnO-500, ZnO-700, and ZnO-1150 were 11, 5, 3, and 0.13 m^2/g , respectively. The pore volumes of ZnO-as syn, ZnO-500, and ZnO-700 were 0.036, 0.008, 0.004 cm^3/g , respectively. For ZnO-1150, no pores were observed. These results suggested that the meso pores of zinc oxide were totally collapsed at calcinations temperature about 1150°C . It can be obviously seen that BET surface area and pore volumes zinc oxide dramatically decreased with increasing calcinations temperature; in the other hand, average pore sizes increased. These changes in pore structure were attributed to the collapse of micro and meso pores.

After Pd loading, it can be seen that BET surface area, pore volume, and average pore sizes of Pd catalysts prepared from ZnO supports slightly diminished in the same as those of the Pd/ZnAl₂O₄ and Pd/Al₂O₃. The BET surface areas of Pd/ZnO-as syn, Pd/ZnO-500, Pd/ZnO-700, and Pd/ZnO-1150 are 9, 5.2, 3.3, and 0.086 m^2/g , and their pore volumes are 0.026, 0.01, 0.005, and n.d. cm^3/g , respectively.

Table 5.3 N₂ physisorption properties of zinc oxide supports and Pd catalysts

Samples	Surface Area (m ² /g)	N ₂ Physisorption	
		Pore Volume (cm ³ /g)	Avg. Pore Diameter (nm)
ZnO-as syn	11	0.036	10.9
ZnO-500	5	0.008	23.9
ZnO-700	3	0.004	26.9
ZnO-1150	0.13	-	-
Pd/ZnO-as syn	9	0.026	12.6
Pd/ZnO-500	5.2	0.01	16.8
Pd/ZnO-700	3.3	0.005	21.9
Pd/ZnO-1150	0.086	-	-

**Figure 5.6** Pore size distributions of zinc oxide calcined at various temperatures

5.1.1.3 X-Ray Diffraction (XRD)

Bulk crystal structure and chemical phase composition of a crystalline material having crystal domains of greater than 3-5 nm can be detected by diffraction of an X-ray beam as a function of the angle of the incident beam. The measurements were carried out at the diffraction angles (2θ) between 10° and 80° . Broadening of the diffraction peaks were used to estimate crystallite diameter from Scherrer Equation.

5.1.1.3.1 X-Ray Diffraction (XRD) Patterns of ZnAl_2O_4 , Al_2O_3 , and ZnO Supports

The XRD patterns of ZnAl_2O_4 , Al_2O_3 , and ZnO supports calcined at various temperatures were carried out at the diffraction angles (2θ) between 10° and 80° , and are shown in Figure 5.7, 5.8, and 5.9, respectively. There were significant differences in ZnAl_2O_4 and Al_2O_3 supports, but no indicative different in ZnO support. According to the Table 5.4, the ZnAl_2O_4 -as syn has a small crystallite size and low crystalline in spinel phase. After it was calcined at higher temperature, the crystallite size grew much more. In the same way, Al_2O_3 -as syn has low crystalline chi-phase, but it appears to be more crystalline if it is calcined at higher temperature. The Al_2O_3 -700 appears to be the chi phase such as Al_2O_3 -as syn as reported by Mekasuvandumrong *et al.*, and Al_2O_3 -1150 is the alpha alumina. The ZnO revealed the same result as before. In addition, the ZnO-as syn evidenced high crystallinity before calcination.

5.1.1.3.2 X-Ray Diffraction (XRD) Patterns of Supported Pd Catalysts

The XRD patterns of the Pd/ ZnAl_2O_4 , Pd/ Al_2O_3 , and Pd/ZnO prepared by impregnation method in the calcined state are shown in Figure 5.10, 5.11, and 5.12, respectively. The XRD characteristic peak for Pd at 2θ of 40.2° was observed only for the Pd/ Al_2O_3 -1150 catalysts. XRD characteristic peaks for PdO at 2θ of 33.8 and less so at 42.0 , 54.8 , 60.7 , and 71.4° were not observed for all the prepared catalysts suggesting that Pd was probably highly dispersed and its average particle size was smaller than XRD detectable limit. The average Pd crystallite sizes on Pd/ Al_2O_3 -1150

were calculated from the full width at half maximum of the XRD peak at $40.2^\circ 2\theta$ using Scherrer's equation (Klug and Alexander) to be 5.9 nm and are shown in Table 5.4.

Table 5.4 Crystallite sizes of supports and catalysts

Catalysts	Crystallite size (nm)	
	Pd	Support
Pd/ZnAl ₂ O ₄ -as syn	n.d.*	8.2
Pd/ZnAl ₂ O ₄ -300	n.d.	8.7
Pd/ZnAl ₂ O ₄ -400	n.d.	8.8
Pd/ZnAl ₂ O ₄ -500	n.d.	9.0
Pd/ZnAl ₂ O ₄ -700	n.d.	10.9
Pd/ZnAl ₂ O ₄ -900	n.d.	17.6
Pd/ZnAl ₂ O ₄ -1150	n.d.	33.3
Pd/Al ₂ O ₃ -as syn	n.d.	8.1
Pd/Al ₂ O ₃ -700	n.d.	12.6
Pd/Al ₂ O ₃ -1150	5.9	77.1
Pd/ZnO-as syn	n.d.	66.6
Pd/ZnO-500	n.d.	67.0
Pd/ZnO-700	n.d.	80.5
Pd/ZnO-1150	n.d.	90.3

* n.d. = not determined

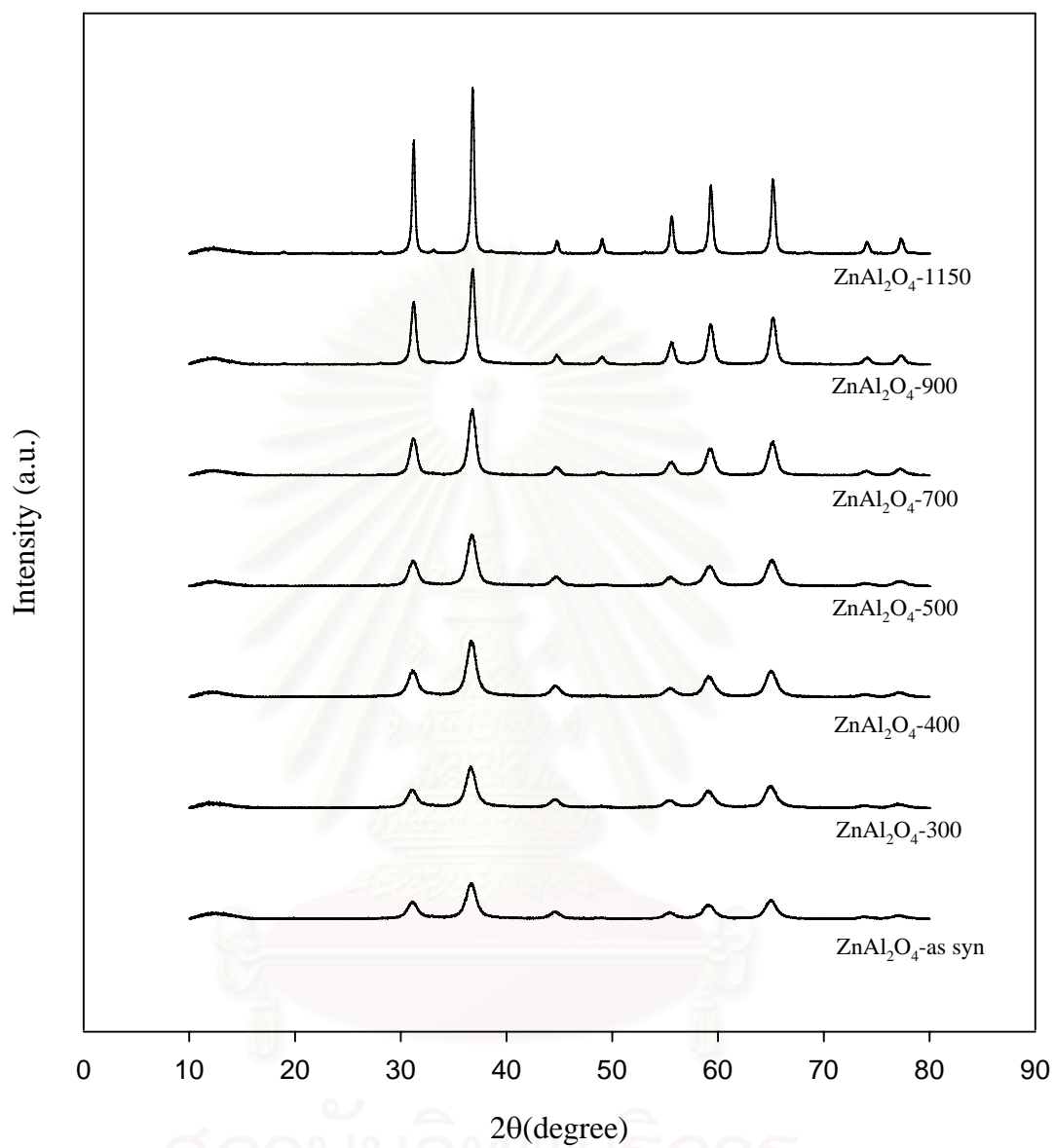


Figure 5.7 XRD patterns of ZnAl₂O₄ calcined at various temperatures

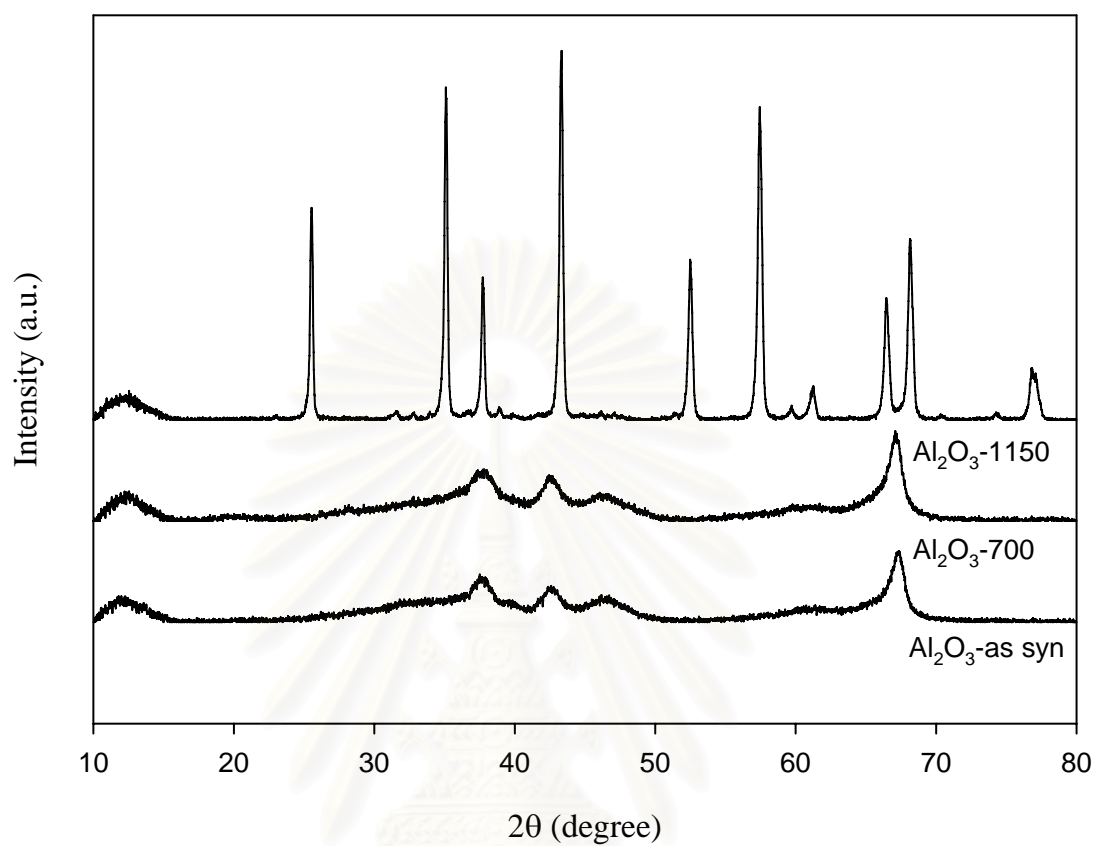


Figure 5.8 XRD patterns of Al_2O_3 calcined at various temperatures

สถาบันวิทยบริการ
จุฬาลงกรณ์มหาวิทยาลัย

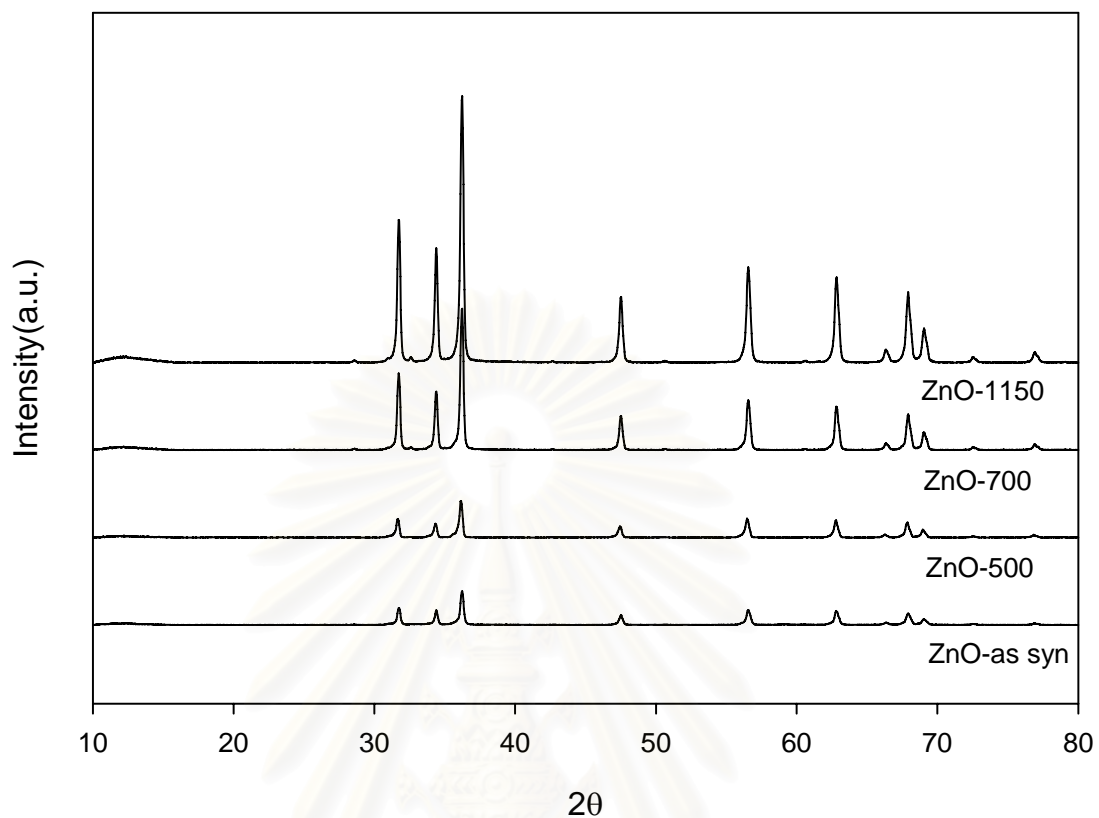


Figure 5.9 XRD patterns of ZnO calcined at various temperatures

สถาบันวิทยบริการ
จุฬาลงกรณ์มหาวิทยาลัย

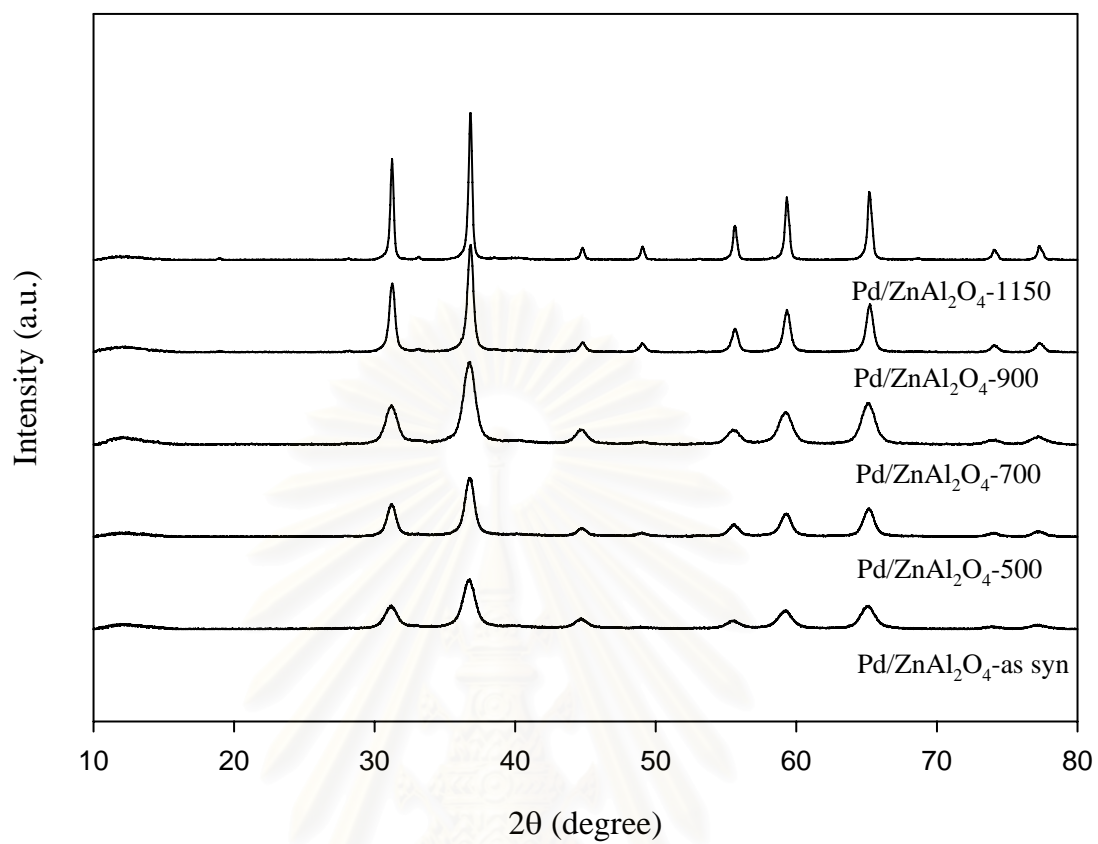


Figure 5.10 XRD patterns of Pd/ZnAl₂O₄ calcined at various temperatures

สถาบันวิทยบริการ
จุฬาลงกรณ์มหาวิทยาลัย

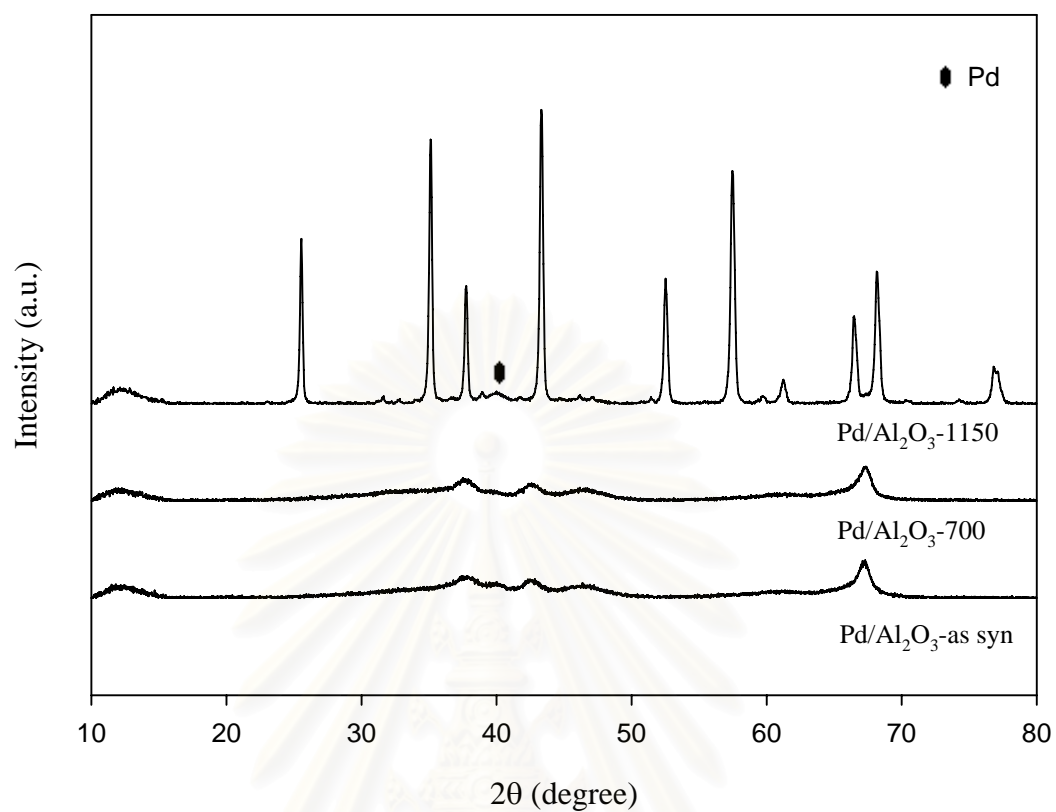


Figure 5.11 XRD patterns of Pd/Al₂O₃ calcined at various temperatures

สถาบันวิทยบริการ
จุฬาลงกรณ์มหาวิทยาลัย

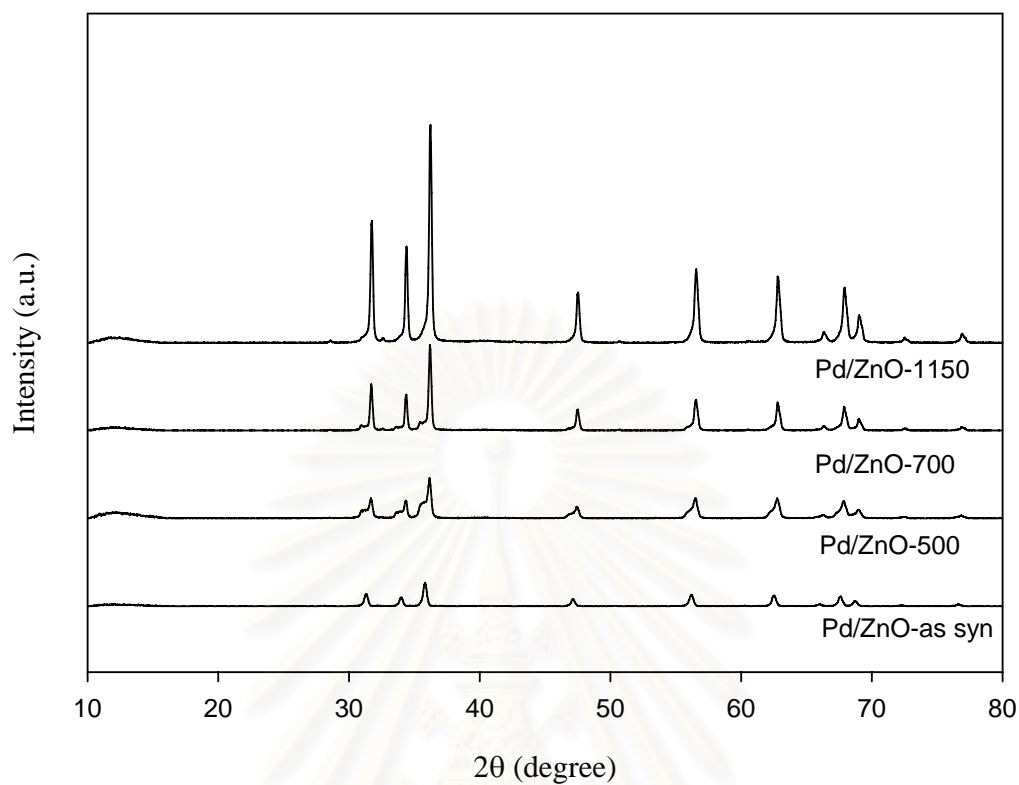


Figure 5.12 XRD patterns of Pd/ZnO calcined at various temperatures

สถาบันวิทยบริการ
จุฬาลงกรณ์มหาวิทยาลัย

5.1.1.4 X-Ray Photoelectron Spectroscopy (XPS)

Surface compositions of the catalysts were analyzed using a Kratos Amicus X-ray photoelectron spectroscopy. The XPS analysis were carried out with following conditions: Mg Ka X-ray source at current of 20 mA and 12 keV, resolution 0.1 eV/step, and pass energy 75 eV. The operating pressure is approximately 1×10^{-6} Pa.

A survey scan was performed in order to determine the elements on the catalyst surface. The elemental scan was carried out for C 1s, O 1s, Zn 2p, Al 2s, and Pd 3d. Binding energies of each element was calibrated internally with carbon C 1s at 285.0 eV. Photoemission peak areas are determined by using a linear routine. Deconvolution of complex spectra are done by fitting with Gaussian (70%)–Lorentzian (30%) shapes using a VISION 2 software equipped with the XPS system.

The percentages of atomic concentration for Zn 2p, Al 2p, O 1s and Pd 3d are given in Table 5.5. The atomic ratios of Zn/Pd for the zinc aluminate supported Pd catalysts are constant for the calcinations temperature of zinc aluminate up to 900°C, and significantly decreased for the Pd/ZnAl₂O₄-1150 catalyst. Furthermore, the atomic ratios of Al/Pd for the alumina supported Pd catalysts drastically decreased when using alumina calcined at higher temperature as the support. Although, the average pore sizes of Pd/ZnAl₂O₄-1150 and Pd/Al₂O₃-1150 catalysts are larger than those of the catalysts with supports was calcined at lower temperature, the Zn/Pd and Al/Pd ratios were lower suggesting that most of the palladium existed on the outer surface than inside the pore of supports. It can also be suggested that the pores of ZnAl₂O₄-1150 and Al₂O₃-1150 were collapsed. Besides, it can be seen obviously that the Zn/Pd ratio of Pd/ZnO-1150 catalyst is very low because there were almost no pores in the ZnO-1150. Furthermore, from Table 5.6 and 5.7, it was found that no electronic effects were observed among all the prepared catalysts.

Table 5.5 Atomic concentrations of catalysts from XPS

Catalysts	Atomic Concentration (%)				Zn/Pd	Al/Pd
	Zn 2p	Al 2s	O 1s	Pd 3d		
Pd/ZnAl ₂ O ₄ -500	10.8	22.29	66.68	0.22	49.1	101.3
Pd/ZnAl ₂ O ₄ -700	8.23	22.76	68.84	0.16	51.4	142.3
Pd/ZnAl ₂ O ₄ -900	7.12	25.37	67.39	0.13	54.8	195.2
Pd/ZnAl ₂ O ₄ -1150	4.73	26.11	69.01	0.15	31.5	174.1
Pd/Al ₂ O ₃ -as syn	-	27.79	72.2	0.01	-	2779.0
Pd/Al ₂ O ₃ -1150	-	31.23	68.64	0.13	-	240.2
Pd/ZnO-1150	14.34	-	83.1	2.56	5.6	-

Table 5.6 Binding energy position (eV) of catalysts from XPS

Catalysts	Position BE (eV)			
	Zn 2p	Al 2s	O 1s	Pd 3d
Pd/ZnAl ₂ O ₄ -500	1021.7	119.0	531.3	329.0
Pd/ZnAl ₂ O ₄ -700	1025.6	122.5	534.7	334.0
Pd/ZnAl ₂ O ₄ -900	1022.4	119.2	531.6	330.4
Pd/ZnAl ₂ O ₄ -1150	1022.2	119.2	531.4	335.2
Pd/Al ₂ O ₃ -as syn	n.d	120.6	532.7	331.1
Pd/Al ₂ O ₃ -1150	n.d.	119.2	531.6	336.1
Pd/ZnO-1150	1022.3	n.d.	532.0	335.3

* n.d. = not determined

Table 5.7 Full width of half maximum (eV) of catalysts from XPS

Catalysts	FWHM (eV)			
	Zn 2p	Al 2s	O 1s	Pd 3d
Pd/ZnAl ₂ O ₄ -500	3.04	3.11	3.22	2.74
Pd/ZnAl ₂ O ₄ -700	2.94	2.99	3.44	2.28
Pd/ZnAl ₂ O ₄ -900	2.67	2.82	2.92	1.17
Pd/ZnAl ₂ O ₄ -1150	2.30	2.33	2.56	1.28
Pd/Al ₂ O ₃ -as syn	n.d	2.89	3.17	0.42
Pd/Al ₂ O ₃ -1150	n.d.	2.43	2.63	1.41
Pd/ZnO-1150	2.05	n.d.	2.96	1.43

* n.d. = not determined

5.1.1.5 CO-Pulse Chemisorption

Chemisorption is the relatively strong, selective adsorption of chemically reactive gases on available metal sites or metal oxide surfaces at relatively higher temperatures (i.e. 25-400°C); the adsorbate-adsorbent interaction involves formation of chemical bonds and heats of chemisorption in the order of 50-300 kJ mol⁻¹.

Since H₂ chemisorption on Pd bridge bonding may occur so there is no precise ratio of atom to Pd metal surface. H/Pd stoichiometry may be varied from 1, 1/2 or 1/3. However, for CO chemisorption, CO/Pd stoichiometry is normally equal to 1. Exposed active surface areas of Pd of the catalysts were calculated from the irreversible pulse CO chemisorption technique based on the assumption that one carbon monoxide molecule adsorbs on one palladium site (Mahata and Vishwanathan, Ali and Goodwin, Sales *et al.*, Sarkany *et al.*, and Nag). The amounts of CO chemisorption on the catalysts are given in Table 5.6. For the Pd/ZnAl₂O₄ catalysts, the amounts of CO chemisorption on Pd active sites seem to be not significantly different; despite the BET surface areas drastically decreased at higher calcinations temperature. However, for the Pd/Al₂O₃ catalysts, the amounts of CO chemisorption on Pd active sites decreased with decreasing of BET surface area of supports, and this result was similar to the Pd/ZnO catalysts. For Pd/ZnO-1150 catalyst, the active sites were not found from the amounts of CO chemisorption. It should be noted that all the Pd/ZnAl₂O₄ have the similar Pd crystallite size. The Pd crystallite size of Pd/Al₂O₃ significantly increased with calcinations temperature of Al₂O₃ above 700°C. For the Pd/ZnO catalysts, Pd crystallite size grew up when temperature above 500°C.

Table 5.8 CO- pulse chemisorption results

Catalysts	Active sites (10^{18} sites/g _{catalyst})	% dispersion	Avg. crystallite size of Pd (nm)
Pd/ZnAl ₂ O ₄ -as syn	7.36	13	7.82
Pd/ZnAl ₂ O ₄ -500	7.44	13	7.78
Pd/ZnAl ₂ O ₄ -700	7.23	13	7.43
Pd/ZnAl ₂ O ₄ -900	7.25	13	7.98
Pd/ZnAl ₂ O ₄ -1150	8.68	15	6.67
Pd/Al ₂ O ₃ -as syn	12.73	23	2.12
Pd/Al ₂ O ₃ -700	12.60	22	2.26
Pd/Al ₂ O ₃ -1150	8.21	15	7.05
Pd/ZnO-as syn	3.36	6	17.25
Pd/ZnO-500	2.26	4	27.35
Pd/ZnO-700	0.96	2	59.75
Pd/ZnO-1150	-	-	-

5.1.2 Reaction Study in 1-Heptyne Hydrogenation

The catalytic properties of the catalysts prepared on three different supports were investigated in selective hydrogenation of 1-heptyne. The reaction was carried out in toluene solvent at 30°C and 1 bar H₂ pressure. The substrate/toluene ratio was 1/49. The products are analyzed by gas chromatography with flame ionization (GC-FID) using GS-alumina column.

Hydrogenation activity and selectivity of all the catalysts are presented in Table 5.5. The hydrogenation activities of the Pd/ZnAl₂O₄-as syn, Pd/ZnAl₂O₄-500, Pd/ZnAl₂O₄-700, and Pd/ZnAl₂O₄-900 catalysts were not significantly different, but those of Pd/ZnAl₂O₄-1150 rapidly increased. These results were coincident with the amounts of CO chemisorption. The turnovers of frequencies (TOFs) were calculated using the number of surface metal atoms measured by CO-chemisorption and are given in Table 5.8. The TOFs of Pd/ZnAl₂O₄-as syn, Pd/ZnAl₂O₄-500, Pd/ZnAl₂O₄-700, Pd/ZnAl₂O₄-900, and Pd/ZnAl₂O₄-1150 were 0.24, 0.23, 0.22, 0.24, and 0.32 s⁻¹, respectively. It can be seen that there are no notable differences in TOFs. The TOFs results suggested that there was no pore diffusion limitation.

For the hydrogenation activities of the Pd/Al₂O₃ catalysts, the Pd/Al₂O₃-1150 is the most active. However, considering the amounts of CO chemisorption, it revealed that the Pd/Al₂O₃-as syn and Pd/Al₂O₃-700 have the amounts of CO chemisorption much higher than Pd/Al₂O₃-1150. The TOFs of Pd/Al₂O₃-as syn, Pd/Al₂O₃-700, and Pd/Al₂O₃-1150 were 0.08, 0.10, and 0.26 s⁻¹, respectively. According to previous studies (Marin-Astorga *et al.*), it is suggested that changes in the metal dispersion, i.e. different particle sizes, lead also to changes in TOFs and selectivity. Furthermore it has been reported that the specific activity decreased with decreasing metal particle size (Molnar *et al.*, Duca *et al.*, Carturan *et al.*, Sarkany *et al.*, Albers *et al.*, and Angel *et al.*), whereas others found that the TOFs increased upon increasing the metal dispersion (Duca *et al.*). Such results are consistent with this work that the TOFs of Pd/Al₂O₃-as syn and Pd/Al₂O₃-700 were less than those of the Pd/Al₂O₃-1150 due to its higher dispersion and smaller Pd crystallite size. Furthermore, it should be noted that this reaction is a structure-sensitive reaction.

For the Pd/ZnO catalysts, it was found that catalytic activities were primarily related to the amounts of CO chemisorption. From the performance curve in the Figure 5.13, the selectivity to 1-heptene of all catalysts is very high about 96 % even for 100 % of conversion. The selectivity to 1-heptene dropped very slightly when percentage of conversion increased. It suggests that all prepared catalysts are excellent in performance.

For comparison of the Pd/ZnAl₂O₄, Pd/Al₂O₃, and Pd/ZnO catalysts, the results revealed that the Pd/ZnAl₂O₄ and Pd/Al₂O₃ have almost identical activities and performance, especially Pd/ZnAl₂O₄-1150 and Pd/Al₂O₃-1150. Moreover, both catalysts show higher overall performance than Pd/ZnO catalysts.



สถาบันวิทยบริการ
จุฬาลงกรณ์มหาวิทยาลัย

Table 5.9 Results of 1-heptyne hydrogenation

Catalysts	Conversion (%)	Selectivity (%)	
		Selectivity to Heptene	Selectivity to Heptane
Pd/ZnAl ₂ O ₄ -as syn	52	97	3
Pd/ZnAl ₂ O ₄ -500	51	100	0
Pd/ZnAl ₂ O ₄ -700	45	100	0
Pd/ZnAl ₂ O ₄ -900	49	96	4
Pd/ZnAl ₂ O ₄ -1150	66	100	0
Pd/Al ₂ O ₃ -as syn	30	100	0
Pd/Al ₂ O ₃ -700	31	100	0
Pd/Al ₂ O ₃ -1150	59	100	0
Pd/ZnO-as syn	33	100	0
Pd/ZnO-500	48	100	0
Pd/ZnO-700	39	100	0
Pd/ZnO-1150	n.d.	n.d.	n.d.

* n.d. = not determined

สถาบันวิทยบริการ
จุฬาลงกรณ์มหาวิทยาลัย

Table 5.10 TOFs of various Pd catalysts

Catalysts	TOF(s ⁻¹)
Pd/ZnAl ₂ O ₄ -as syn	0.24
Pd/ZnAl ₂ O ₄ -500	0.23
Pd/ZnAl ₂ O ₄ -700	0.22
Pd/ZnAl ₂ O ₄ -900	0.24
Pd/ZnAl ₂ O ₄ -1150	0.32
Pd/Al ₂ O ₃ -as syn	0.08
Pd/Al ₂ O ₃ -700	0.10
Pd/Al ₂ O ₃ -1150	0.26
Pd/ZnO-as syn	0.35
Pd/ZnO-500	0.98
Pd/ZnO-700	1.45
Pd/ZnO-1150	n.d.

* n.d. = not determined

สถาบันวิทยบริการ
จุฬาลงกรณ์มหาวิทยาลัย

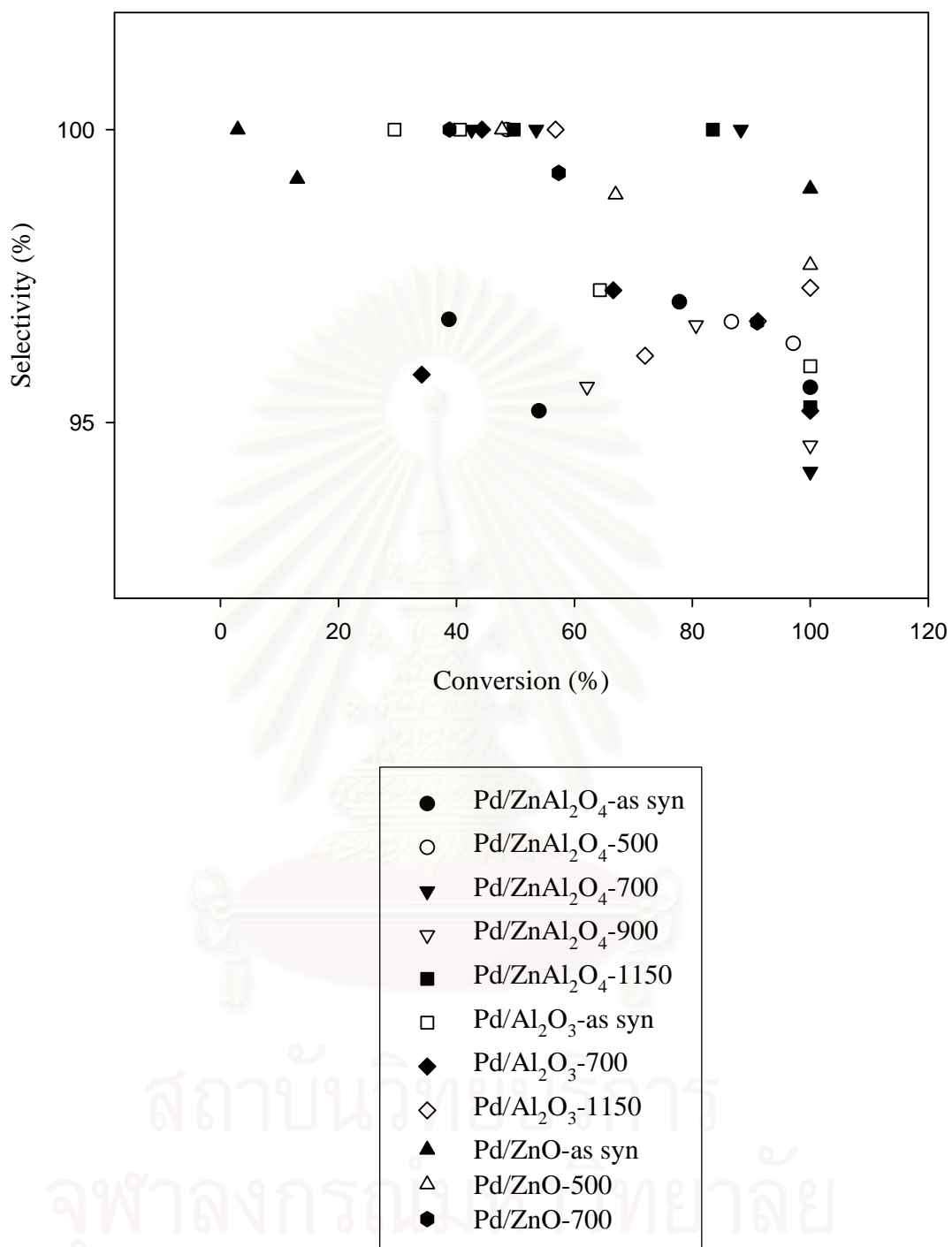


Figure 5.13 Performance curves of Pd/ZnAl₂O₄, Pd/Al₂O₃, Pd/ZnO catalysts in 1-heptyne hydrogenation

5.1.3 Catalyst Deactivation

Atomic absorption spectroscopy is a very common technique for quantitative measurement of atomic composition based on photon absorption of a vaporized aqueous solution prepared from the starting material.

The actual amounts of palladium loading before and after reaction determined by atomic adsorption spectroscopy are given in Table 5.9. The palladium loadings on the each catalyst are not similar values resulting from errors of preparation and measurement. The palladium loading on the fresh catalyst is about 1 wt.% and those on the spent catalysts are always lower than that on the fresh catalyst, meaning that palladium was leached in the course of the reaction. Leaching of active metal is another main cause of catalyst deactivation in liquid phase reaction. In general, it depends upon the reaction medium (pH, oxidation potential, chelating properties of molecules) and upon bulk and surface properties of the metal (Besson and Gallezot). For the Pd/ZnAl₂O₄, the percentages of Pd leached in the Pd/ZnAl₂O₄-as syn, Pd/ZnAl₂O₄-500, Pd/ZnAl₂O₄-700, and Pd/ZnAl₂O₄-900 catalysts were 36, 38, 30, and 35 %, respectively. It can be seen that percentages of Pd leaching is not significantly changed. On the other hand, the Pd/ZnAl₂O₄-1150 catalyst has only 8 % of the Pd leaching decreasing obviously from the Pd catalysts supported on the ZnAl₂O₄ calcined at lower temperature. It is suggested that Pd can be formed stably on the outer surface, and it can be attached strongly on the higher crystalline surface. According to the Pd/Al₂O₃ catalysts, they show that the Pd leaching were similar to the patterns of Pd leaching of Pd/ZnAl₂O₄ catalysts. For the Pd/ZnO catalysts, the Pd leaching was very low for all the catalysts because they are very high crystalline and have very little pore volume in all the Pd/ZnO catalysts. Furthermore, it should be noted that the smaller Pd crystallite sizes are more likely to be leached.

Table 5.11 The actual amounts of palladium loading and the percentage of Pd leaching

Catalysts	Amounts Pd of fresh catalysts (wt.%)	Pd leached (%)
Pd/ZnAl ₂ O ₄ -as syn	0.95	36
Pd/ZnAl ₂ O ₄ -500	0.94	38
Pd/ZnAl ₂ O ₄ -700	0.94	30
Pd/ZnAl ₂ O ₄ -900	1.2	35
Pd/ZnAl ₂ O ₄ -1150	1.2	8
Pd/Al ₂ O ₃ -as syn	1.2	27
Pd/Al ₂ O ₃ -700	1.2	25
Pd/Al ₂ O ₃ -1150	1.3	8
Pd/ZnO-as syn	1.1	9
Pd/ZnO-500	1.1	9
Pd/ZnO-700	1.2	8

5.2 Comparison of Pd Catalysts on the Solvothermal-derived Supports and the Commercial Ones in 1-Heptyne Hydrogenation

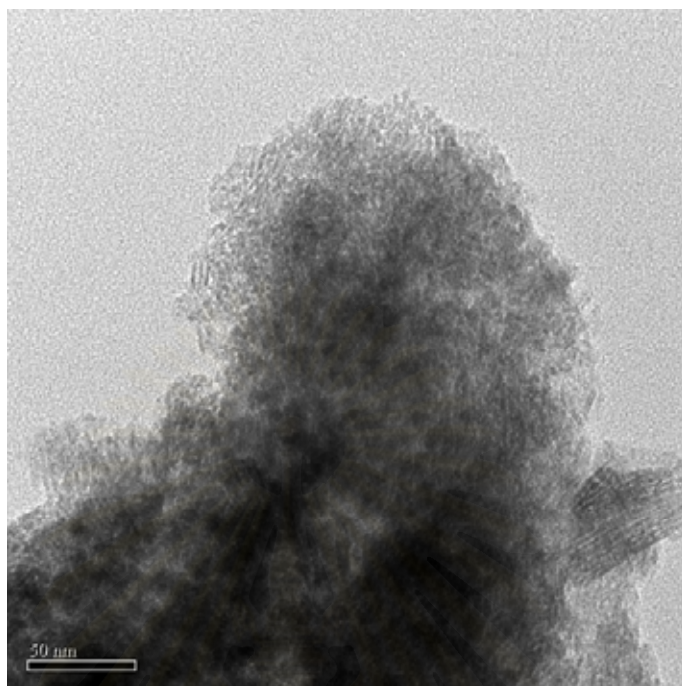
5.2.1 Characterization of the Commercial Catalysts

5.2.1.1 Transmission Electron Microscopy (TEM)

The morphology of commercial alumina as viewed by transmission electron microscope is shown in Fig. 5.14. It is revealed that the commercial gamma alumina is composed of many small particles with an average particle size of ca. 6 nm, and the average particle size of commercial alpha alumina is about 100 nm. Furthermore, from selected area diffraction (SAD) patterns, the commercial gamma alumina does not have any patterns indicating the single crystal pattern, while the commercial alpha alumina is single crystalline.



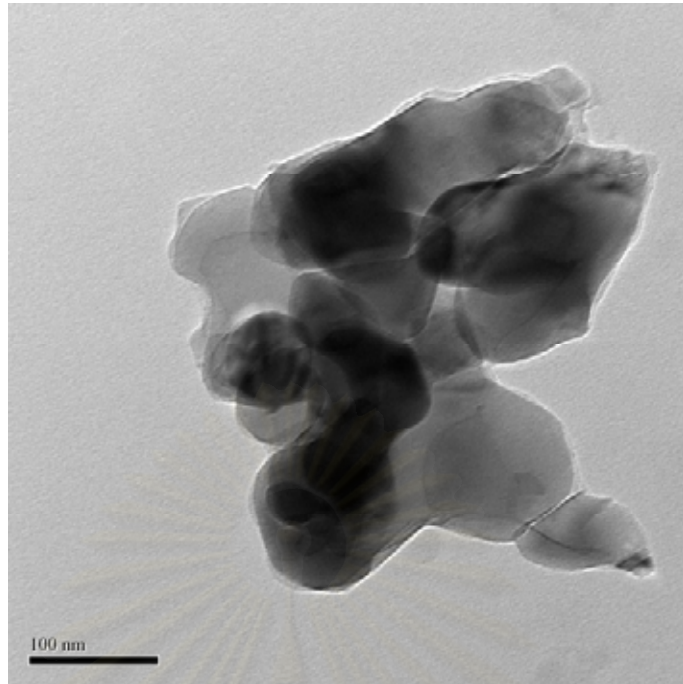
สถาบันวิทยบริการ
จุฬาลงกรณ์มหาวิทยาลัย



(a)



(b)



(c)



(d)

Figure 5.14 TEM micrographs and SAD patterns of commercial Al_2O_3 of (a), (b) Al_2O_3 -gamma com and (c), (d) Al_2O_3 -alpha com

5.2.1.2 N₂ Physisorption

The pore size distributions of the alumina-gamma com, alumina-alpha com, and silica-com are shown in Figure 5.15, 5.16, and 5.17, respectively, and BET surface areas, pore volumes and pore diameters of the commercial supports are shown in Table 5.12. It is indicated that alumina-gamma com composed of micro pores, meso pores, and macro pores, such as alumina-alpha com and silica-com. The BET surface area of Al₂O₃-gamma com, which is 282 m²/g, is much higher than Al₂O₃-as syn and Al₂O₃-700 which are also gamma alumina because of smaller pores of Al₂O₃-gamma com in micro size, and the total pore volumes are equal. According to Table 5.12, it is revealed that Al₂O₃-alpha com and Al₂O₃-1150, which is alpha phase, have almost equal surface areas, pore volume, and average pore sizes; however, from Figure 5.16, it shows that the pore size distribution of Al₂O₃-alpha com shifted toward smaller size. For the SiO₂-com, the BET surface area is 62 m²/g, as well as the pore volume and the average pore size diameter is about 0.17cm³/g and 11.5 nm, respectively.

For the supported Pd catalysts, it can be seen that BET surface areas, pore volumes, and average pore sizes of Pd catalysts prepared from Al₂O₃ supports slightly changed. The BET surface areas, pore volumes, and average pore sizes of Pd/Al₂O₃-gamma com, Pd/Al₂O₃-alpha com, and Pd/SiO₂-com are 268, 15, and 59 m²/g, 0.41, 0.07, and 0.23 cm³/g, and 4.6, 22.2, and 16.7 nm, respectively.

Table 5.12 N₂ physisorption properties of various supports and Pd catalysts

Samples	Surface Area (m ² /g)	N ₂ Physisorption	
		Pore Volume(cm ³ /g)	Avg. Pore Diameter(nm)
Al ₂ O ₃ -as syn	170	0.39	6.4
Al ₂ O ₃ -700	133	0.41	8.2
Al ₂ O ₃ -1150	11	0.05	14.5
Al ₂ O ₃ -gamma com	282	0.40	4.6
Al ₂ O ₃ -alpha com	14	0.06	13.1
SiO ₂ (com)	62	0.17	11.5
Pd/Al ₂ O ₃ -as syn	152	0.29	5.2
Pd/Al ₂ O ₃ -700	116	0.33	6.6
Pd/Al ₂ O ₃ -1150	10	0.05	17.3
Pd/Al ₂ O ₃ -gamma com	268	0.41	4.6
Pd/Al ₂ O ₃ -alpha com	15	0.07	22.2
Pd/SiO ₂ -com	59	0.23	16.7

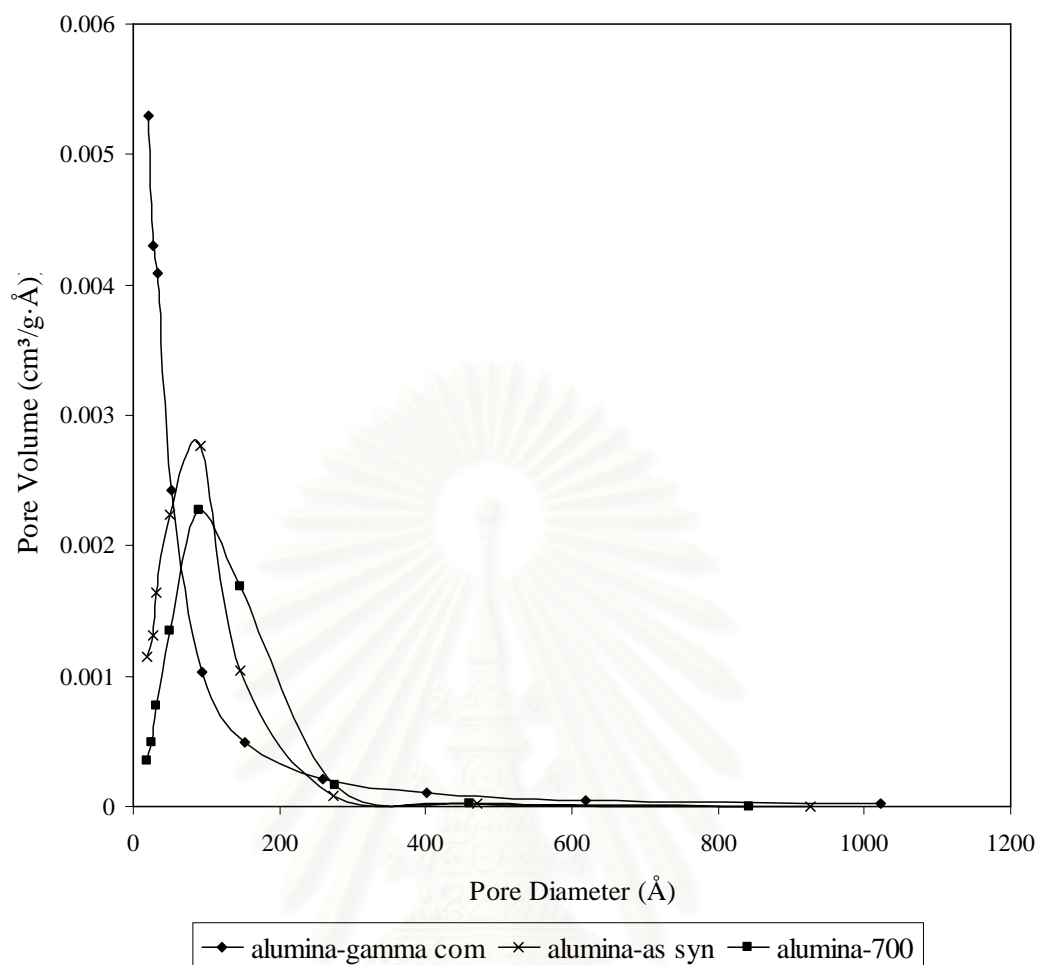


Figure 5.15 Pore size distributions of solvothermal-derived gamma Al_2O_3 and commercial gamma Al_2O_3

สถาบันวิทยบริการ
จุฬาลงกรณ์มหาวิทยาลัย

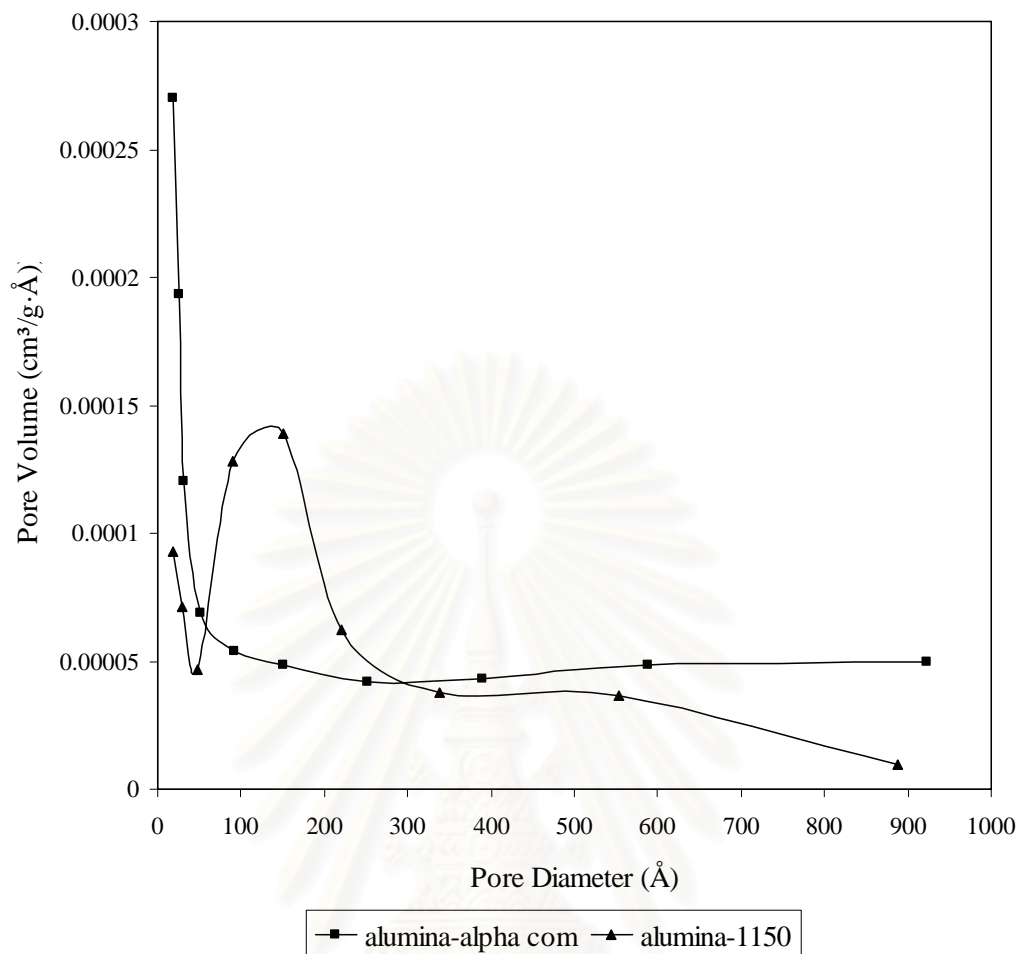


Figure 5.16 Pore size distributions of solvothermal-derived alpha Al₂O₃ and commercial alpha Al₂O₃

สถาบันวิทยบริการ
จุฬาลงกรณ์มหาวิทยาลัย

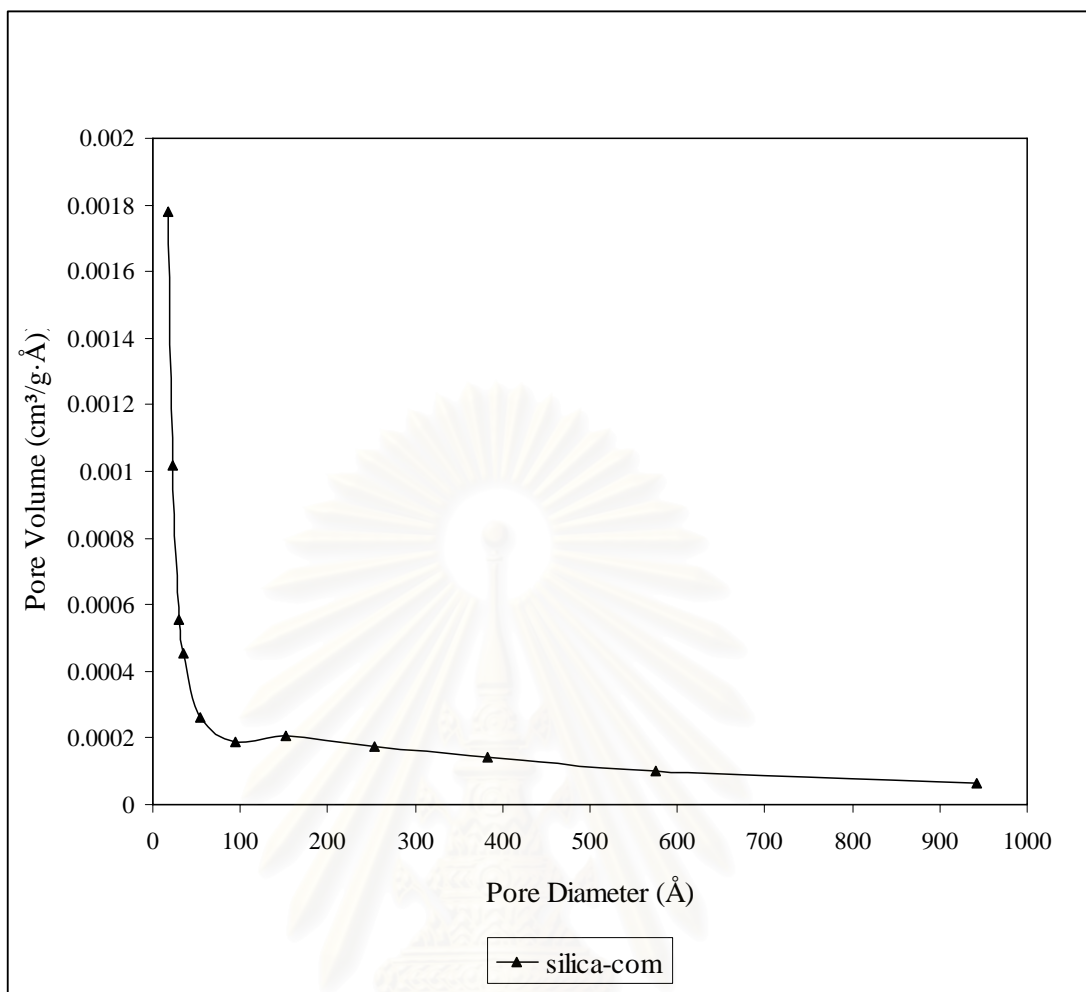


Figure 5.17 Pore size distributions of commercial SiO₂ (15 nm)

สถาบันวิทยบริการ
จุฬาลงกรณ์มหาวิทยาลัย

5.2.1.3 X-Ray Diffraction (XRD)

The XRD patterns of Al₂O₃-as syn, Al₂O₃-700, and Al₂O₃-gamma com supports were carried out at the diffraction angles (2θ) between 10° and 80° and are shown in Figure 5.18. The peaks of Al₂O₃-as syn and Al₂O₃-700 showed that they were chi phase of alumina. In the Figure 5.19, all the three catalysts revealed the Pd peaks at 2θ of 40.2°, but they can not be used to calculate the Pd crystallite size because it was overlapped with the XRD peaks of Al₂O₃. According to the Table 5.13, the crystallite size of Al₂O₃-as syn, Al₂O₃-700, and Al₂O₃-gamma supports were 8.7, 12.6, and 4.45, respectively. It can be seen that the crystallite size decreased with increasing the BET surface area.

The XRD patterns of Al₂O₃-1150 and Al₂O₃-alpha com supports are shown in Figure 5.20. It shows that both Al₂O₃-1150 and Al₂O₃-alpha com have very highly narrow peaks of the XRD patterns of alpha alumina. The crystallites sizes of Al₂O₃-1150 and Al₂O₃-alpha com were 77.1 and 63.8 nm, respectively. From the Figure 5.21, both catalysts revealed the Pd peak at 2θ of 40.2°, and it was calculated that the crystallite size of Pd of Pd/Al₂O₃-1150 and Pd/Al₂O₃-alpha com were 5.9 and 7.0, respectively. It can be suggested that there are no much differences in crystallite size between of Pd/Al₂O₃-1150 and Pd/Al₂O₃-alpha.

Table 5.13 Crystallite sizes of supports and catalysts

Catalysts	Crystallite size (nm)	
	Pd	Support
Pd/Al ₂ O ₃ -as syn	n.d.	8.1
Pd/Al ₂ O ₃ -700	n.d.	12.6
PdAl ₂ O ₃ -gamma com	n.d.	4.45
Pd/Al ₂ O ₃ -1150	5.9	77.1
Pd/Al ₂ O ₃ -alpha com	7.0	63.8
Pd/SiO ₂ -com	n.d.	n.d.

* n.d. = not determined

สถาบันวิทยบริการ
จุฬาลงกรณ์มหาวิทยาลัย

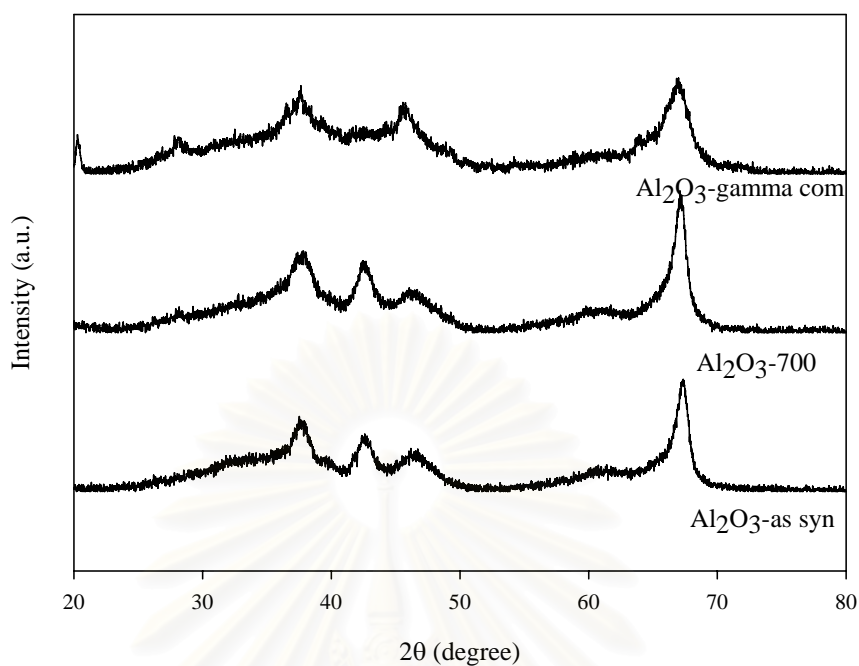


Figure 5.18 XRD patterns of solvothermal-derived alumina and commercial gamma alumina

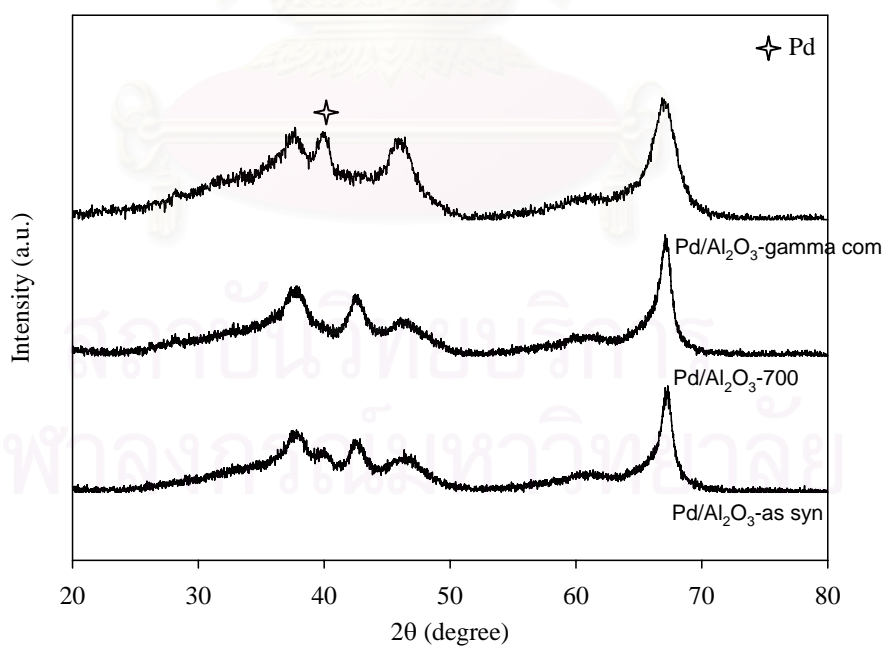


Figure 5.19 XRD patterns of Pd catalysts supported on solvothermal-derived alumina and commercial gamma alumina

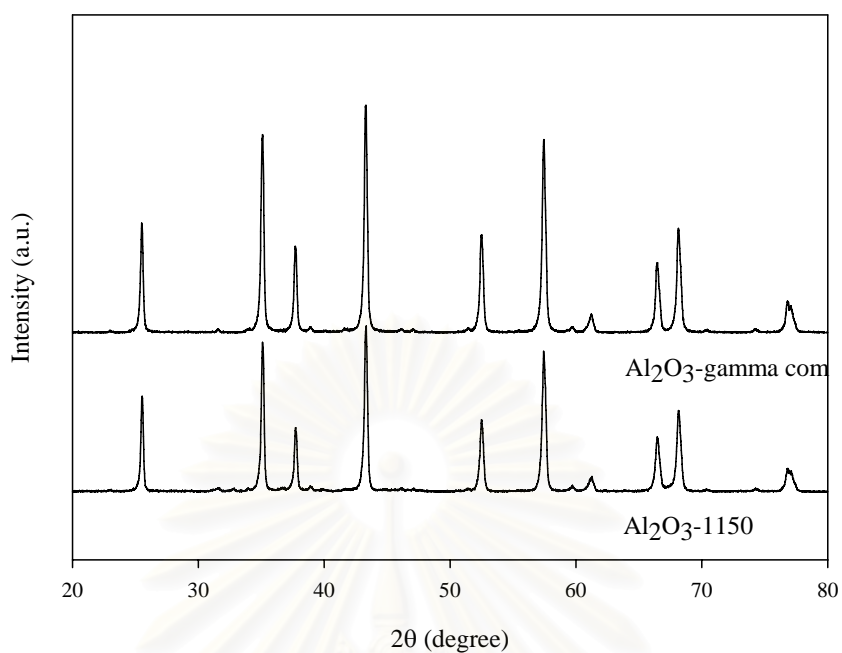


Figure 5.20 XRD patterns of solvothermal-derived alpha alumina and commercial alpha alumina

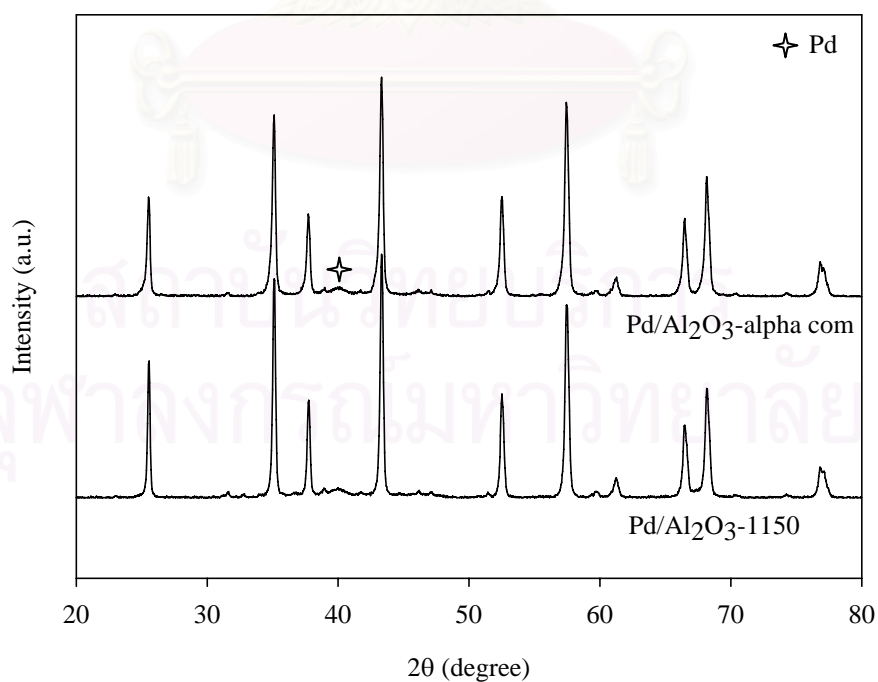


Figure 5.21 XRD patterns of Pd catalysts supported on solvothermal-derived alpha alumina and commercial alpha alumina

5.2.1.4 CO-Pulse Chemisorption

The amounts of CO chemisorption on the catalysts are given in Table 5.14. It can be seen that the amounts of CO chemisorption on Pd active sites of Pd/Al₂O₃-as syn, Pd/Al₂O₃-700, and Pd/Al₂O₃-gamma com are very identical in agreement with equal surface area. For the Pd/alpha Al₂O₃ catalysts, the amounts of CO chemisorption on Pd active sites seem to be not significantly different, so it is also in agreement with BET surface areas which are nearly constant. In addition, it was found that the amount of CO chemisorption on Pd active sites of Pd/SiO₂-com catalyst were lowest.

Table 5.14 CO- pulse chemisorption results

Catalysts	Active sites (10 ¹⁸ sites/g catalyst)	% dispersion	Avg. crystallite size of Pd (nm)
Pd/Al ₂ O ₃ -as syn	12.73	22.51	2.12
Pd/Al ₂ O ₃ -700	12.60	22.27	2.26
PdAl ₂ O ₃ -gamma com	14.20	25.10	2.04
Pd/Al ₂ O ₃ -1150	8.21	14.52	7.05
Pd/Al ₂ O ₃ -alpha com	8.79	15.54	6.59
Pd/SiO ₂ -com	4.02	7.11	14.34

5.2.2 Reaction Study in 1-Heptyne Hydrogenation and Catalyst Deactivation

The catalytic properties of the catalysts prepared by solvothermal-derived supports and commercial supports were investigated in 1-heptyne hydrogenation. The reaction was carried out in toluene solvent at 30°C and 1 bar H₂ pressure. Hydrogenation activity and selectivity of all catalysts are presented in Table 5.15. It was found that the hydrogenation activities of the Pd/Al₂O₃-as syn, Pd/Al₂O₃-700, and Pd/Al₂O₃-gamma com catalysts were not significantly different; therefore, it is in good agreement with the CO chemisorption results that amounts of CO chemisorption were nearly identical. These results are also consistent with the TOFs results that the catalytic activities do not depend on pore diffusion. From Table 5.16, it shows that percentage of Pd leaching of Pd/Al₂O₃-gamma com is lower than the Pd catalysts supported on the synthesized gamma Al₂O₃ catalysts. It is suggested that Pd particles of Pd/Al₂O₃-gamma com were impregnated on the outer surface which Pd can strongly interact because the pores of Al₂O₃-gamma com is too small to allow Pd solution impregnated easily by impregnation method.

In comparison of Pd/Al₂O₃-1150 with Pd/Al₂O₃-alpha com, from Table 5.15, it reveals that activity of Pd/Al₂O₃-1150 is higher than Pd/Al₂O₃-alpha com. However, amounts of CO chemisorption and the N₂ physisorption measurement results of both catalysts were nearly identical. It can be suggested that this reaction is structure-sensitive. The reasons of these results might be investigated by further research using other analysis. For the Pd/SiO₂ catalysts, it has very poor catalytic activity. It may be due to combination of nano-size particle and amorphous of silica.

From the Figure 5.22, the selectivity to 1-heptene of all catalysts is very high about 96 % even for 100 % of conversion. The selectivity to 1-heptene has a very little drop when percentage of conversion increased. Hence, the selectivity does not play an important role in 1-heptyne hydrogenation.

Table 5.15 Results of 1-heptyne hydrogenation

Catalysts	Conversion (%)	Selectivity (%)		TOFs (s ⁻¹)
		Selectivity to Heptene	Selectivity to Heptane	
Pd/Al ₂ O ₃ -as syn	30	100	0	0.08
Pd/Al ₂ O ₃ -700	31	100	0	0.10
Pd/Al ₂ O ₃ -gamma com	34	96	4	0.09
Pd/Al ₂ O ₃ -1150	57	100	0	0.26
Pd/Al ₂ O ₃ -alpha com	37	100	0	0.15
Pd/SiO ₂ -com (15nm)	2	100	0	0.02

Table 5.16 The actual amounts of palladium loading and the percentage of Pd leaching

Catalysts	%Pd of fresh catalysts	% Pd leaching
Pd/Al ₂ O ₃ -as syn	1.2	27
Pd/Al ₂ O ₃ -700	1.2	25
Pd/Al ₂ O ₃ -gamma com	1.2	17
Pd/Al ₂ O ₃ -1150	1.3	8
Pd/Al ₂ O ₃ -alpha com	1.2	8

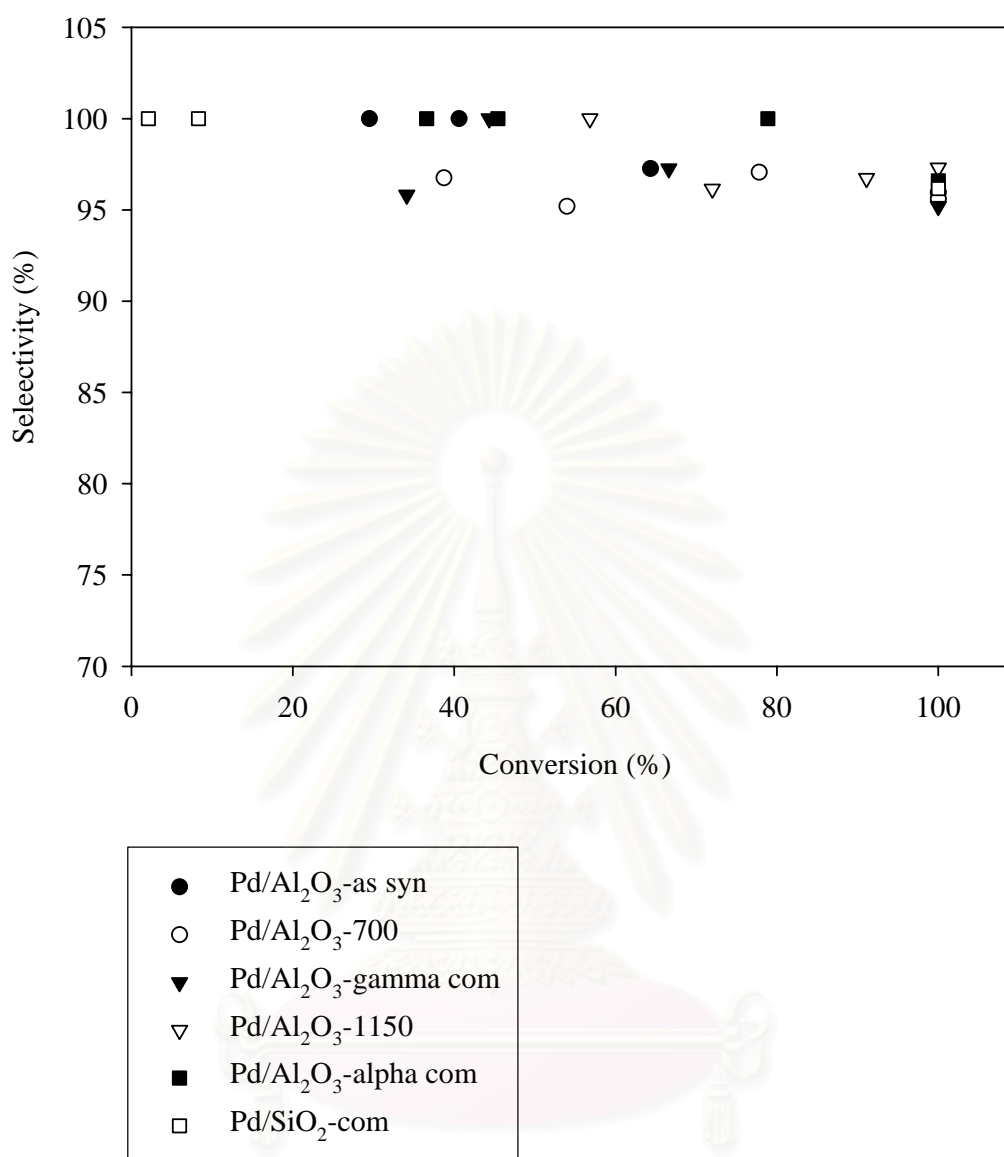


Figure 5.22 Performance curves of various catalysts in 1-heptyne hydrogenation

CHAPTER VI

CONCLUSIONS AND RECOMMENDATIONS

6.1 Conclusions

In this chapter, the conclusions are divided into two parts as following:

6.1.1 Selective Hydrogenation of 1-Heptyne on Pd catalysts on the solvothermal-derived ZnAl_2O_4 , Al_2O_3 , and ZnO supports

1. The solvothermal-derived ZnAl_2O_4 , Al_2O_3 , and ZnO supports are composed of single crystalline.
2. The pore structure of all solvothermal-derived supports were meso-pores around 2-50 nm. For calcination, the pore structure of zinc aluminate and alumina were stable up to 1150°C whereas that of ZnO was at 500°C.
3. The Pd catalysts supported on zinc aluminate calcined at 1150°C exhibited similar performances compared to those supported on alumina calcined at 1150°C and were better than those on the supports calcined at lower temperatures. The Pd/ ZnO catalysts show the lowest performance.
4. Less catalyst deactivation due to metal leaching occurred for those prepared using the supports calcined at higher temperature because Pd can be formed stably on the outer surface and it can be attached strongly on the higher crystalline surface.

6.1.2 Liquid Phase hydrogenation on Pd catalysts supported on solvothermal-derived alumina and commercial alumina

1. The Pd catalysts supported on commercial gamma alumina exhibited the same activities compared to the solvothermal-derived gamma alumina. However, Pd leaching of those supported on commercial gamma alumina is lower.
2. The Pd catalysts supported on commercial alpha alumina exhibited the lower activities compared to the solvothermal-derived alpha alumina. However, Pd leaching of those supported on commercial alpha alumina is the same.

6.2 Recommendations

1. The conditions used in solvothermal synthesis of ZnAl_2O_4 should be varied in order to obtain vary crystallite sizes.
2. The mechanism for deactivation of metal catalyst due to metal leaching during liquid phase hydrogenation should be studied.
3. The preparation of catalysts by ion-exchange and flame spray pyrolysis methods should be studied to compare with the impregnation method.

สถาบันวิทยบริการ
จุฬาลงกรณ์มหาวิทยาลัย

REFERENCES

- Alber, P., Pietsch, J., and Parker, S.F., Poisoning and deactivation of palladium catalyst. *J. Mol. Catal. A* 173 (2001): 275-286.
- Albers, P., Seibold, K., Prescher, G., and Muller, H. XPS and SIMS studies of carbon deposits on Pt/Al₂O₃ and Pd/SiO₂ catalysts applied in the synthesis of hydrogen cyanide and selective hydrogenation of acetylene. *Appl. Catal. A*. 176 (1999): 135-146.
- Albers, P., Pietsch, J., Stewart, F., and Parker, C., Poisoning and deactivation of palladium catalysts. *J. Mole. Catal. A: Chem.* 173 (2001): 275–286
- Ali, S.H., and Goodwin, J.G., Investigation of palladium precursor and support effects on CO hydrogenation over supported Pd catalysts. *J.Catal.* 176 (1998): 3–13.
- Angel, G.D., and Benitez, J.L., Ammonia and sulfur poisoning effects on hydrogenation of phenylacetylene over Pd supported catalysts. *J. Mol. Catal. A* 94 (1994): 409-416.
- Argentiere, P.C.L., Cagnola, E.A., Quiroga, M.E., Liprandi, D.A., A palladium tetra-coordinated complex as catalyst in the selective hydrogenation of 1-heptyne. *App. Catal. A: Gen.* 226 (2002): 253–263
- Argentiere, P.C.L., Lederhos, C.R., and Figoli, N.S., 1-Heptyne Selective Hydrogenation over Pd Supported Catalysts. *Ind. Eng. Chem. Res.* 44 (2005): 1752-1756.
- Besson, M., and Gallezot, P., Deactivation of metal catalysts in liquid phase organic reactions *Catal. Today* 81 (2003): 547-559.
- Carturan, G., Facchin, G., Cocco, G., Enzo, S., and Navazio, G., Influence of metal dispersion on selectivity and kinetics of phenylacetylene hydrogenation catalyzed by supported palladium. *J. Catal.* 76 (1982): 405-417.
- Cagnola, E., Liprandia, D., Quiroga, M., and Argentiere, P.C.L., 1-Heptyne semihydrogenation catalysed by [PdCl₂(NH₂(CH₂)₅CH₃)₂], *React.Kinet.Catal.Lett.* 80, No. 2, (2003): 277-283
- Cagnola, E.A., Liprandi, D.A., Quiroga, M.E., and Argentiere, P.C.L., Rhodium(I) complex with hexylamine and chloride ligands, catalytically active in the selective hydrogenation of 1-heptyne. *Ind. Eng. Chem. Res.* 45 (2006): 5836-5840.

- Dominguez-Quintero, O., Martinez, S., Henriquez, Y., D'Ornelas, L., Krentzien, H., and Osuna, J., Silica-supported palladium nanoparticles show remarkable hydrogenation catalytic activity *J. Mol. Catal. A* 197 (2003): 185-191.
- Duca, D., Liotta, L.F., and Deganello, G., Liquid phase hydrogenation of phenylacetylene on pumice supported palladium catalysts. *Catal. Today* 24 (1995): 15-21.
- Fengyu, Z., Kenji, M., Masayuki, S., and Masahiko, A., Recyclable homogeneous/heterogeneous catalytic systems for heck reaction through reversible transfer of palladium species between solvent and support *J. Catal. A* 194 (2000): 479–483.
- Fengyu, Z., Masayuki, S., Yutaka, I., and Masahiko, A., The leaching and re-deposition of metal species from and onto conventional supported palladium catalysts in the Heck reaction of iodobenzene and methyl acrylate in *N*-methylpyrrolidone. *J. Mol. Catal. A* 180 (2002): 211–219.
- Heidenreich, R.G., Krauter, J.G.E., Pietsch, J., and Kohler K., Control of Pd leaching in Heck reactions of bromoarenes catalyzed by Pd supported on activated carbon *J. Mol. Catal. A* 182-183 (2003): 499-509.
- Joice, P.M., and Srinivasan, M., Photoelectron Spectroscopy (XPS) studies on some palladium catalysts. *Eur. Polym. J.* 31 (1994): 835-839.
- Jianjun, G., Hui, L., Zhao, H., Wang, X., Zheng, X., Novel synthesis of high surface area MgAl₂O₄ spinel as catalyst support. *Mat. Letters* 58 (2004): 1920– 1923
- Mahata, N., and Vishwanathan, V., Influence of palladium precursors on structural properties and phenol hydrogenation characteristics of supported palladium catalysts. *J. Catal.* 196 (2000): 262–270.
- Marin-Astorga, N., Pecchi, G., Fierro, J.L.G., and Reyes, P., Alkynes hydrogenation over Pd-supported catalysts. *Catal. Lett.* 91, Nos. 1–2, November 2003: (2003)
- Marin-Astorga, N., Alvez-Manoli, G., Reyes, P., Stereoselective hydrogenation of phenyl alkyl acetylenes on pillared clays supported palladium catalysts. *J. Mol. Catal. A* 226 (2005): 81-88.
- Mekasuwandumrong, O., Pavarajarn, V., Inoue, M., and Praserttham, P., Preparation and phase transformation behavior of χ -alumina via solvothermal synthesis. *Mat. Chem. Phys.* 100 (2006): 445-450.

- Nag, N.K., A study on the dispersion and catalytic activity of gamma alumina supported palladium catalysts. *Catal. Lett.* 24 (1994): 37-46.
- Nijhuis, T.A., van Koten, G., Moulijn, J.A., Optimized palladium catalyst systems for the selective liquid-phase hydrogenation of functionalized alkynes. *App. Catal. A: Gen.* 238 (2003): 259–271.
- Nozoe, T., Tanimoto, K., Takemitsu, T., Kitamura, T., Harada, T., Osawa, T. and Takayasu, O., Non-solvent hydrogenation of solid alkenes and alkynes with supported palladium catalyst. *Sol. St. Ion.* 141 (2001): 695-700.
- Panpranot, J., Pattamakomsan, K., Praserthdam, P. and Goodwin, G.J., A comparative study of Pd/SiO₂ and Pd/MCM-41 catalysts in liquid-phase hydrogenation. *Catal. Com.* 5 (2004): 583-590.
- Panpranot, J., Pattamakomsan, K., Praserthdam, P. and Goodwin, G.J., Impact of the silica support structure on liquid phase hydrogenation on Pd catalysts. *Ind. Eng. Chem. Res.* 43 (2004): 6014-6020.
- Panpranot, J., Tangjitwattakorn, O., Praserthdam, P., and Goodwin, G.J., Effects of Pd precursors on the catalytic activity and deactivation of silica-supported Pd catalysts in liquid phase hydrogenation. *App. Catal. A: Gen.* 292 (2005): 322–327.
- Panpranot, J., Phandinthong, K., Sirikajorn, T., Arai, M., and Praserthdam, P., Impact of palladium silicide formation on the catalytic properties of Pd/SiO₂ catalysts in liquid-phase semihydrogenation of phenylacetylene. *J. Mol. Catal. A: Chem.* 261 (2006): 29–35.
- Rylander, P.N., “Hydrogenation Methods”, (1985a)
- Rylander, P.N., Hydrogenation Olefins, in “Hydrogenation Methods”, (1985b)
- Sales, E.A., Bugli, G., Ensuque, A., Mendes, M.J., Bozon-Verduraz, F., Palladium catalysts in the selective hydrogenation of hexa-1,5-diene and hexa-1,3-diene in the liquid phase. Effect of tin and silver addition-part 1. Preparation and characterization: from the precursor species to the final phases. *Chem. Phys.* (1999): 491-498.
- Sarkany, A., Weiss, A.H., and Guzzi, L., Structure sensitivity of acetylene-ethylene hydrogenation over Pd catalysts. *J. Catal.* 98 (1986): 550-553.
- Sarkany, A., Zsoldos, Z., Furlong, B., Hightower, J.W., and Guzzi, L., Hydrogenation of 1-butene and 1,3-butadiene mixtures over Pd/ZnO catalysts. *J. Catal.* 141 (1993): 566-582.

- Singh, U.K. and Vannice, M.A., Liquid-phase citral hydrogenation over SiO₂-supported group VIII metals *J. Catal.* 199 (2001): 73-84.
- Stanger, K.J., Tang, Y., Andereg, J., and Angelici, R.A., Arene hydrogenation using supported rhodium metal catalysts prepared from [Rh(COD)H]₄, [Rh(COD)₂]⁺BF₄⁻, and [Rh(COD)Cl]₂ adsorbed on SiO₂ and Pd-SiO₂ *J. Mol. Catal. A.* 202 (2003): 147–161.
- Yamada, H. and Goto, S., The effect of solvents polarity on selective hydrogenation of unsaturated aldehyde in gas-liquid-solid three phase reactor *J. Chem. Eng. Japan* 36 (2003): 586-589.
- Wagner, C. D., Riggs, W. M., Davis, L. E., Moulder, J. F., In Handbook of X-ray Photoelectron Spectroscopy; Muilenberg, G. E., Ed.; Perkin-Elmer Corporation: Eden Prairie, MN, (1978).
- Wrzyszczyk, J., Zawadzki, M., Trzeciak, A.M., Ziolkowski, J.J., Rhodium complexes supported on zinc aluminate spinel as catalysts for hydroformylation and hydrogenation: preparation and activity. *J. Mol. Catal. A:* 189 (2002): 203–210.
- Xiuhua, W., Donghua, C., Synthesis and characterization of nanosized zinc aluminate spinel by sol–gel technique *Mat. Lett.* 60 (2006): 823–827.
- Zawadzki, M., Wrzyszczyk, J., Hydrothermal synthesis of nanoporous zinc aluminate with high surface area. *Materials Research Bulletin* 35 (2000): 109–114.
- Zawadzki, M., Synthesis of nanosized and microporous zinc aluminate spinel by microwave assisted hydrothermal method (microwave–hydrothermal synthesis of ZnAl₂O₄) *Sol. St. Sci.* 8 (2006): 14–18.



APPENDICES

สถาบันวิทยบริการ
จุฬาลงกรณ์มหาวิทยาลัย

APPENDIX A

CALCULATION FOR CATALYST PREPARATION

Preparation of 1%Pd/ZnAl₂O₄ catalysts by the incipient wetness impregnation is shown as follows:

Reagent: - Palladium (II) nitrate hydrate (99.99%)

Molecular weight. = 338.52

- Support: ZnAl₂O₄, Al₂O₃, ZnO

Example Calculation for the preparation of 1%Pd/ZnAl₂O₄

Based on 100 g of catalyst used, the composition of the catalyst will be as follows:

Palladium	=	1 g	
ZnAl ₂ O ₄	=	100-1 =	99 g

For 1 g of catalyst

Palladium required	=	1×(1/100)	=	0.01 g
--------------------	---	-----------	---	--------

Palladium 0.01 g was prepared from Pd(NO₃)₂.6H₂O and molecular weight of Pd is 106.42

The Pd(NO₃)₂.6H₂O(99.99%)content =
$$\frac{\text{MW of Pd(NO}_3)_2.6\text{H}_2\text{O} \times \text{Palladium required}}{\text{MW of Pd} \times 0.9999}$$

$$= (338.52/(106.42 \times 0.9999)) \times 0.01 = 0.0321 \text{ g}$$

สถาบันวิทยบริการ
จุฬาลงกรณ์มหาวิทยาลัย

APPENDIX B

CALCULATION OF THE CRYSTALLITE SIZE

Calculation of the crystallite size by Debye-Scherrer equation

The crystallite size was calculated from the half-height width of the diffraction peak of XRD pattern using the Debye-Scherrer equation.

From Scherrer equation:

$$D = \frac{K\lambda}{\beta \cos \theta} \quad (\text{B.1})$$

- where
- D = Crystallite size, Å
 - K = Crystallite-shape factor = 0.9
 - λ = X-ray wavelength, 1.5418 Å for CuK α
 - θ = Observed peak angle, degree
 - β = X-ray diffraction broadening, radian

The X-ray diffraction broadening (β) is the pure width of a powder diffraction free from all broadening due to the experimental equipment. α -Alumina is used as a standard sample to observe the instrumental broadening since its crystallite size is larger than 2000 Å. The X-ray diffraction broadening (β) can be obtained by using Warren's formula.

From Warren's formula:

$$\beta = \sqrt{B_M^2 - B_S^2} \quad (\text{B.2})$$

- Where
- B_M = The measured peak width in radians at half peak height.
 - B_S = The corresponding width of the standard material.

Example: Calculation of the crystallite size of Pd/ZnAl₂O₄-900

$$\begin{aligned} \text{The half-height width of 111 diffraction peak} &= 0.60^\circ \text{ (from the figure B.1)} \\ &= (0.60 \times \pi) / 180 \\ &= 0.1047 \text{ radian} \end{aligned}$$

The corresponding half-height width of peak of α -alumina (from the B_s value at the 2θ of 34.08° in figure B.2) = 0.00405 radian

$$\begin{aligned} \text{The pure width, } \beta &= \sqrt{B_M^2 - B_S^2} \\ &= \sqrt{0.1047^2 - 0.00405^2} \\ &= 0.1046 \text{ radian} \end{aligned}$$

$$B = 0.1046 \text{ radian}$$

$$2\theta = 36.8^\circ$$

$$\theta = 18.4^\circ$$

$$\lambda = 1.5418 \text{ \AA}$$

$$\begin{aligned} \text{The crystallite size} &= \frac{0.9 \times 1.5418}{0.1046 \cos 18.4} = 171.66 \text{ \AA} \\ &= 17.16 \text{ nm} \end{aligned}$$

สถาบันวิทยบริการ
จุฬาลงกรณ์มหาวิทยาลัย

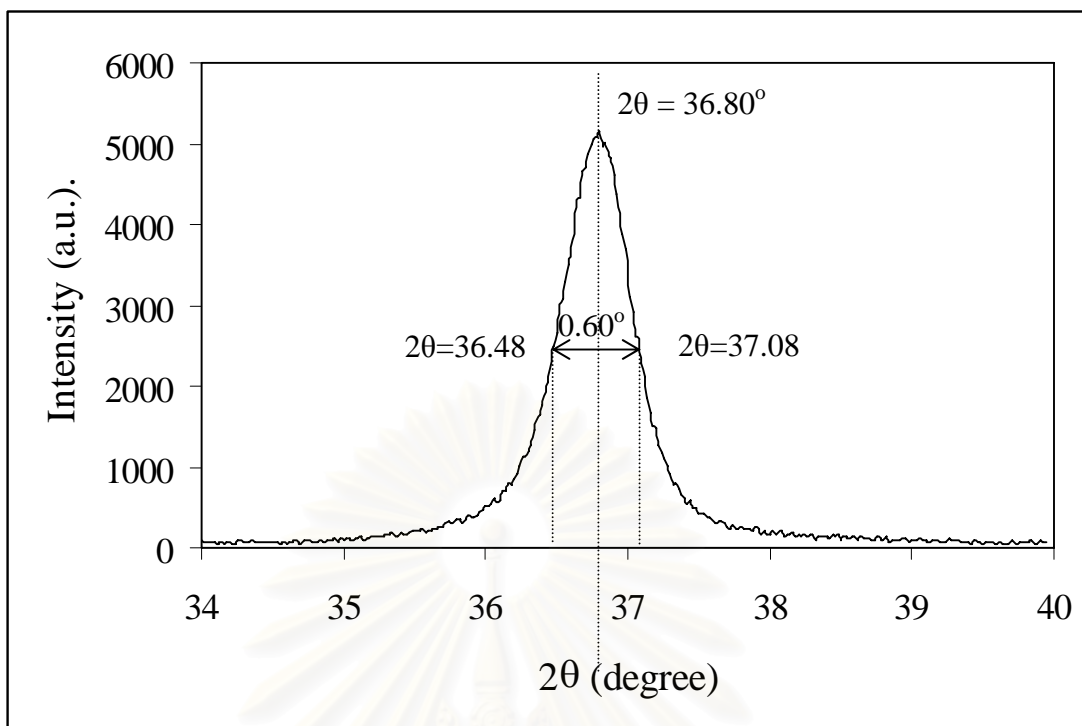


Figure B.1 The diffraction peak of Pd/ZnAl₂O₄-900 for calculation of the crystallite size

สถาบันวิทยบริการ
จุฬาลงกรณ์มหาวิทยาลัย

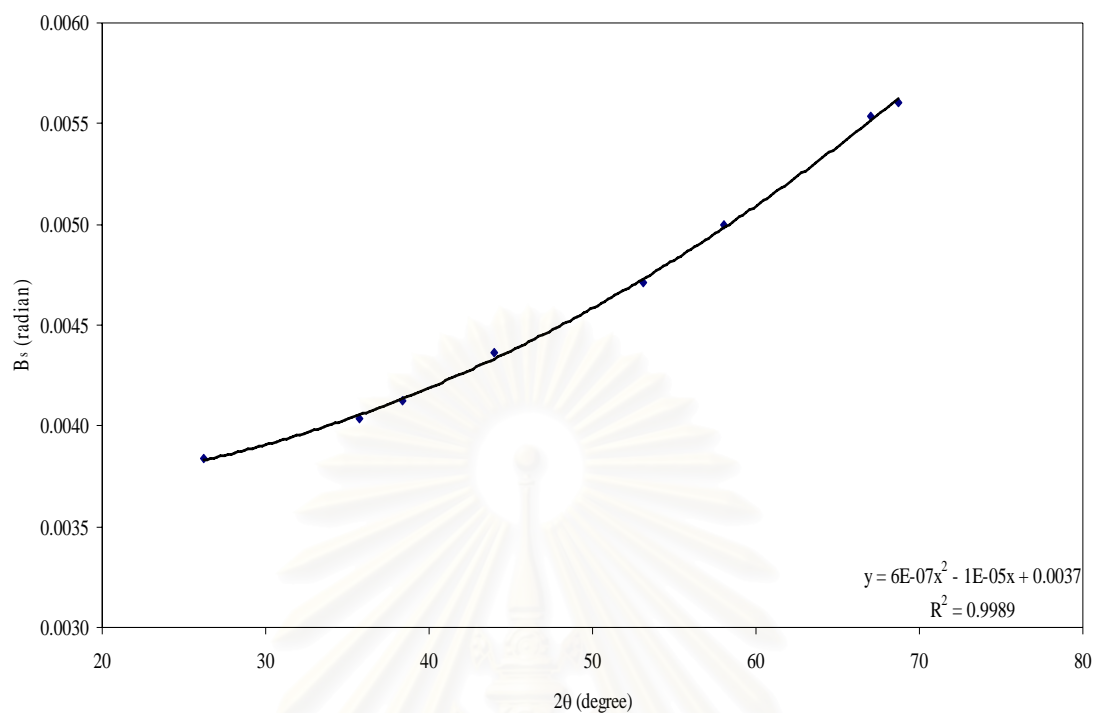


Figure B.2 The plot indicating the value of line broadening due to the equipment. The data were obtained by using α -alumina as a standard

สถาบันวิทยบริการ
จุฬาลงกรณ์มหาวิทยาลัย

APPENDIX C

CALCULATION FOR METAL ACTIVE SITES AND DISPERSION

Calculation of the metal active sites and metal dispersion of the catalyst measured by CO adsorption is as follows:

Let the weight of catalyst used	= W	g
Integral area of CO peak after adsorption	= A	unit
Integral area of 100 μ l of standard CO peak	= B	unit
Amounts of CO adsorbed on catalyst	= B-A	unit
Volume of CO adsorbed on catalyst	= $100 \times [(B-A)/B]$	μ l
Volume of 1 mole of CO at 30°C	= 24.86×10^6	μ l
Mole of CO adsorbed on catalyst	= $[(B-A)/B] \times [40/24.86 \times 10^6]$	mole
Molecule of CO adsorbed on catalyst	= $[1.61 \times 10^{-6}] \times [6.02 \times 10^{23}] \times [(B-A)/B]$	molecules
Metal active sites	= $9.68 \times 10^{17} \times [(B-A)/B] \times [1/W]$	molecules of CO/g of catalyst
Molecules of Pd loaded	= $[\% \text{ wt of Pd}] \times [6.02 \times 10^{23}] / [\text{MW of Pd}]$	molecules/g of catalyst
Metal dispersion (%)	= $100 \times [\text{molecules of Pd from CO adsorption} / \text{molecules of Pd loaded}]$	

สถาบันวิทยบริการ
จุฬาลงกรณ์มหาวิทยาลัย

APPENDIX D

CALIBRATION CURVES

This appendix shows the calibration curves for calculation of composition of reactant and products in 1-heptyne hydrogenation. The reactant is 1-heptyne and products are 1-heptene and heptane.

The flame ionization detector (FID), gas chromatography Shimadzu modal 14B was used for analyzing the concentration of 1-heptyne, 1-heptene, and heptane by using GS-alumina column.

The GS-alumina column was used with a gas chromatography equipped with a flame ionization detector (FID), Shimadzu modal 14B, for analyzing the concentration of phenylacetylene, styrene and ethylbenzene. Conditions uses in GC are illustrated in Table B.1.

Mole of reagent in y-axis and area, which was reported by gas chromatography, in x-axis is exhibited in the curves. The calibration curves of 1-heptyne and 1-heptene.

สถาบันวิทยบริการ
จุฬาลงกรณ์มหาวิทยาลัย

Table D.1 Conditions uses in Shimadzu modal GC-14B

Parameters	Conditions of Shimadzu GC-14B
Width	5
Slope	29
Drift	0
Min. area	100
T.DBL	2.7
Stop time	40
Atten	0
Speed	2
Method	1
Format	1
SPL.WT	100
IS.WT	0

สถาบันวิทยบริการ
จุฬาลงกรณ์มหาวิทยาลัย

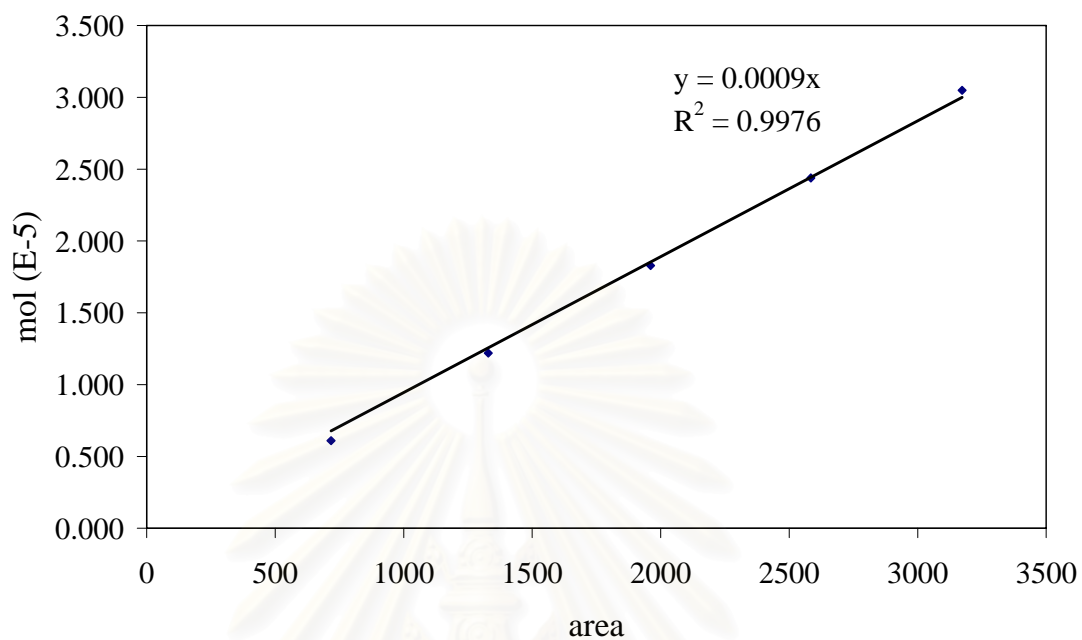


Figure D.1 The calibration curve of 1-heptyne

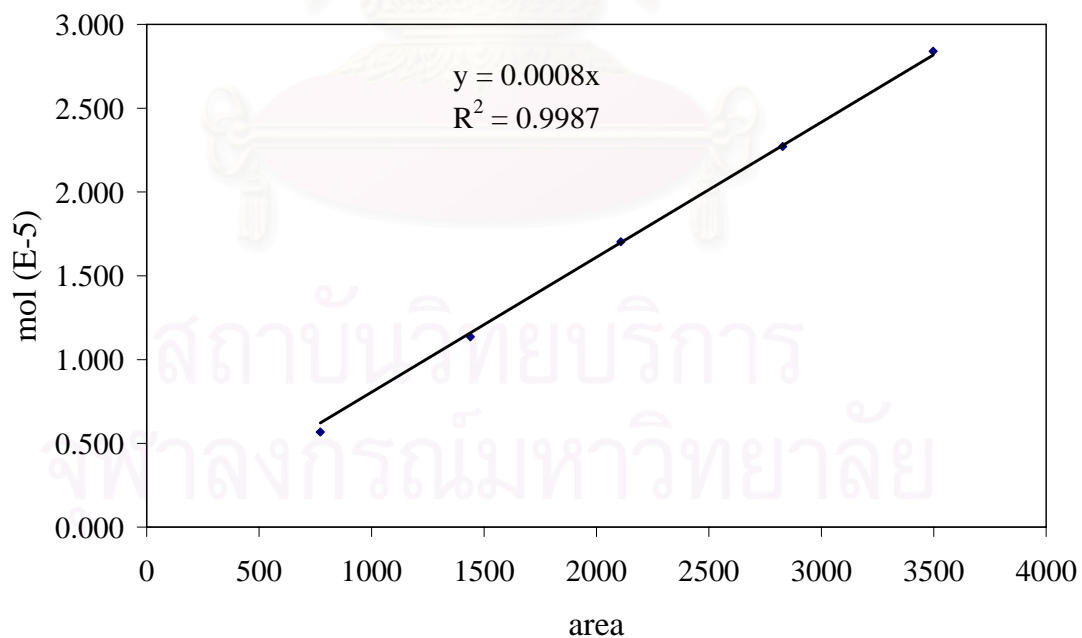


Figure D.2 The calibration curve of 1-heptene

APPENDIX E

CALCULATION OF PHENYLACTYLENE CONVERSION AND SELECTIVITY

The catalytic performance for the 1-heptyne hydrogenation was evaluated in terms of activity for 1-heptyne conversion and selectivity.

Activity of the catalyst performed in term of 1-heptyne conversion. 1-Heptyne conversion is defined as moles of 1-heptyne converted with respect to 1-heptyne in feed:

$$1\text{-heptyne conversion}(\%) = \frac{\text{mole of 1-heptyne in feed} - \text{mole of 1-heptyne in product}}{\text{mole of 1-heptyne in feed}} \times 100 \quad (\text{E.1})$$

Where mole of 1-heptyne can be measured employing the calibration curve of 1-heptyne in Figure D.1, Appendix D., i.e.

$$\text{Mole of 1-heptyne} = (\text{Area of 1-heptyne peak from integrator plot on GC - 14B}) \times 9 \times 10^{-9} \quad (\text{E.2})$$

Selectivity of product is defined as mole of 1-heptene formed with respect to mole of 1-heptyne converted:

$$\text{Selectivity of 1-heptene}(\%) = \frac{\text{mole of 1-heptene formed}}{\text{mole of total product}} \times 100 \quad (\text{E.3})$$

Where mole of 1-heptene can be measured employing the calibration curve of 1-heptene in Figure D.2, Appendix D., i.e.,

$$\text{Mole of 1 - heptene} = (\text{Area of 1 - heptene peak from integrator plot on GC - 14B}) \times 8 \times 10^{-9} \quad (\text{E.4})$$



สถาบันวิทยบริการ
จุฬาลงกรณ์มหาวิทยาลัย

APPENDIX F

CALCULATION OF TURNOVER OF FREQUENCY

Calculation of Turnover frequencies (TOF)

Metal active site = y molecule/g cat.

$$\begin{aligned}
 \text{TOF} &= \frac{\text{rate}}{(\text{numbers of active site})} \\
 &= \frac{\text{molecule substrate converted}}{[\text{g cat.}] [\text{min}]} \left| \frac{[\text{g cat.}]}{y [\text{active site}]} \right| \left| \frac{[\text{min}]}{60[\text{s}]} \right| \\
 &= [\text{s}^{-1}]
 \end{aligned}$$

สถาบันวิทยบริการ
จุฬาลงกรณ์มหาวิทยาลัย

APPENDIX G**LIST OF PUBLICATIONS**

1. Terachai Sirikajorn and Joongjai Panpranot, “Liquid-Phase Hydrogenation on Pd Catalyst Supported on Solvothermal-Derived ZnAl_2O_4 ”, Proceedings of the Regional Symposium on Chemical Engineering 2006, Singapore, Dec. 3 –5, 2006.



สถาบันวิทยบริการ
จุฬาลงกรณ์มหาวิทยาลัย

Liquid-Phase Hydrogenation on Pd Catalyst Supported on Solvothermal-Derived ZnAl_2O_4

Terachai Sirikajorn^a and Joongjai Panpranot^{a,*}

^aCenter of Excellence on Catalysis and Catalytic Reaction Engineering
Department of Chemical Engineering, Faculty of Engineering,
Chulalongkorn University, Bangkok 10330, Thailand

* Corresponding author, E-mail: joongjai.p@eng.chula.ac.th

ABSTRACT

A solvothermal method is proposed for the preparation of uniform particle size of nanosized ZnAl_2O_4 spinel with high surface area, which is relatively stable after high temperature exposure. In this technique, ZnAl_2O_4 spinel was obtained by reaction between Zn and Al precursors using toluene as solvent at 300 °C, followed by calcination of the as-synthesized ZnAl_2O_4 spinel at different temperatures (400-1150 °C). Powder X-ray diffraction (XRD) shows that the as-synthesized ZnAl_2O_4 spinel is single-phase cubic material having the spinel-type structure, which has crystallite size of 8 nm. The particle sizes of the products observed from the transmission electron microscopy (TEM) are in good agreement with the crystallite sizes determined by the XRD technique. This suggests that each particle is a single crystal of spinel. The specific surface area determined by BET surface area measurement was found to be 110 m² g⁻¹. A Pd/ ZnAl_2O_4 catalyst prepared based on the nanosized ZnAl_2O_4 spinel was reacted in catalytic hydrogenation of heptyne to study the behavior of solvothermal-derived nano-sized ZnAl_2O_4 .

1. INTRODUCTION

Catalytic hydrogenation is one of the most useful, versatile, and environmentally acceptable reaction routes available for organic syntheses because the scope of the reaction type is very broad and many functional groups can be hydrogenated with high selectivity and high conversion. A large number of these reactions are carried out in liquid phase using batch type slurry processes. Hydrogenation reactions are mostly catalyzed by noble metals or group VIII transition metals. The major advantages of noble metal catalysts are their relatively high activity, mild process conditions, easy separation, and better handling properties. Noble metals such as, Pt, Pd, Rh, and Ru are particularly effective in hydrogenation. The important problem in catalytic liquid phase hydrogenation is the activity and selectivity decay due to catalyst deactivation such as sintering, leaching and poisoning. In order to improve the properties of catalytic materials, great interest has focused on the use of spinel-type structures. Among these materials, aluminates seem to be a good option because of their properties such as high thermal stability, high mechanical resistance, hydrophobicity, and low surface acidity. These properties make them interesting materials as catalysts and carriers for active metals to substitute the more traditional systems. Furthermore, it is known that some aluminate spinels, including zinc aluminate, tend to prevent sintering of noble metals due to a strong metal-support interaction. The sintering resistance and chemical stability of catalytically active phases are a very important problem for high-temperature processes.

2. MATERIALS AND METHODS

Zinc aluminate was first synthesized by solvothermal method described in detail in previous work [1]. Aluminium isopropoxide and appropriate amount of zinc (II) acetylacetonate were suspended in toluene and heated under autogeneous pressure in an autoclave at 300°C for 2 h. The obtained zinc aluminate was then calcined at different temperature for 1 h. The Pd/ ZnAl_2O_4 catalyst with 1% palladium loading was prepared by incipient wetness impregnation of zinc aluminate with aqueous solutions of palladium (II) nitrate. And then catalyst precursor was calcined in air at 400°C for 6 h prior to reducing with hydrogen. The characterization of powder included X-ray diffraction (XRD), scanning electron microscope (SEM), transmission electron microscope (TEM) and surface area/porosity measurement via N₂ physisorption method. The liquid-phase hydrogenation reaction was studied at reduce temperature, 150 °C and reaction condition is 30 °C, 1 atm. The products will be analyzed by gas chromatography technique in order to evaluate the catalytic activity and selectivity of products.

3. RESULTS AND DISCUSSION

The XRD analysis of the obtained powder confirmed that the product was zinc aluminate in spinel phase without contamination from other crystalline phases. The crystallite size of as-synthesized samples calculated from the Scherrer equation was approximately 8 nm. Surface area was found to be 110 m²/g. TEM micrographs revealed that the obtained powder was nanometered particles. The particle sizes are in good agreement with the crystallite sizes determined by the XRD technique. This suggests that each particle is a single crystal of spinel phase. According to Table 1, the calcined products have growth of crystallite size and decreasing of surface area.

Table 1 Surface area and crystallite size of zinc aluminate at different calcined temperature

Calcined temperature (°C)	Crystallite size (nm)	Surface area (m ² /g)
as-synthesized	8.25	110
300	8.66	109
400	8.84	106
500	9.03	86
700	10.87	48
900	17.63	28
1150	33.27	10

The liquid-phase hydrogenation of heptyne shows high selectivity of heptene above 90 percents for all catalysts. According to Table 2, Pd catalyst supported on as-synthesized zinc aluminate shows the highest activity, resulting from high surface area. The activity decreases as Pd catalyst supported on higher calcined temperature, respectively.

Table 2 Results of reaction study from hydrogenation of heptyne

catalyst	% Conversion	% Selectivity	
		heptene	heptane
Pd/ZnAl ₂ O ₄ (as-syn)	78.21	96.76	3.24
Pd/ZnAl ₂ O ₄ (700°C)	66.16	95.44	4.56
Pd/ZnAl ₂ O ₄ (1,150°C)	52.34	93.19	6.81

The performance of these catalysts is very effective. Although conversion of heptyne is complete, the selectivity of heptene is above 90 percent.

REFERENCE

- Kanyanucharat, A., Prasertthdam, P. and Tanakulrungsank, W.** (2001). Determination of the thermal stability of CoAl₂O₄, ZnAl₂O₄ and NiAl₂O₄ single nanocrystals. pp 1-93. Chulalongkorn University, Bangkok.
- Zawadzki, M., Mista, W. and Kepinski, L.** (2001). Metal-support effects of platinum supported on zinc aluminate. *Vacuum* **63**, 291-296.
- Zawadzki, M.** (2006). Synthesis of nanosized and microporous zinc aluminate spinel by microwave assisted hydrothermal method (microwave-hydrothermal synthesis of ZnAl₂O₄). *Solid State Sci.* **8**, 14-18.
- Wrzyszczyk, J., Zawadzki, M., Trzeciak, A. M. and Ziolkowski, J. J.** (2002). Rhodium complexes supported on zinc aluminate spinel as catalysts for hydroformylation and hydrogenation: preparation and activity. *J. Mol. Cat. A: Chem.* **189**, 203-210

VITAE

Mr. Terachai Sirikajorn was born in December 17th, 1983 in Bangkok, Thailand. He finished high school from Yothinburana School, Bangkok in 2001, and received bachelor's degree in Chemical Engineering from the department of Chemical Engineering, Faculty of Engineering, Chulalongkorn University, Bangkok, Thailand in 2005.



สถาบันวิทยบริการ
จุฬาลงกรณ์มหาวิทยาลัย